DEPARTAMENTO DE INGENIERÍA NUCLEAR
MÁSTER EN CIENCIA Y TECNOLOGÍA NUCLEAR

UNIVERSIDAD POLITÉCNICA DE MADRID

PROYECTO FIN DE MÁSTER

Preliminary approach to neutron instrument selection at ESS-Bilbao based on experience at ISIS molecular spectroscopy group

JESÚS PEDRO DE VICENTE BUENO SEPTIEMBRE 2013

DIRECTORES: **Dr. FERNANDO SORDO BALBÍN** & **Dr. FÉLIX FERNÁNDEZ-ALONSO**
TUTOR: **Prof. Dr. JOSÉ MANUEL PERLADO MARTÍN**

«Neutrons tell you where the atoms are
and what the atoms do»

C. Shull and B. Brockhouse (1994)

Edited by LaTeX

Contents

List of Figures

DOCUMENT 1: CHARACTERIZATION OF THE NEUTRON SOURCE

DOCUMENT 2: APPENDICES

List of Tables

DOCUMENT 1: CHARACTERIZATION OF THE NEUTRON SOURCE

DOCUMENT 2: APPENDICES

1 MOTIVATION

One of the purposes of the ESS-Bilbao project, hereinafter ESSB, is to produce useful neutrons to several research areas, from nuclear physics to material and irradiation sciences. Nevertheless the focus of the present report was on neutron scattering, a very useful technique for material sciences, biology and engineering.

This report is the result of a two-moth stay at the molecular spectroscopy group of ISIS. The goal was to get a general view of the neutron scattering technique emphasizing the main parameters required to design instruments. Simulation tools were used trying to materialize the concepts learned.

I would like to express a special gratitude to Prof. Félix Fernández-Alonso who let me feel as a member of his group. He transmitted me the motivation for the neutron scattering and guided my learning. His wise advices constitute the guidelines of the present report.

I am also very grateful to the molecular spectroscopy group, i.e. to Dr. A. Seel, Dr. F. Demmel, Dr. V. García, Dr. S. Mukhopadhyay, Dr. S. Parker, Dr. T. Ramírez and especially to Dr. S. Rudic who taught me the molecular spectroscopy principles and let me feel like at home

Dr. Stuart Ansell, thank you very much for the invitations to your group meetings and your advices.

I would like to appreciate the effort of the two instituions involved, ISIS and ESS-Bilbao, to let me this experience.

Finally I would like to show my pride for belonging to the Target & Neutron Applications Group which effort and assiduously let me to contribute with this little grain of sand.

Thank you very much.

MÁSTER EN CIENCIA Y TECNOLOGÍA NUCLEAR

DOCUMENT 1: CHARACTERIZATION OF THE NEUTRON SOURCE

1 THE ESS-BILBAO PROJECT

1.1 History

Research with neutrons has traditionally been performed around fission reactors. However, in the late 1990s a necessity to build a new generation of high-intensity neutron sources was identified. Projects for large spallation neutron source were launched in the US, Japan and Europe.

The project to build a European Spallation Source (ESS) [1] is a cooperation among several European countries. During the early 2000s, several European cities, including Bilbao, contended to hosting of the ESS. In 2009 it was decided that the ESS will be built in Lund, Sweden. However, ESS-Bilbao (ESSB) will collaborate with the European Project and build a smaller neutron source in Spain. While the ESS is expected to be fully operational in 2025, ESSB will be online by 2016. Hence, it will be possible to test and support the design of components for the ESS at ESSB.

An important remark is that the ESSB neutron source will not be a spallation neutron source but a compact source where neutrons will be produced by (p, n) reactions [2].

The construction of ESSB stands as a reference among science projects in Spain. Upon its completion, not only will it be an important support to the ESS project but it will also be capable of producing relevant scientific results on its own.

1.2 Facilities

The ESSB facilities will be located at the Leioa campus of University of the Basque Country (UPV/EHU). Among others, the School of Science and Technology is in this campus, which is situated in the town of Leioa, close to the city of Bilbao in the Basque Country, North of Spain.

As of September 2012, works have already started where the buildings will be erected. The grounds have been flattened and foundations are being lain.

According to the most updated design, the layout of the main building is shown in Figure 1-1. The main components of the facility are highlighted in the Figure.

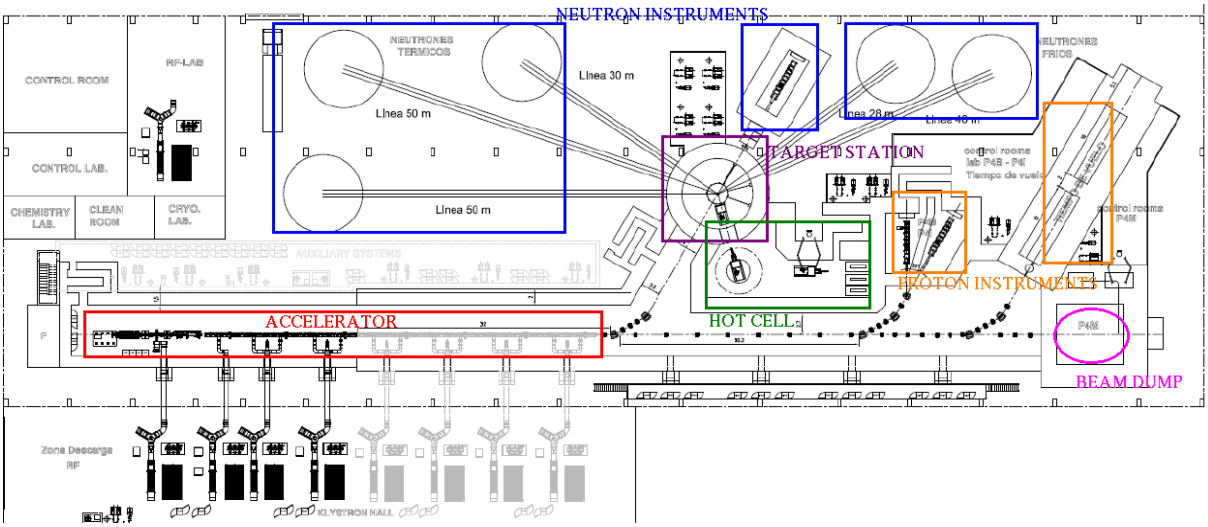

Figure 1-1: ESSB building layout

A proton **Accelerator** goes along the main building, accelerating protons up to 50 MeV before bending towards the **Target Station** (TS), situated in the center of the building. When neutrons are produced, they are directed to different **Neutron Instruments** located around the TS, while **Proton Instruments** are situated further down in the beam direction. Next to the TS there is also a **Hot Cell** for storage and decay of activated components. Finally, the **Beam Dump** (BD) is located in a straight line from the LINAC.

The following sections summarize the main aspects of some of these components.

1.2.1 ACCELERATOR

The proton LINAC is the instrument in charge of generating a pulsed proton beam and directing it to the target. It consists of different components that increase the proton energy or shape the proton beam. Figure 1-2 shows a schematic layout of the main components of the LINAC.

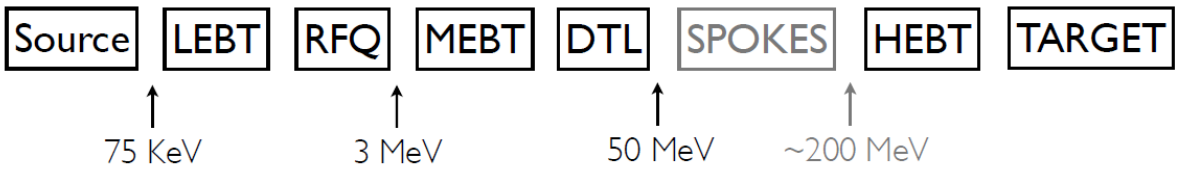

Figure 1-2: ESSB LINAC Overview [3].

Protons are extracted from a plasma chamber at the ion source. In fact, two Ions Sources will be installed: a H^+ source and a H^-, although they will work one at a time. Protons exit the Ion Source at 75 keV, and are directed by the Low Energy Beam Transport (LEBT) to the Radio

Frequency Quadrupole (RFQ). At the RFQ protons are grouped in *bunches* and accelerated up to 3 MeV, and the beam is compacted. Then the Medium Energy Beam Transport (MEBT) takes the beam to the Drift Tube LINAC (DTL), where the beam is finally accelerated up to 50 MeV. Future upgrades of the facility could include acceleration up to 200 MeV by means of Spoke Cavities and a High Energy Beam Transport (HEBT)[3].

According to the most updated LINAC design status, beam parameters at the end of the accelerator are listed on Table **??**.

Species	H^+
Particle Energy	$50 - 60$ MeV
Peak Current	75 mA
Average Current	$2 - 5$ mA
Repetition Rate	$20 - 50$ Hz

Table 1-1: Beam Parameters

1.2.2 TARGET STATION

The TS is the part of the facility that hosts the neutron producing target and its auxiliary components.

ESSB target [4] will consist of a rotating aluminium alloy (6061 T6) wheel with beryllium plates shown in Figure 1-3. Beryllium was compared to other materials for the plates, but it was chosen for its best relation of neutron production and neutron average energy, with a production of 0.065 neutrons per incident proton at an average energy of 7.76 MeV [2] . This target is cooled by water channels that are formed between the different parts of the component.

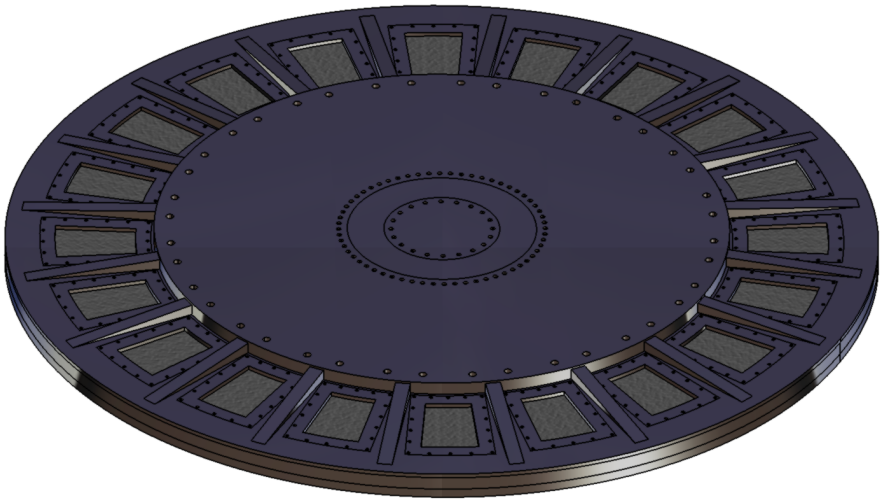

Figure 1-3: ESSB rotating target wheel [4]

The current design of the target wheel includes 20 Beryllium plates. Given that 20 Hz is the design value for beam frequency at the target, each plate would see a frequency of 1 Hz. The total beam power, taking into account the other design parameters, is 112.5 kW.

The rotating target is located inside a Target Vessel (TV), which is a steel vessel that includes moderators, reflector, shielding, a Target Positioning Unit and the different proton and neutron guides. The TV, shown in Figure 1-4 has the objective of shielding radiation from the target, confinement of possible radioactive products as well as providing the target with rotation and coolant.

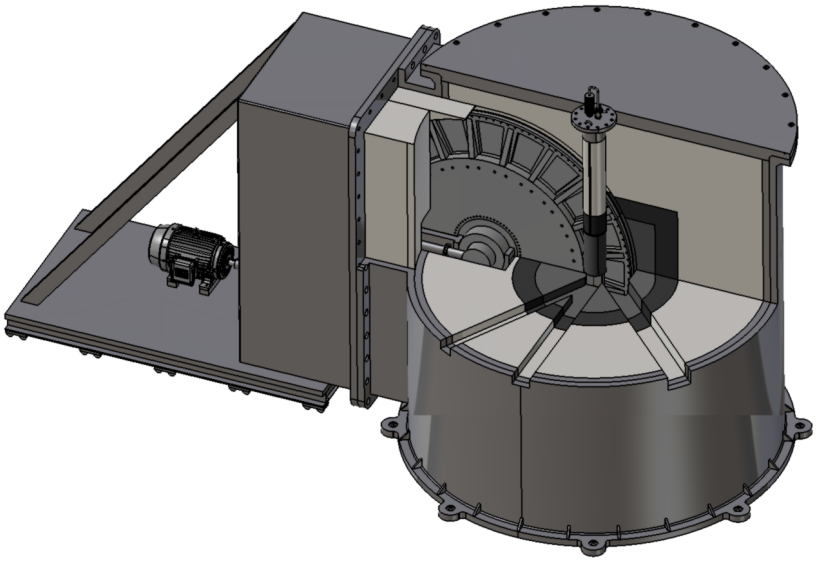

Figure 1-4: ESSB Target Vessel [4]

The TV is located in the TS, which is a large concrete structure hosting the TV, neutron and proton guides. Its purpose is to shield radiation coming from the TV and allow space for operation and maintenance of the target, moderators and reflector. An overview of the TS is shown in Figure 1-5.

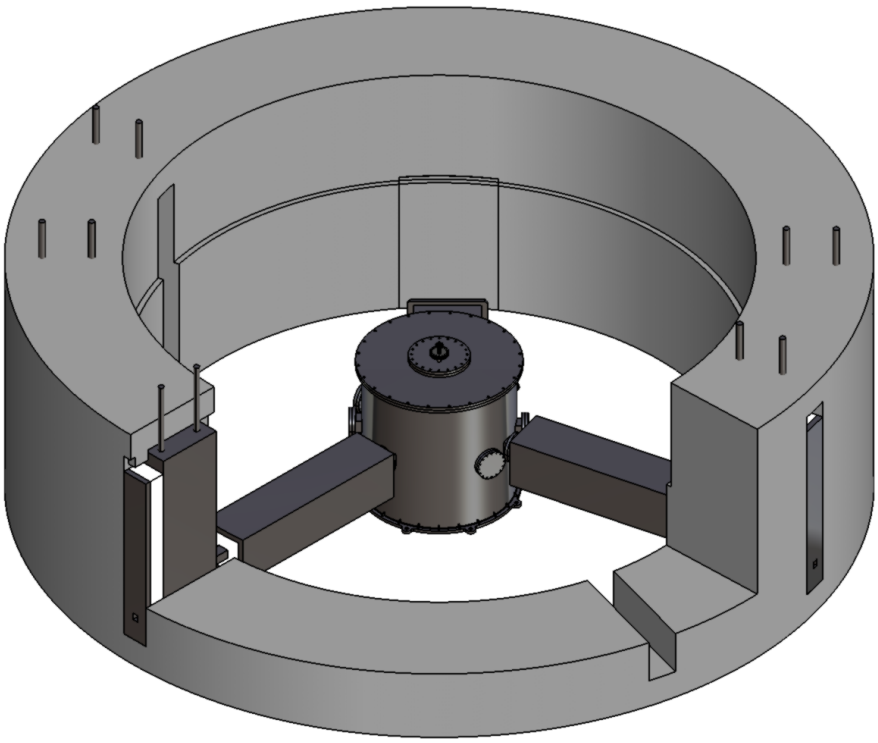

Figure 1-5: Overview of ESSB Target Station [4]

2 NEUTRONS FROM MODERATOR

This chapter will try to analyze the raw neutron pulses emerging from the moderator at the ESSB Target Station, i.e., without any adjustment required for any neutron scattering instrument, like chopping, focussing, collimation, and so on. All the neutron pulses will emerge from the nuclear interaction of the a beryllium-target with **(75 mA and 50 MeV)-proton pulses** from the accelerator, whose time lengths could vary from **0.1 ms (at 50 Hz) to 1.5 ms (at 10 Hz)** (the target cooling system could remove the deposited heat over the rotating target in safety conditions for every of these accelerator operation modes).

The neutron source model taken into account was the conceptual design of the Target Station of ESSB [5] , Figure 2-1. In that model the neutrons are produced by a **nuclear stripping reaction over the beryllium target** due to the impact of protons at 50 MeV of energy. The Be(p,n) reaction is the most efficient reaction for neutron production with protons at these energies [6] . The moderator material is methane at 22 K in order to take the advantage of the cold neutrons for neutron scattering. The beryllium target and the moderator are also rounded at the same time by a beryllium reflector. This reflector gives another moderation opportunity to the escaped neutrons in order to increase the flux, but as it will be seen later this will produce long pulse tails. Other components or configurations like premoderators, grooves or filters were also taken into account.

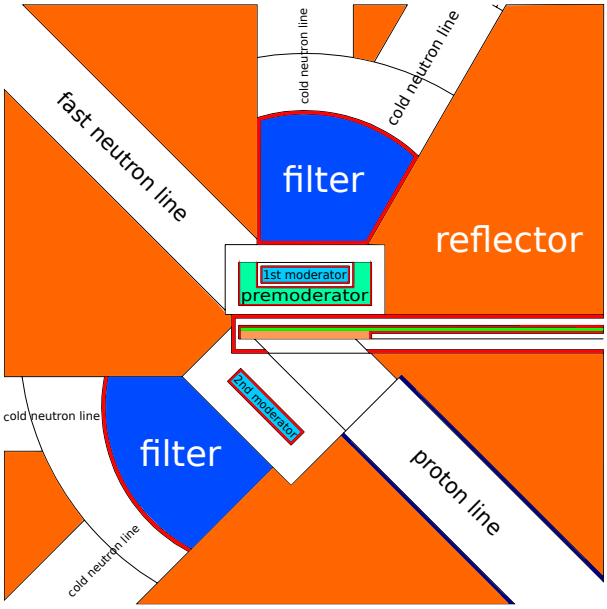

Figure 2-1: TMR assembly with the advanced moderator configuration

Neutrons emerging from a stripping reaction maintain most of the momentum and direction of the proton beam. This is the reason why the ESSB model (Figure 2-1) will have a fast neutron line and several cold neutron lines for experiments. Hence a moderator SLAB con-

figuration could be benefited by a high energy neutron reduction (background). This report will just focus into the cold neutron line that has a direct line-of-sight to the moderator face.

Two moderator system configurations will be analyzed, such as an only methane moderator (**the baseline configuration**) and another with grooved faces, a water premoderator and a beryllium filter in front of the moderator face (**the advanced proposal**) [7]-[8].

The neutron pulses were estimated with the MCNPX code while the their analysis was carried out with the BILBAO_source McStas component (APPENDIX A, pag. 57).

2.1 The time-integrated flux

This section will try to analyze the time-integrated flux, i.e., the total neutron emerging from the moderator as a function of the wavelength regardless their time of emerging. Figure 2-2 plots this time-integrated flux (**per pulse**) for several cases, such as a only methane moderator, two methane moderators and the addition of a water premoderator (Figure 2-3). All of them without filters. This Figure shows how the use of a second moderator reduces the flux at the face of the first one. The responsible of this reduction is the gap into the reflector to host the second moderator that could not reflect the neutrons to the first one. In spite of this flux reduction, a second moderator will allow to ESSB the use of more neutron beamlines. Nevertheless the cold neutron flux could be briefly increased with the use of a previous water premoderator that improves the moderation performance.

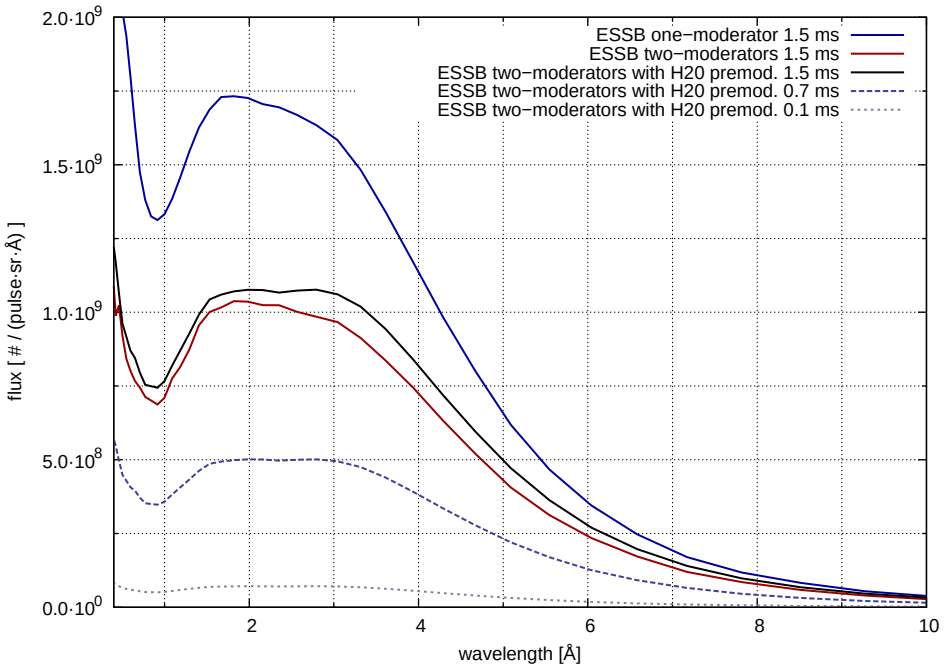

Figure 2-2: Time integrated flux per pulse for configurations without filter

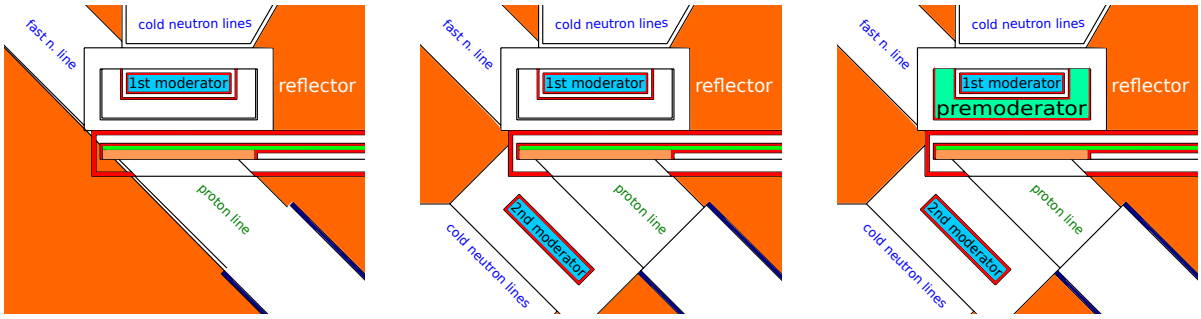

Figure 2-3: Sketchs of the moderator system with just one moderator, two moderators and with a water premoderator

Figure 2-4 plots also the time integrated flux per pulse for the baseline configuration (two methane moderators) in comparison with the advanced one [8] (with a beryllium filter and grooved faces). The effect of the beryllium filter will return some high energy neutrons to the TMR assembly and moderate some epithermal ones, hence the advanced config. can reduce the background and produce 20% more cold neutrons (above 0.35 Å) than the baseline configuration. Then a peak of flux around 1.5 Å will appear, but as it will be seen later this increase will be useful just for coarse resolution applications (where the time distribution would not be relevant). The low inelastic versus elastic cross section of the Be-filter between 2 and 4 Å will produce a valley where the flux will be also reduced to the 50% of the baseline config. Nevertheless these effect could increase the flux above 4 Å 60% higher than the baseline configuration.

In order to find out what would be the ESSB neutron performance, it would interesting to compare the ESSB moderator configurations with the ISIS-TS2 cold moderators (hydrogen and grooved faces). Figure 2-5 plots the time-integrated flux for ESSB and ISIS-TS2 (**per pulse**). This Figure shows how a single long pulse (1.5 ms) of cold neutrons (above 0.35 Å) from the ESSB baseline/advanced configuration could produce between 20 and 30% of total cold neutrons than a single ISIS-TS2 pulse. Between 1 and 2 Å ESSB advanced proposal could produce a similar time-integrated flux than ISIS-TS2. But between 2 and 4 Å the ESSB values can reach just up to the 20% of ISIS-TS2, with the baseline configuration. Nevertheless ESSB increases gradually this ratio above 4 Å, where the performance of these two facilities begin to decrease but the drop of ISIS-TS2 will be higher. So the ESSB avanced proposal could achieve its best ratio of, 50% of the ISIS-TS2 hydrogen face, above 6 Å.

It can be taken into account the ESSB accelerator operation modes, i.e. the time and length of the proton pulses that reach the target, in order to determine the time-intergrated flux **per second** (not per pulse) at the moderator face. As already discussed, ESSB could operate between the short pulse (0.1 ms at 50 Hz) and the long pulse (1.5 ms at 20 Hz). Figure 2-6 shows the time-integrated flux per second for the ESSB short and long pulses compared with ISIS-TS2 (100 ns length for the proton pulse at 10 Hz). At first glance, this Figure shows again how the long pulse could deliver more neutrons than the short one (six times more),

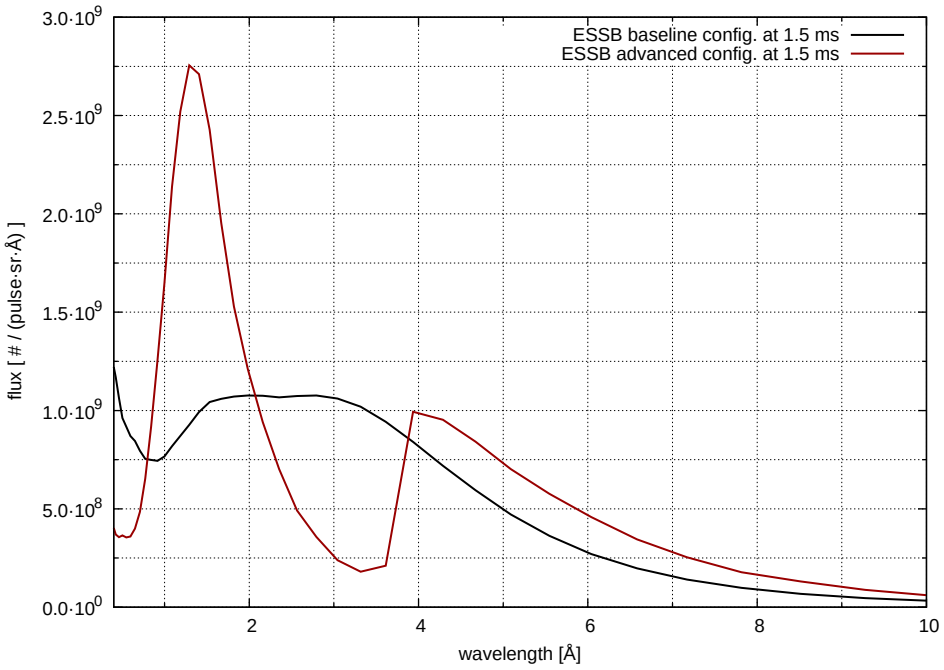

Figure 2-4: Time integrated flux per pulse for baseline and the advanced configurations

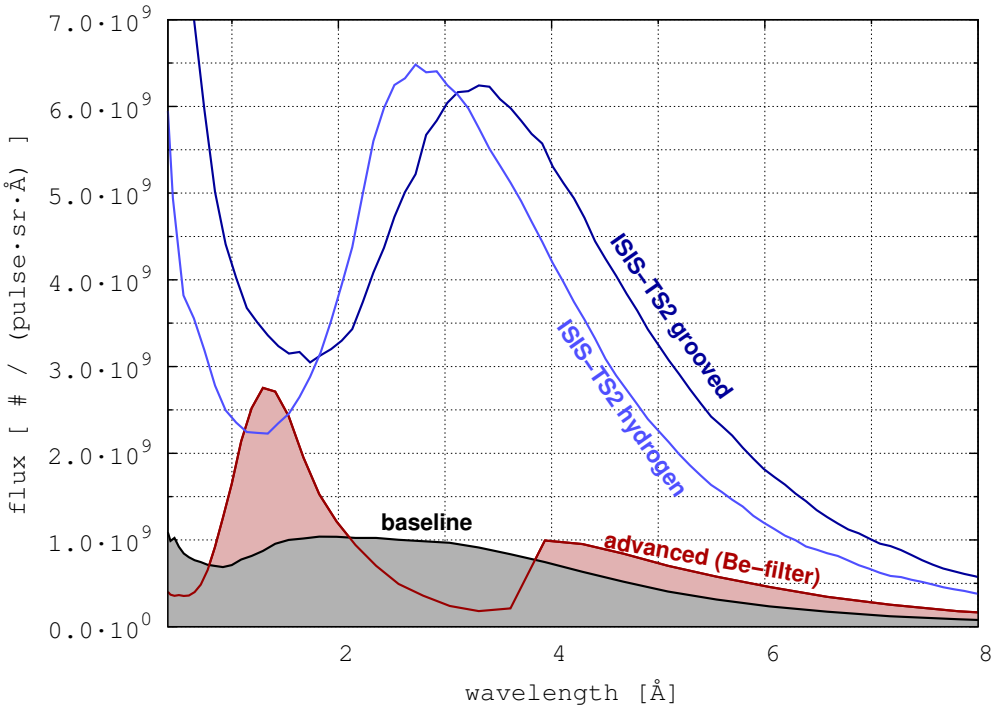

Figure 2-5: Time integrated flux per pulse for ESSB baseline config. and advanced proposal versus ISIS-TS2 hydrogen and grooved faces

although with a not optimal time distribution, as it will be seen later. An overall view also shows how, regarding ISIS-TS2 (at 10 Hz), the long pulse (at 20 Hz) could improve its ratio of time-integrated flux "per second" respect to "per pulse" in a factor of two (20 Hz / 10 Hz). But, as it will be seen later again, with a lower dynamic range available (at 20 Hz the pulses will be closer each other). Table 2-1 shows the ratios of time-integrated flux per second for several wavelength intervals, taken the long pulse over the baseline configuration as the reference value.

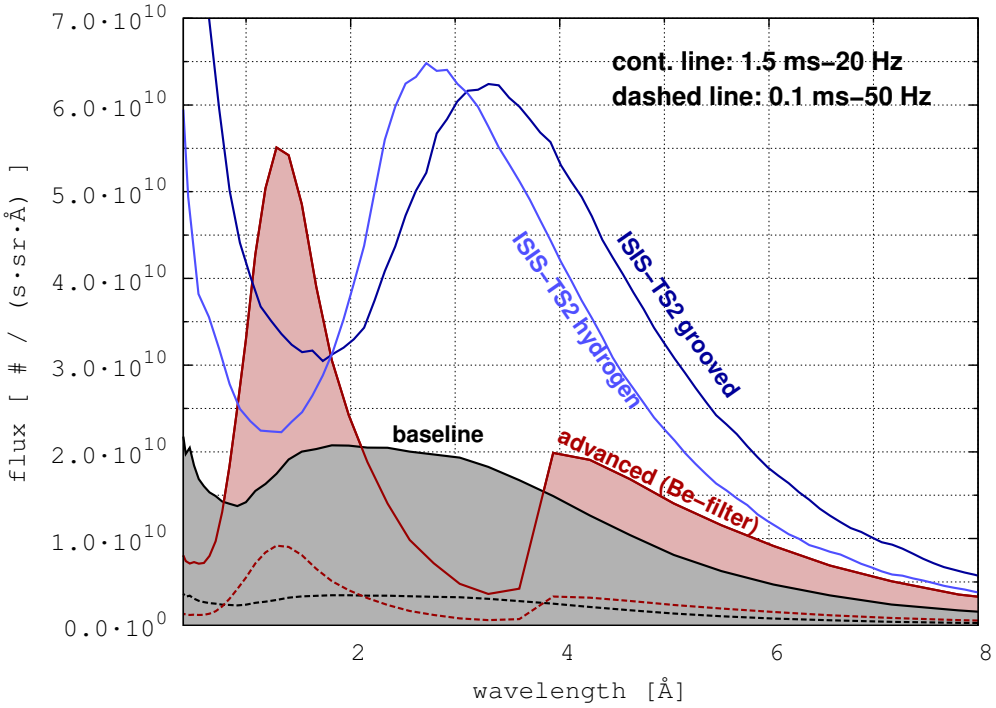

Figure 2-6: Time integrated flux per second for ESSB baseline config. and advanced proposal versus ISIS-TS2 hydrogen and grooved faces

Table 2-1: Time-integrated flux per second ESSB vs ISIS-TS2

	1-2 Å	2-3 Å	3-4 Å	4-5 Å	5-6 Å	6-7 Å	7-8 Å
ISIS-TS2 grooved @ 10 Hz	x1.69	x2.09	x3.09	x3.40	x3.48	x3.29	x3.26
ISIS-TS2 hydrogen @ 10 Hz	x1.32	x2.62	x2.78	x2.52	x2.36	x2.16	x2.15
Advanced propol. 1.5 ms 20 Hz	x2.20	x0.58	x0.40	x1.37	x1.58	x1.75	x1.83
Advanced propol. 0.1 ms 50 Hz	x0.37	x0.10	x0.07	x0.23	x0.26	x0.29	x0.30
Baseline conf. 1.5 ms 20 Hz (ref.)	**x1.0**	**x1.0**	**x1.0**	**x1.0**	**x1.0**	**x1.0**	**x1.0**
Baseline conf. 0.1 ms 50 Hz	x0.17	x0.17	x0.17	x0.17	x0.17	x0.17	x0.17

So a ESSB pulse will produce about 20-30% of total cold neutrons than a ISIS-TS2 pulse. If it is taken into account the repetition rate of these two facilities, the cold neutrons flux per second from ESSB can be similar than the ISIS-TS2 one at certain wavelengths. Nevertheless

this ratios can be achieved with the ESSB long pulse, where its neutron application will be limited to coarse resolution.

2.2 The pulse peaks

The time-integrated flux could be a right way to compare the total cold neutron production (useful for coarse resolution applications) between ESSB and ISIS-TS2, but it is interesting to compare the potential useful cold neutrons (for high resolution scattering applications), where the spectral resolution should be adjusted. So the time-integrated flux would not be the best way to compare the potential applications in these two facilities due to two main aspects, such as,

- the length of the most ESSB pulses will be too long than the ISIS-TS2 ones, and
- the ESSB pulses will have longer tails (worse ratio useful/non-useful neutrons).

A better way two compare these two facilities could be the comparison of the pulse peaks, becuase they could be isolated from the pulse shape (the length and the tail). How to isolate the pulse peak will be addressed in Section 3.6, pag. 37 . Figure 2-7 plots the pulse peaks values for ESSB and ISIS-TS2 (logarithmic scale). It can be seen that ISIS-TS2 can provide around two order of magnitude higher peaks than ESSB, because ESSB pulses will be too outspread along the time and will have long tails. The maximum peak difference can be observed at 1 Å, where any moderator response will be too fast, hence the ISIS pulses will be very concentrated while ESSB pulses will be too outspread (dominated by the accelerator proton pulse). On the other hand, between 2 Å and 4 Å, it can be seen how the baseline configuration can provide higher peaks than the advanced proposal, so this configuration would be better for high resolution applications.

It could be taken into account the repetition rate of the pulses, and compare the peak-ratios per second (not per pulse). The histogram plotted by Figure 2-8 compares the peak-ratios per second taking the long pulse baseline config. as the reference value. It shows how the ESSB pulse peaks will be again far away from the ISIS-TS2 ones at wavelengths below 1 Å, for the same reason as commented on the previous paragraph. But this ratio tends to improve at higher wavelengths (the ISIS pulses tend to spread out), e.g. at 8 Å the peak of the long avanced proposal pulse will be six times lower (ratios per second) than the peak of ISIS-TS2 hydrogen face pulse at this wavelength.

On the other hand, the long pulses (1.5 ms) at 20 Hz could provide higher peaks than the short pulses (0.1 ms) at 50 Hz (the level of pulse saturation in long pulses wins over the higher repetition rate of short pulses). Another point of favour of the long pulse, as it will be seen later, would be its low repetition rate that could allow higher dynamic ranges (Section 3.4, pag. 33).

The pulse peak comparison should be complemented with the analyzis of the amount of useful neutrons that ESSB could provide at a certain specified time-width by the user (time-width shown by Figure 2-9. This time-width is connected to the spectral resolution, as it will

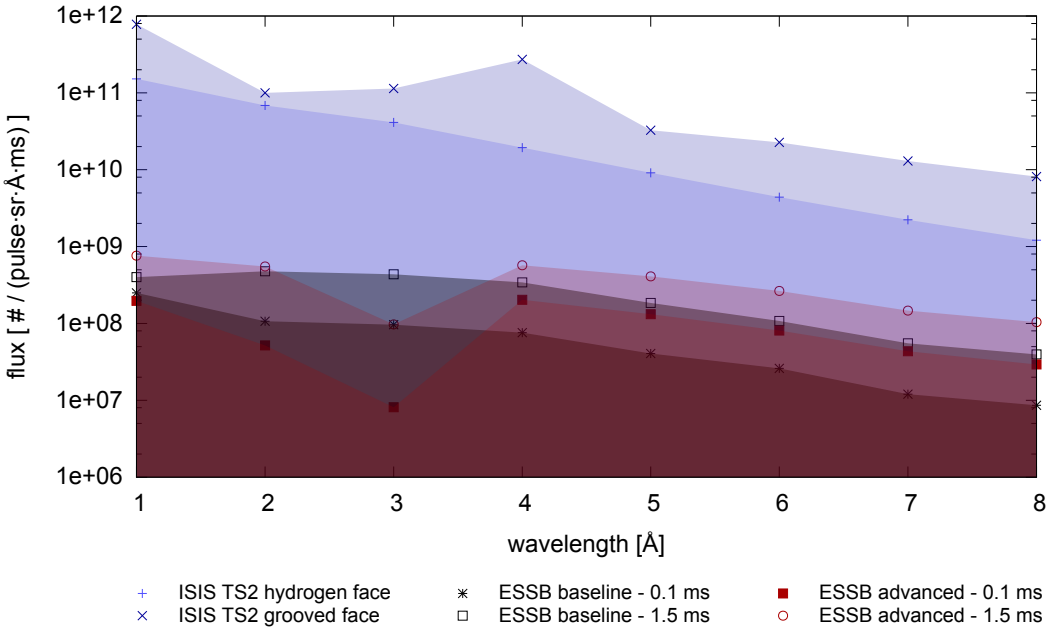

Figure 2-7: Pulse peak comparison for ESSB baseline config. and advanced proposal versus ISIS-TS2 hydrogen and grooved faces

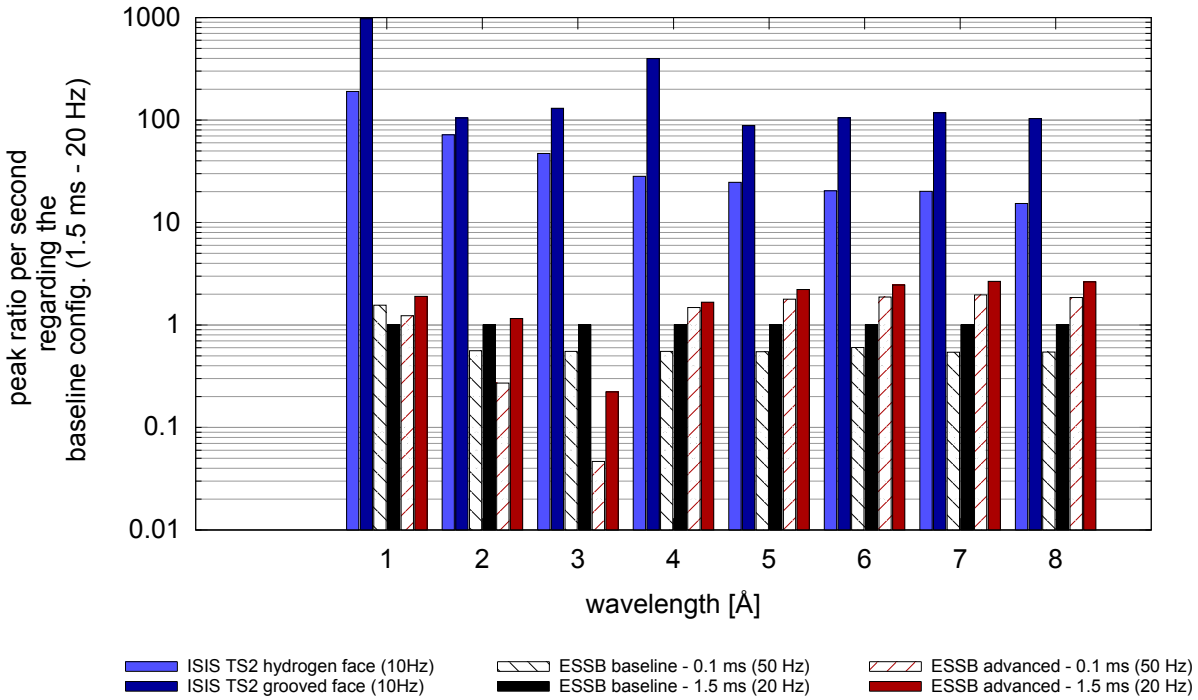

Figure 2-8: Pulse peak ratio per second comparison for ESSB baseline config. and advanced proposal versus ISIS-TS2 hydrogen and grooved faces. Long pulse baseline config. as reference

be shown in Section 3.3, pag. 31 . Figure 2-10 plots the amount of neutrons contained in 0.6, 0.2, and 0.08 ms, all of them before the peak time of the long pulse (when the amount of neutrons is maximum). This figure would show a truly useful information for the final user. It must be taken into account that these values cannot not be obtained from the same pulse because it would be needed a perfect chopper placed just at the face of the moderator, and this would no be technically possible.

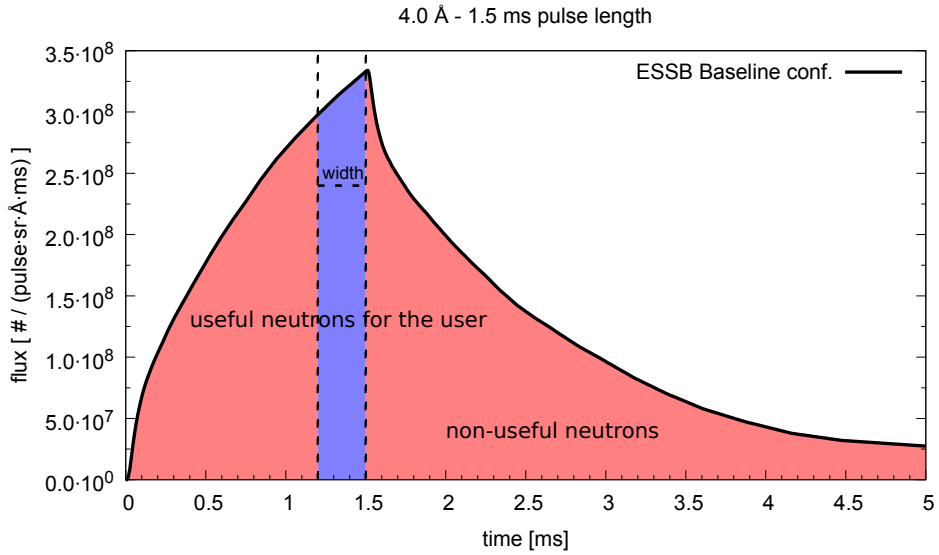

Figure 2-9: Example of the time width that determines the useful neutrons for the user

Hence the potential use of ESSB for high resolution neutron applications will be on the order of 100 times less than ISIS-TS2 for lower wavelengths. Nevertheless it will be improved above 4-5 Å up to 7 times less.

2.3 The response of the moderator system

The response of the moderator (in fact it is the response of all the components together, such as the target, reflector, premoderadors, filters and so on) is important to be analyzed for two main reasons, such as,

- it is the guilty of the pulse tails (in most of the cases non-useful neutrons). As it will be seen later ESSB produces long tails due to a coupling between the moderator and the reflector,
- it is one of the responsibles (together with the length of the proton pulse) of the shape of the neutron pulses, specifically for the short pulse case (not for the long pulse on, where the contribution of the proton pulse to the shape would be dominant).

If the length of the proton pulse is much shorter than the length of the moderator response then the neutron pulse will be dominated by the moderator response (the ISIS-TS2 case, i.e,

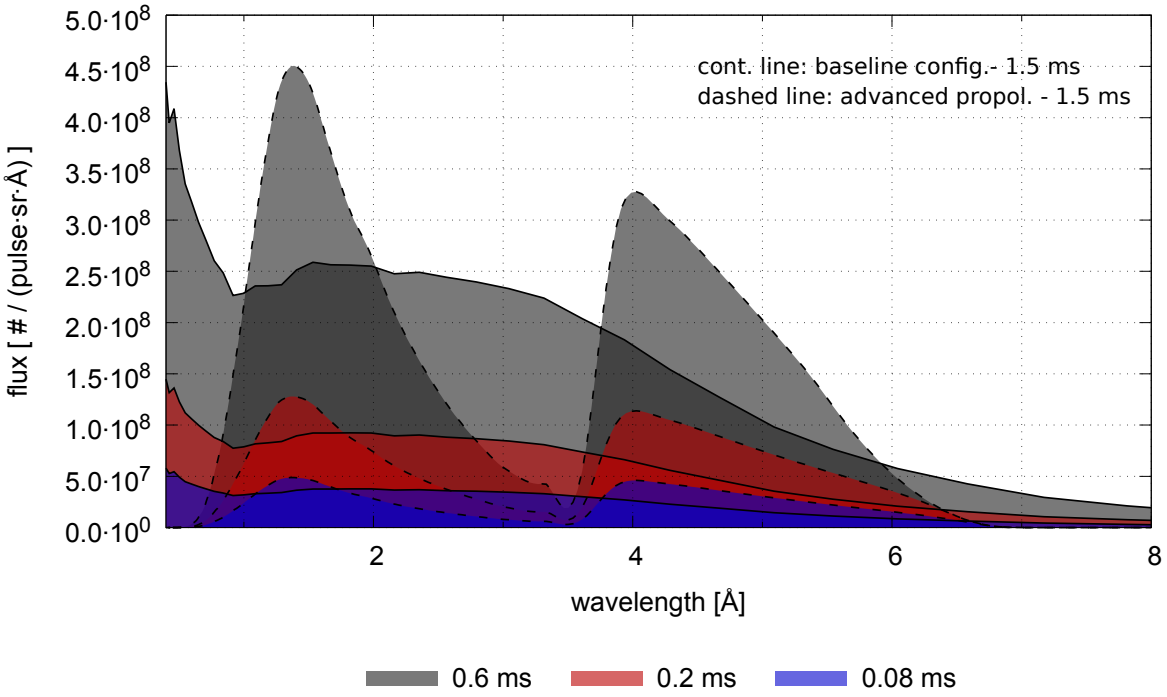

Figure 2-10: Flux of useful neutrons contained by various time widths as a funcion of wavelength

a compressor ring deliver two 100 ns proton pulses which are shorter than the moderator response for cold neutrons). Otherwise, if the proton pulse is much longer, the neutron pulse will be dominated by the proton pulse (the ESSB long pulse case, i.e., the accelerator could deliver protons during 1.5 ms). Exceptional attention is required by the ESSB short pulse case, where the length of the moderator response and the proton pulse are similar.

Figure 2-11, and Figures B.1-1 to B.1-8 from the APPENDIX B, pag. 63 , show the intrisic moderator response of the baseline configuration, the advanced proposal and the ISIS-TS2 hydrogen and grooved faces at wavelengths from 1 to 8 Å. They show how the length of the baseline response will be similar to the ISIS-TS2 ones (the temperatures of the moderators are similar), nevertheless it will be different for the avanced proposal from 2 to 3 Å, where the effect of the filter will expand too much its response over time, producing very long tails and very long signals.

These Figures also show a briefly displacement of the advanced proposal response because it is taking neutrons emerging from the filter face for that case. Hence there was be a small TOF inside the filter.

It can also be observed that the neutron production per proton at ESSB will be around 250 time less than the ISIS-TS2 one. This is due to the higher performance on neutron production of a spallation reaction at 800 MeV (≈16 n/p) over a stripping reaction at 50 MeV (≈1/15 n/p). Nevertheless ESSB will try to improve its total neutron production increasing its proton average current from the accelerator (2.25 mA for ESSB and 0.2 mA for ISIS).

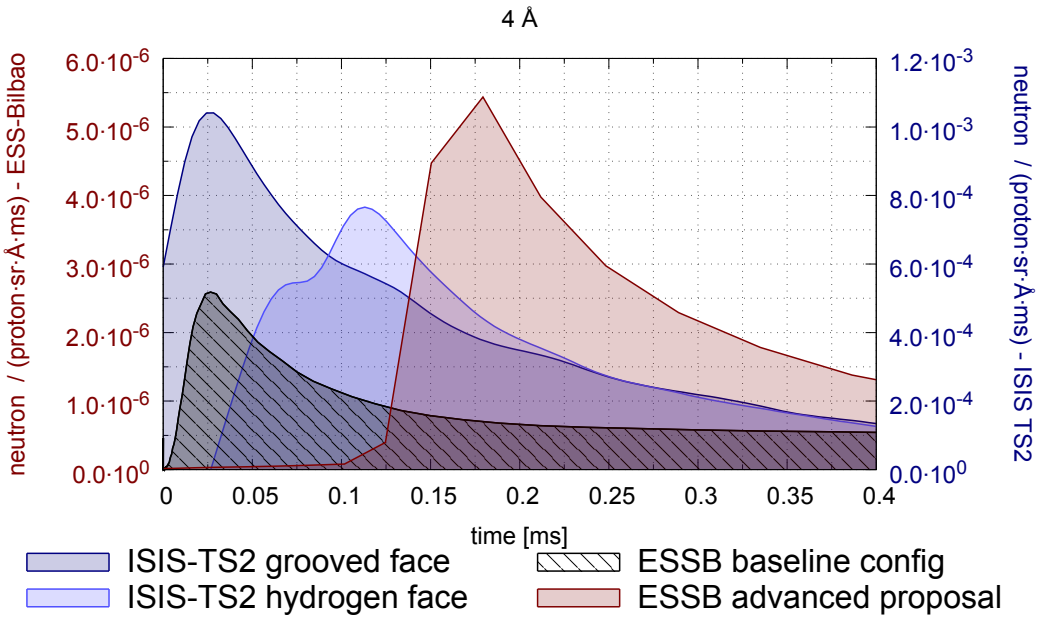

Figure 2-11: Intrinsic moderator response ESSB vs ISIS-TS2 at 4 Å

The ESSB moderator system responses will produce long tails due to a coupling effect between the moderator and the reflector. Nevertheless the width of the baseline reponse will be similar than the ISIS-TS2 one (both moderator temperatures will be around the same value). But the advanced response will be too longer at certain wavelengths due to the beryllium filter effect.

2.4 The neutron pulses

Plotting the shape of the neutron pulses over time would be important in order to visualise the effect of the proton pulse and the moderator response together. The neutron pulses emerge from the convolution for the signals from the proton pulse and the moderator response system to just one proton, as shown by Figure 2-12.

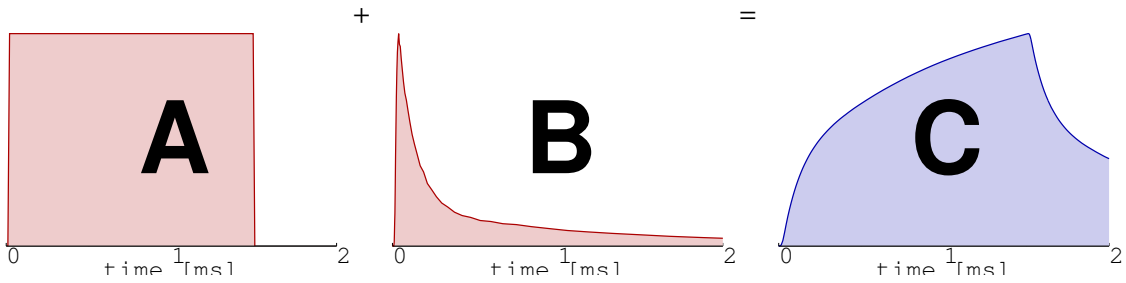

Figure 2-12: Example of convolution bettwen the long pulse of protons (1.5 ms) with the ESSB baseline config. moderator response system

Figures 2-13, and Figures C.1-1 to C.1-8 in APPENDIX C, pag. 68 , compare the neutron pulses of the ESSB **short pulse** operation mode (baseline config. and advanced proposal) versus ISIS-TS2 ones. At 1, 2 and 3 Å the length of the ESSB pulses will be longer than the ISIS-TS2 ones because at these wavelengths the moderator response, which dominates de ISIS pulses, will be shorter than the ESSB proton short pulse (0.1 ms) (Figure 2-11). Up to 3-4 Å the neutron pulses of ESSB short pulse will be dominated by the proton pulse, while above 4 Å these pulses would be dominated by the proton pulse and the response together. This is, in spite of the coupling moderator-reflector, one of the reasons of producing higher tails than ISIS-TS2 (governed always for the moderator response only). These figures also show the same brief displacement on time of the advanced proposal as was commented in Section 2.3, pag. 15 , about the intrinsic moderator response.

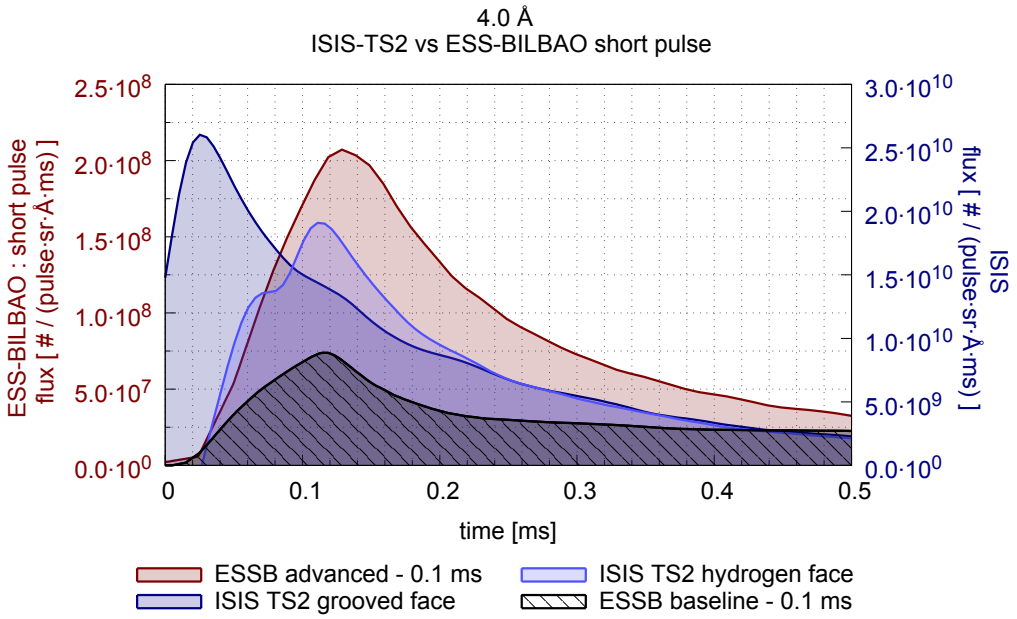

Figure 2-13: Neutron pulse for the ESSB short pulse cases vs ISIS-TS2 at 4 Å

Figures 2-14, and Figures C.2-1 to C.2-8, plot the ESSB **long pulse** cases, where the ESSB neutrons pulses are clearly dominated by the proton pulse. Hence no direct comparison with ISIS-TS2 cabe be performed.

Figure 2-15, and Figures C.1-9 to C.2-10, let the comparison of all the wavelengths together for every ESSB configuration in order to have a general view of their magnitudes. Also these Figures show the importance of the tails in the advanced proposal around 1 Å.

Another issue about these Figures is that there is non-greater neutron producction of the advanced proposal for short pulse case around 1 Å, than the short pulse baseline configuration. This could be due to the plain advanced moderator response at this wavelength that would not allow the pulse to be satured enough.

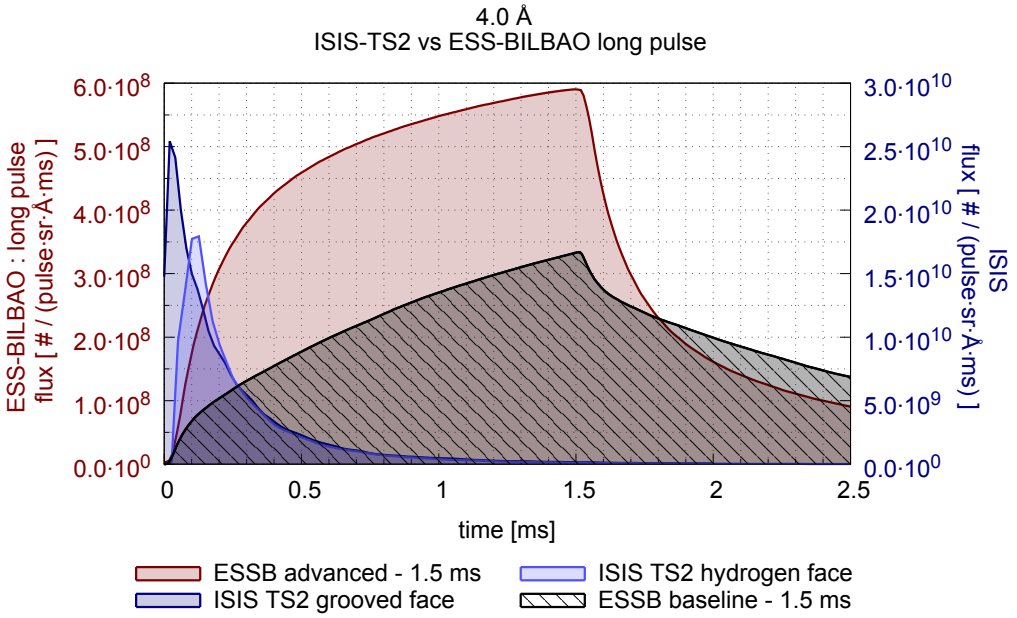

Figure 2-14: Neutron pulse for the ESSB long pulse cases vs ISIS-TS2 at 4 Å

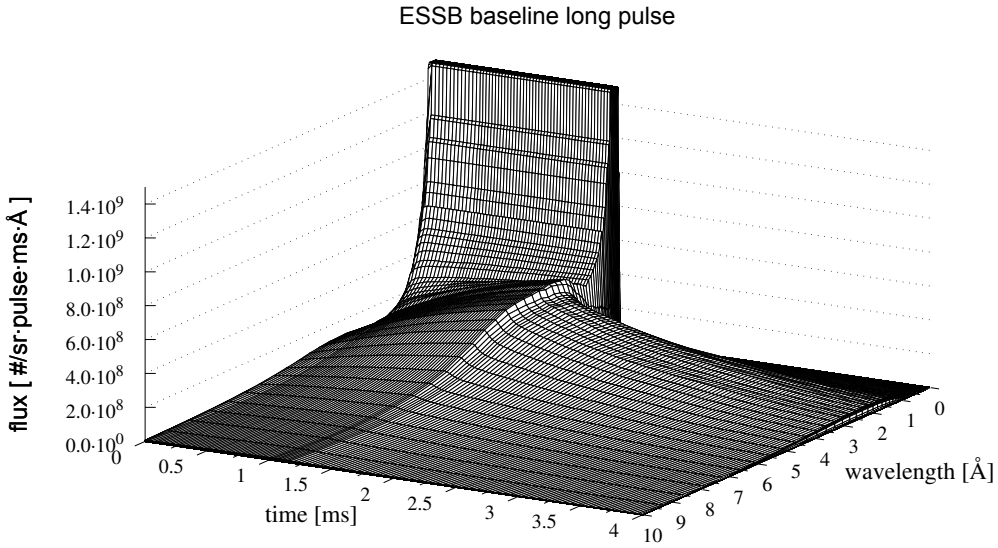

Figure 2-15: Neutron pulses of the ESSB long baseline configuration

So the ESSB long pulses will be dominated by the accelerator proton pulse, while for the ESSB short pulses the effect of the accelerator and the moderator response will dominate together.

2.5 Central moment analysis

A general analysis of the pulse shapes (for every wavelength) could be interesting in order to figure out how these shapes can influence the potential neutron information, which will be useful for the user. As it will be seen on Chapter 3, pag. 25 , this useful information can be generally characterized by the spectral resolution, the dynamic range and the amount of useful neutrons. All of them depend on the width, the slope and the ratio signal/tail of the pulse, i.e. the pulse shape in general.

A tool that could be useful to characterize the pulse shapes would be the high-order central moment analysis of the pulse time distributions. The expression of the n-order central moment (M_n) is given by equation (1). This expression consider the nth-root of the moments in order to can plot the same unit for all of them. These moments were refered to the peak times (μ), instead of the means (M_1), in order to get the relationship between the signal and the tail, or neutrons beyond the peak-time

$$M_n = \left(\int_0^\infty (t-\mu)^n \cdot f(t) dx \right)^{1/n} \tag{1}$$

where,

M_n, *is the moment of n-order, in milliseconds.*
t, *is time of every point of the pulse, in milliseconds.*
μ, *is the time of the peak of the pulse, in milliseconds.*
$f(t)$, *is the probability density function for every point of the pulse.*

Up to 4-order moments have been considered, such us,

- the 0th-order (**prob. distrib.**), it is the time-integrated flux, that it was analyzed on Section 2.1, pag. 9 ,
- the 1st-order (**the mean**), it indicates the amount of neutrons in the pulse signal relative to the tail (non-useful neutrons),
- the 2nd-order (**deviation**), it is an indirect measure of the pulse width which is connected to the spectral resolution,
- the 3rd-order (**skewness**), it measures the pulse asymmetry. If positive, then tail will be longer than the signal, and
- the 4th-order (**kurtosis**), it indicates the pulse shape itself. If positive, then the values will be around the mean.

Figure 2-16 shows the high order central moments for the baseline config. and the advanced proposal. This figure also shows the peak-time for every wavelength.

In the relation to **peak-times**, for the baseline short pulse case, **a)**, it can be perceived a brief increase of the peak time above 0.1 ms (the length of the proton short pulse) with wavelength. This is due to the similar width of the moderator response and the proton pulse for the short pulse operation mode. This effect is not considerable for the long pulse case, **b)**, because its

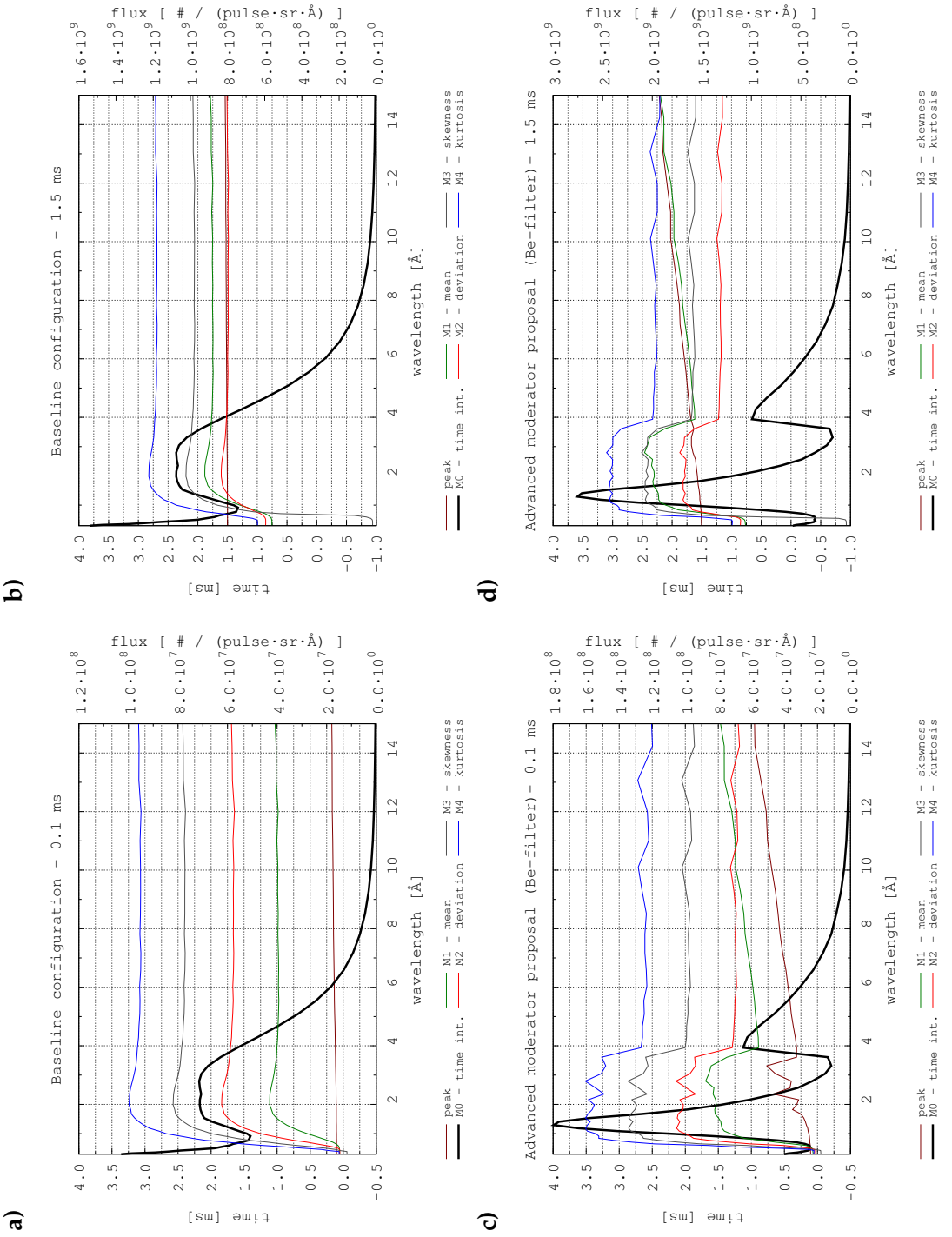

Figure 2-16: High order central moments for the baseline config. and the advanced proposal (short and long pulses)

peaks happen when the pulse is close to saturation (too much inertia to maintain when the proton pulse finishs). This effect also happens for the advanced proposal adding a small TOF

indise the beryllium fiter (as was commented in Section 2.3, pag. 15 , neutrons from the filter face were considered for the advanced proposal instead of of the moderator face).

Regarding to the **mean**, it tends to the half proton pulse width at lower wavelengths indicating that most of the neutrons will be in the signal, because the moderator response is too fast (the neutron pulses will follow the proton pulse very well at these wavelengths). But it increases with wavelength (the moderation process becomes more and more slowly) up to 1 ms for the short pulse and 1.5 ms for the long one. This indicates that there will be more neutrons on the tail than in the signal for the short pulse because the inertia of the moderator response wins over the proton pulse. While for the long pulse case the amount of neutrons in the signal and in the tail tends to be similar. Neverthess, the mean functions have maximums at certain wavelengths, around 2 Å (baseline) and 1-3.5 Å (advanced), where the ratio signal/tail will be the lowest. This indicates the worst efficient wavelength ranges, as can be checked by Figure 2-17, becuase the temperature of the moderator is around the same value (the moderation process is maximum) producing high tails.

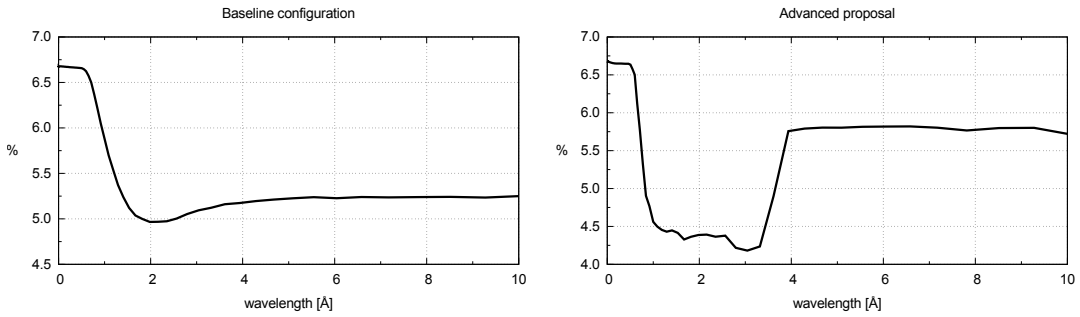

Figure 2-17: Ratio of neutrons in 0.1 ms around the pulse peak relative to the total neutrons in the pulse

Up to 1-1.5 Å the **deviation** grows quickly from the half of the proton pulse width to a constant value around 1.5 ms for every operation mode. This indicates the relative importance of the tail, specifically for the short pulse operation mode, because the deviation of its pulses will go far beyond the proton pulse width (0.1 ms). The avadvanced proposal, **c)** and **d)**, shows a plateau where the width of the pulses will be too wide due to the already commented effect of the beryllium filter. This plateau is a problem for resolution applications at the wavelengths those it happens.

At very low wavelengths, the **skewness** is negative indicating a pulse signal longer than its tail. But this situation quickly turns because ESSB will produce big tails due to the moderator-reflector coupling.

The **kurtosis** begins from a low value, hence the time distrubution is spread out around the peak (the neutron pulse will follow the square proton pulse shape). But it also rises with wavelength, so there will be a high data concentration around the peak and also a high frequency of data far away. Hence the pulse peaks will be high (useful to cut them with a fast chopper) and the pulse tails will be longer (too much non-useful neutrons).

A central momentum analysis can be carried out in order to determine to the main aspects of the pulse shape. The shapes of the baseline pulses will follow the natural evolution that corresponds to a moderator at a certain cold temperature, i.e., very short and squared pulse at low wavelengths, and longer and sharper at higher ones. Special attention requieres the short pulse due to the similar widths of the moderator response and the proton pulse (0.1 ms). While the shapes of the advanced proposal pulses will have some peculiarities due to the distorsion of the beryllium filter.

2.6 Alternative to central moment analysis

On the other hand, the tail of the neutron pulse ($\{f(x)\},, \forall x > \mu$) can be fitted by an expression like $f(x > \mu) = t^{-\alpha}$. In those cases where $\alpha < n$, the expression (1) (central moment) will be divergent and it could not be represented the moments of orders higher than α. At this point there would be another parameters that could characterize the neutron pulse shape like the central moments, such as,

- the full width half maximum (FWHM),
- the average (estimator of deviation) and the ratio (estimator of skewness) of the half width half maximum to the right of the peak (HWHM-r) and to the left (HWHM-l),
- and the ratio between the integrals of the pulse to the right and to the left of the pulse (estimator of kurtosis).

Figure 2-18 plots this parameters for the baseline config. and the advanced proposal for the long pulse case.

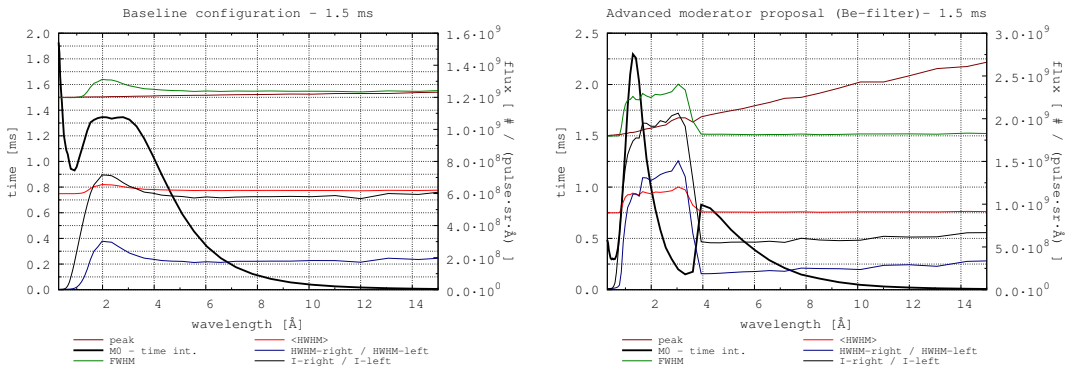

Figure 2-18: Another pulse shape estimators, such us FWHM and HWHM, for the ESSB long pulse (baseline config. and advanced proposal)

2.7 Conclusions

- The **ESSB accelerator** could deliver proton pulse widths from the short pulse-0.1 ms (at 50 Hz) to the long pulse-1.5 ms (at 20 Hz). The long pulse could provide six times more total neutrons per second than the short one.

- The **ESSB long pulse** could deliver between 20 and 30% of total cold neutrons per pulse than large facilities like ISIS-TS2, but with an awful time distribution, limiting its applications to coarse resolution applications.
- The **ESSB short pulse** could produce a similar time distribution than ISIS-TS2 (their moderator response shapes would be similar), but it would be limited to the 5% of ISIS-TS2 cold neutron flux per pulse.
- The **ESSB pulse tails**, i.e. the neutrons emerging after the pulse peak (non-useful neutrons), would be too much longer due to coupling effect between the moderator and the beryllium reflector.
- Due to the pulse saturation on the long pulse, this pulse case could hold more potential **useful neutrons** than the short one that could be obtained with a time selector component, like a fast chopper.
- Depending on the resolution required by the useful neutrons, the **advanced proposal** could provide more neutrons than the baseline config. at certain wavelengths.

3 NEUTRONS FOR SCATTERING TECHNIQUES

On Previous chapter pulses from moderator were analyzed without taking any consideration on how optimized them for neutron scattering instruments. Present chapter will try to show the main pulse parameters requiered by a neutron scattering experiment and how adapt them to optimze the instument performance.

Neutron scattering experiments require as much neutrons as possible at sample in order to compensate

- the weak neutron-matter interaction, compared with other particles, such as electrons or X-rays, nevertheless neutrons collect unique properties that make them extraordinary particles, and
- the low intensity of the available neutron beams.

"The combination of a weak interaction and low fluxes make neutron scattering a signal-limited technique, which is practiced only because it provides information on the structure and dynamic of materials that cannot be obtained by other means." [9].

So one of the goals of every moderator configuration will be maximize the flux at a certain energy range. The previous chapter dealt with the neutron pulses emerging from the moderator baseline config. and advanced proposal, where it was tried to maximize as much as possible the cold neutron flux.

Neutrons of very different energies emerge from the moderator at the same time. And the scattering researcher needs to find out which neutron energy will hit the sample, or which neutron energy will emerge from the sample, at a certain time. But the current detectors (those with good position resolution) cannot distinguish the energy of these neutrons. So the solution will be to move away the sample and take the advantage of the TOF over the detector timing. Thanks to the linar relationship between the neutron wavelength and its TOF, the detector timing can be associated to the wavelength counting.

But neutrons of the same wavelength also emerge from the moderator at different times (due to system response to a proton pulse and due to the repetition rate of theses pulses), hence the TOF never can avoid a small wavelength range contamination (pulses overlapping).

Then it can be deduced that not all the neutrons emerging from the moderator will be signal neutrons, some of them will be noise, so the present chapter will try to characterize, and adjust as much as possible, these neutrons in order to maxime the amount of useful neutrons that reach the sample for certain applications.

A way to measure the mentioned wavelength contamination will be spectral resolution, while those wavelengths where the contamination level will be aceptable for the experiment will determine the dynamic range.

3.1 The background

In spite of the overlapping between the useful wavelength pulses (thermal and cold neutrons), there will be also some high energy neutron pulses that will not be valid for these kind of experiments and will contaminate the signals. These high energy neutrons constitute the background.

On the other hand, the background can cause radiation damage in the detectors and in the samples themselves, and also it can cause noise contamination over the following pulses. So it should be avoided. It will be considered every neutron at wavelengths below 0.35 Å as background.

As it has been already commented, neutrons emerging from the Be(p,n)-stripping reaction will maintain most of the original proton beam momentum, so even the moderator SLAB configuration can be benefited with a reduction on high energy neutrons in those lines which will have a direct line-of-sight to the moderator face.

Figure 3-1 shows the cumulative distribution function of the neutron energy sprectra of the baseline configuration and the advanced proposal [7]-[8] (description on Section 2, pag. 8). It can be appreciated how around 85% of the baseline neutrons will be background. But it shows also that the beryllium filter, on the advanced proposal, could reduce a great fraction of the background until a value of 32%. Nevertheless this figure shows also the same plots for ISIS-TS2 background whose background neutrons are about 50% of the total production.

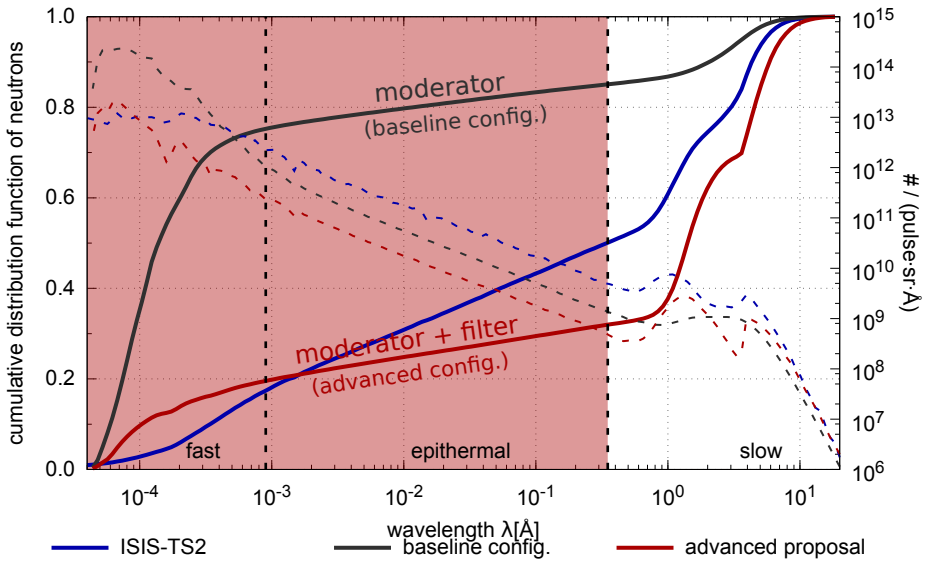

Figure 3-1: Cumulative distribution function of the neutron spectrum (baseline and advanced) vs ISIS-TS2

The ESSB background baseline configuration delivers higher background ratio than ISIS-TS2. Nevertheless this ratio can be improved below the ISIS-TS2 one with the beryllium filter of

the advanced proposal which has a highest cold neutron performance (60% of the neutrons above 1Å).

3.2 The To-chopper

In order to avoid the radiation damage and the noise contamination by high energy particles, the background should be avoided. So, it would be necesary to prevent the direct line-of-sight to the moderator face from the sample. Hence the neutron guides should be bent and high energy neutrons can not be transported. Cold neutrons will be transported properly to the sample, but some thermal neutrons can not do that very efficiently by this solution. It will depend on the required spectrum by the user.

Nevertheless, in order to transport thermal neutrons or to block the background perfectly a To-chopper can be needed. Although this concept could be retained for cold neutron scattering instruments it can be interesting to briefly analyze the concept of a To-chopper.

The To-chopper consists of a robust rotating disk (Figure 3-2) which blocks neutrons hitting its blades while lets neutrons pass through its slits. Its mission will be to block the background, so the depth of its blades shoud be of the order of tens of centimeters (a briefly estimation was carried out on APPENDIX D, pag. 81).

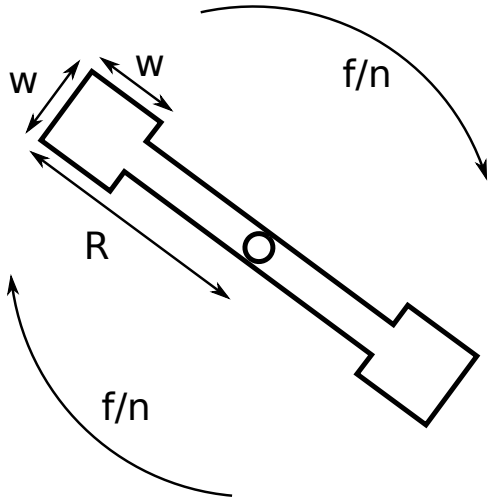

Figure 3-2: A conceptual sketch of a To-chopper with two blades

At this point, it will be assumed that its materials are perfectly efficient, so all neutrons hitting the chopper blades will be stopped. Hence, for the To-chopper conceptual design only its aperture/radius ratio, its rotating frequency and its distance from the moderator will be taken into account.

A To-chopper never will be perfect because it always blocks a small fraction of the useful wavelengths when it is trying to block the background. It happens in pulsed neutron sources, when the fastest and premature neutrons of the useful wavelengths (those coming from the head of the pulse) will reach the To-chopper at the same time than the slowest and late ones

of the background (those coming from the tail of the pulse). So at this time the blades should be in the beam position, in order to block the background, but also they will block a fraction of some useful neutrons, as shown by Figure 3-3. But it does not mean that all the neutrons of a particular wavelength will be blocked because in fact most of them will get to pass throgh the To-chopper.

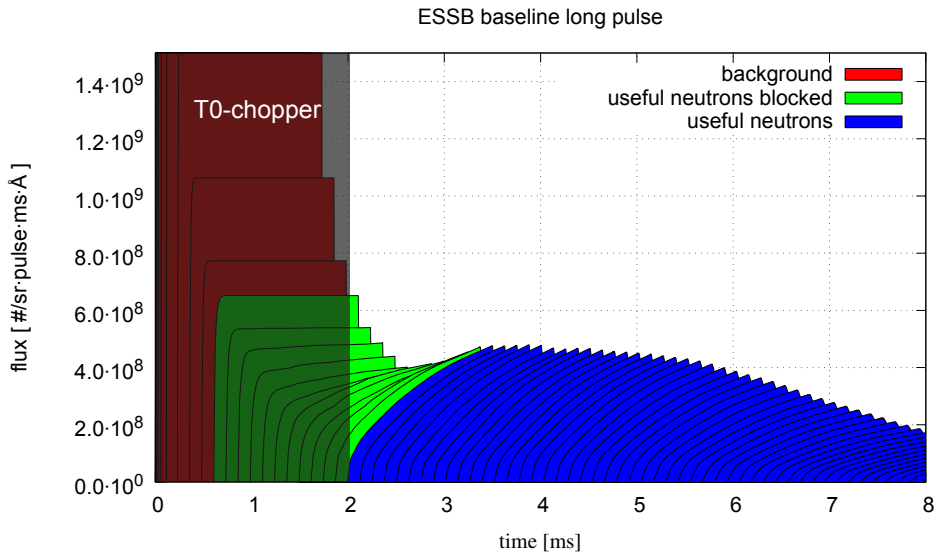

Figure 3-3: TOF of the ESSB baselines long pulses and the time window of a To-chopper at 5 m. Background less than 0.35 Å and useful neutrons blocked by the To-chopper from 0.35 to 1.5 Å

Another point of view for this To-chopper weakness can be the following. If it is wanted to use the full useful neutrons range for the experiment it is needed to let a small fraction of the background to pass also through the To-chopper.

The expression (2) represents the fracction of useful wavelengths that will be partially blocked by the To-chopper, i.e., all wavelengths between λ_b (the lowest neutron energy in the background) and λ_u (the lowest neutron energy in the useful wavelengths which will be blocked). It shows how the range of the blocked wavelenghts will decrase as the distance L increases (L will be the distance of the To-chopper from the moderator). So it will be better to place far away the To-chopper seemingly. But there will be another effect that is not being taken into account, i.e., a far To-chopper can also block some slow neutrons from previous pulses. It will be considered the 18 Å as a possible highest wavelength of interest for experiments (just like a reference value), so the To-chopper should allow to pass this wavelength (and therefore all wavelengths below this value) from the previous pulses. The highest To-chopper rotating frequency, 50 Hz (short pulse), will block the beam every 20 ms, so this time should be the maximum elapsed time of these previous 18 Å-neutrons to arrive the To-chopper before the beam is blocked. During this time (20 ms), these slow neutrons will go throught 4.4 m, that should be the maximum distance to place the To-chopper. Placing away the To-chopper from 4.4 m will block wavelengths below 18 Å.

$$\lambda_u - \lambda_b = \frac{3.96 \cdot \Delta t[ms]}{L[m]} \quad , \quad \forall \lambda_b \leq \lambda_u \tag{2}$$

where,

λ_u, *is the maximum wavelength of useful wavelengths blocked, in angstroms.*
λ_b, *is the maximum wavelength of the background, in angstroms.*
Δt, *is time-length of the background pulses, in milliseconds.*
L, *is the distance between the source and the To-chopper, in meters.*

The previous chapter showed that the high enegy pulses (background) will follow the proton pulse shape properly (a squared shape, i.e. their tails will not be considerable). Hence there will not be a background tail to block, so the Δt of the expression (2) ought to be the length of the proton pulse.

Then the To-chopper should be placed at 4.4 m from the moderator, however in order to guarantee an easy maintenance for this component, it should be place outside of the Target Area (at least 5 m from the moderator) as shown by Figure 3-4. So the To-chopper at 5 m will let pass throught it up to 15.8 Å for the long pulse (50 Hz) and 39.6 Å for the short one (20 Hz).

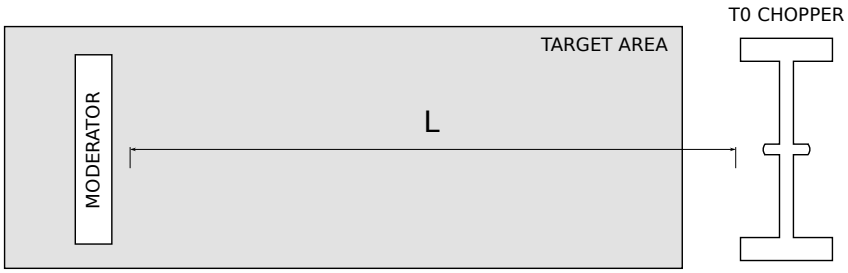

Figure 3-4: A conceptual sketch of a To-chopper place outside the Target Area

Table 3-1 summarizes all of these condiderations for three To-chopper distances, such us, 1.5, 5 and 10 m, also for the short and long pulses. The distance of the To-chopper from the moderator will be selected depending on the requirements of every particular instrument. Neverthess it will be recommended to place it outside the Target Area, so the following section estimations will be for a To-chopper at 5 m.

The To-chopper should block the beam during the proton pulse length (from 0.1 to 1.5 ms) plus the TOF of the slowest background neutrons ($\lambda_b \cdot L/3.96 + FWHM$). And its close position (blocking the beam) must be syncrhonized with the repetition rate of the neutron source. Then these operating parameters will establish the geometry constraints, like it can be observed by the expression (3).

The To-chopper can hold n-blades, that will allow it to rotate at lower frequencies and best mechanical equilibrium. But a higher number of blades will requiered a higher radius for the To-chopper. Nevertheless, the table 3-2 tries to show the To-chopper radius for n=1,2 and for the long-short pulses. It has been supposed a To-chopper at 5 m from the moderator (outside the Target Area) that should block wavelenghts up to 0.35 Å over a section of the same area as

Table 3-1: Range of useful neutrons emerging from a To-chopper at different distances and accelerator operations modes

Case	Distance	Freq.	FWHM	$\Delta\lambda_{useful_B}$	$\Delta\lambda_{useful}$	Maintenance
A	1.50 m	20 Hz	1.5 ms	0.35-4.31 Å	4.31-131.3 Å	hard
B	1.50 m	50 Hz	0.1 ms	0.35-0.61 Å	0.61-52.80 Å	hard
C	5.00 m	20 Hz	1.5 ms	0.35-1.54 Å	1.54-39.60 Å	easy
D	5.00 m	50 Hz	0.1 ms	0.35-0.43 Å	0.43-15.84 Å	easy
E	10.0 m	20 Hz	1.5 ms	0.35-0.94 Å	0.94-19.80 Å	easy
F	10.0 m	50 Hz	0.1 ms	0.35-0.39 Å	0.39-7.920 Å	easy

$$\frac{w}{2\pi R/n} = \left(\frac{\lambda_b}{3.96} \cdot L + \text{FWHM}\right) \cdot \frac{f}{10^3} \tag{3}$$

where,

w, is the width of the guide section at the To-chopper position. Assumed equal to that of the moderator face. In centimeters.
R, is the radius of the To-chopper, in centimeters.
n, is the number of To-chopper blades.
λ_b, is the maximum wavelength of the background that it is wished to block, in .angstroms.
L, is the distance of the To-chopper from the moderator system, in meters.
FWHM, is the width of the neutron pulse. It is supposed the same as the proton pulse width for the background neutrons. In milliseconds.
f, is the frequency of the neutron source, in hertzs.

the moderator face (12x12 cm), nevertheless this window section must be reconsidered after a neutron transport analysis to the sample. So, regardless of mechanical equilibrium issues the one-blade To-chopper can be the best option in order to minimize its radius (C1: 49.17 cm).

Table 3-2: Operation and geometrical parameters for the To-chopper

Case	L	f_{source}	$f_{T0-chopper}$	FWHM	w	n	λ_b	R
C1	5.0 m	20 Hz	20 Hz	1.5 ms	12 cm	1	0.35 Å	49.17 cm
D1	5.0 m	50 Hz	50 Hz	0.1 ms	12 cm	1	0.35 Å	70.48 cm
C2	5.0 m	20 Hz	10 Hz	1.5 ms	12 cm	2	0.35 Å	98.35 cm
D2	5.0 m	50 Hz	25 Hz	0.1 ms	12 cm	2	0.35 Å	140.97 cm

Once the To-chopper will be selected, its rotating speed can be changed in order to follow the neutron source frequency, but its geometrical parameters (w, R, L, n) will be fix. So the same To-chopper will block different background wavelengths as function of the source repetition rate. The expression (4) shows the relationship between the maximum wavelengths that can be avoided from different source frequencies. For example, the C1 case, i.e., a radius of 49.17 cm and just one blade, the To-chopper can block up to 0.35 Å from the long pulse but it will block up to 0.54 Å for the short pulse rotating at 50 Hz.

$$\lambda_{b-2} = \lambda_{b-1} \cdot \frac{f_1}{f_2} + \left(\text{FWHM}_1 \cdot \frac{f_1}{f_2} - \text{FWHM}_2 \right) \cdot \frac{3.96}{L} \tag{4}$$

Hence, in spite of a To-chopper will not be the best option to block the background for cold (not thermal) neutron scattering instrument (a bent neutron guide can be better), a brief review of its concept was made. It showed that the selecction of the geometry parameters of the To-chopper will depend on the desired wavelengths to block and the required quality for this blocking. For example, a premilinary proposal would be to place the 49.17 cm-radius To-chopper at 5 m to block above 0.35 Å.

3.3 Spectral resolution of the beam

As has been already mentioned, the Achilles heel of the neutrons scattering techiques is the neutron detection. The currently detectors cannot distinguish the neutron energy, but the user will need to know it.

Previously it was shown how neutrons of different energies emerge from the moderator at the same time. Then this neutrons need different times to go over the same distance. This will be the way to guess the neutron wavelength, i.e. the time-of-flight (TOF) of the neutron. But the distance to place the detector should be enough in order to the neutrons will be sufficiently separated and the detector timing can differenciate them properly.

Another aspect to be considered should be the length of the neutron pulse. So the longer pulses, the worst the detection will be at the same distance. This is showed by Figure 3-5 where the short pulses will be better separated than the long pulses at the same distance. So the longer pulses will require further distance to reach the same signal quality than the shorter ones.

The TOF use to be measured indirectly by the wavelength rather than the energy in order to take the advantage of their linear relationship. A way to measure whether the distance to place the detector and the pulse length will be enough for a particular instrument will be the espectral resolution. It measures the ratio of the wavelength range that reach the detector at the same time, so a perfect detector (a detector that can meassure an infinitesimal time) can not distinguish the wavelengths inside of this range.

The expression (5) represents the espectral resolution. It can be improved with shorter pulses, as shown by Figure 3-5, or moving away the detector, but it will increase the instrument cost (more neutron guides) and the neutron leaks.

Figures 3-6-a) and 3-6-b) show the spectral resolution at several distances, all of them will fulfill the ESSB building constraints, for the long and the short pulses. It can be percived that long pulse can reach just up to low resolution, so its applications will be limited to coarse and low resolution instruments, such as SANS, reflectometry, imaging, transmission or spin-echo

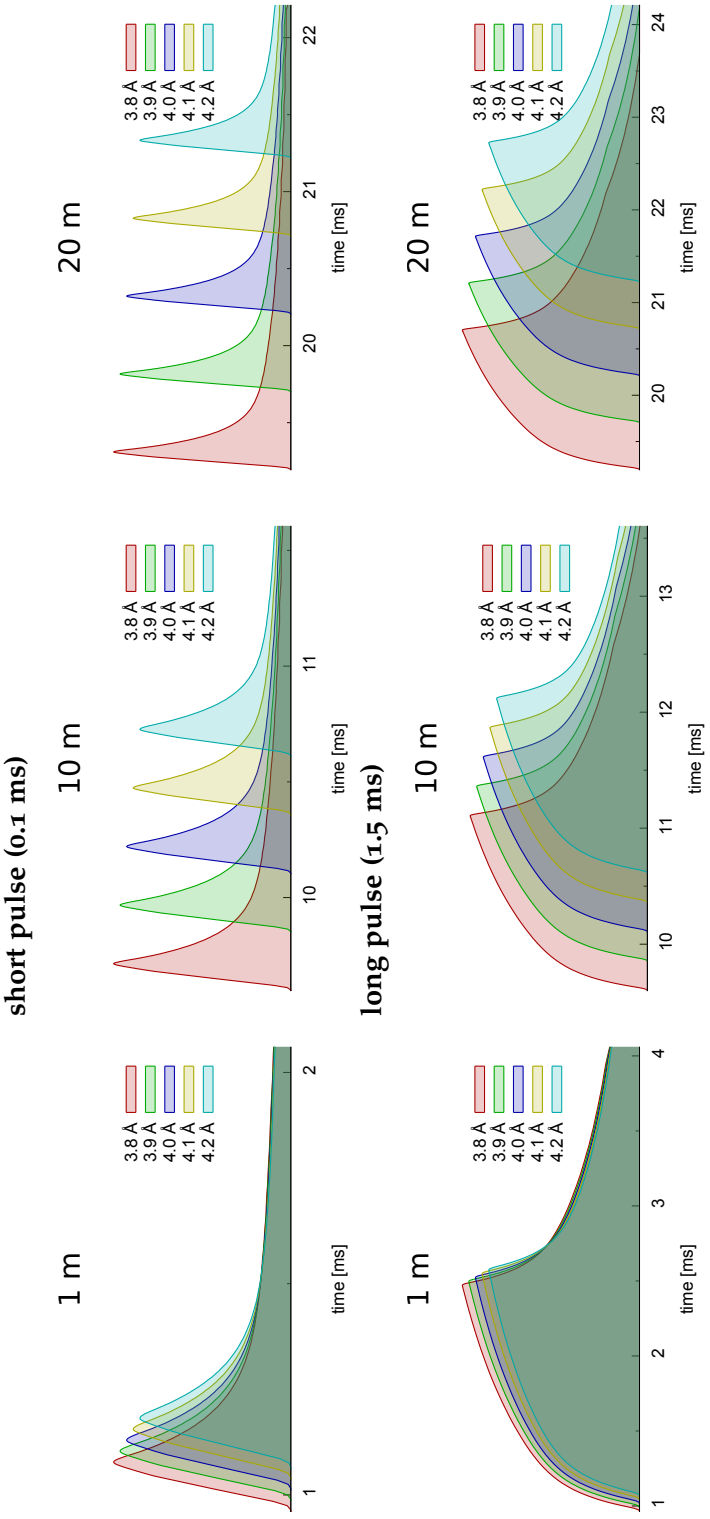

Figure 3-5: Time-of-flight of the short and long pulses at serveral distances

$$R(\lambda) = \frac{3.96}{\lambda[\text{Å}]} \cdot \frac{\Delta t[ms]}{L[m]} \tag{5}$$

where,

R, is the spectral resolution, dimensionless.
λ, is the wavelength for which the resolution is being determined, in angstroms.
Δt, is the neutron pulse width at wavelength λ, in milliseconds.
L, is the distance from the moderator, where resolution is being determined, in meters.

techniques. Nevertheless, the short pulse operation mode can reach up to medium resolution where diffraction and spectroscopy can be used.

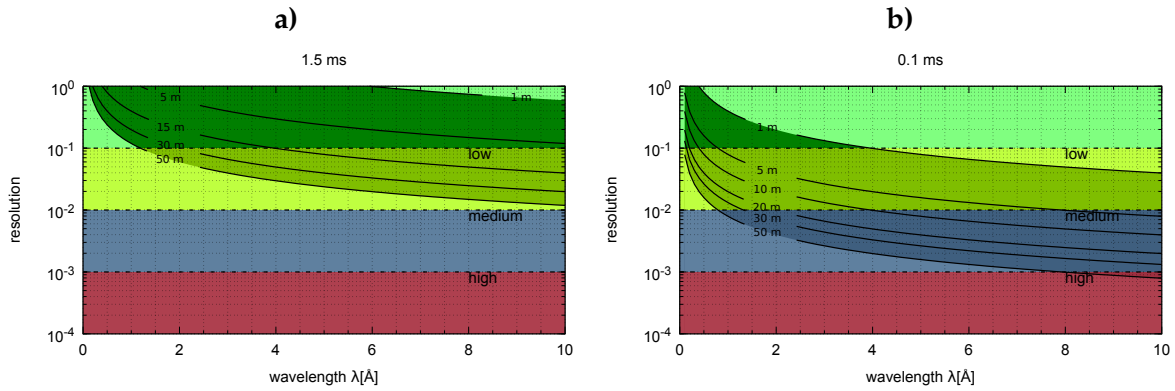

Figure 3-6: Spectral resolution of the long/short pulse as function of the wavelength for several distances

So the short pulse operation mode can provide better spectral resolution at every distance of the instrument.

3.4 Dynamic range of the beam

The dynamic range is those wavelength range that has not been contaminated with neutrons from the next pulse at a particular distance. It happens when high speed neutrons from the next pulse can reach the slowest ones of the current pulse before they arrive to the detector. So the signal will be contaminated. Last section showed that moving away the detector the measured resolution can be improved, but in neutron pulsed sources the dynamic range also will be decreased.

The expression (6) represents the dynamic range as function of the repetition rate, the distance and the pulse length.

$$\Delta\lambda[\text{Å}] = \left(\frac{10^3}{f[Hz]} - \Delta t[ms]\right) \cdot \frac{3.96}{L[m]} \tag{6}$$

Then the main parameters that have influence over the dynamic range are the distance (the longer distance, the lower wavelength will be reached by high speed neutrons) and the repetition rate of the pulses (the higher repetition rate, the lower distance the slowest neutrons can move before the high speed neutrons emerged from moderator catch them). Figure 3-7 shows the time-space diagram of neutrons for the short pulse (50 Hz). For example, 18 Å-neutrons will be reached by 0.35 Å-neutrons from the next pulse at 4.46 m. Figure 3-8 shows how the lower repetition rate of the long pulse (20 Hz) will be better for the dynamic range because this capture will happen at 10.88 m.

On the other hand, Figure 3-9 shows the time-space diagram for three different kind of instruments at ISIS-TS2, i.e. a neutron diffractometer (WISH), a spectrometer (LET) and a small angle instrument (SANS2D). It shows that the higher required dynimic range, the lower distance the detector can be placed.

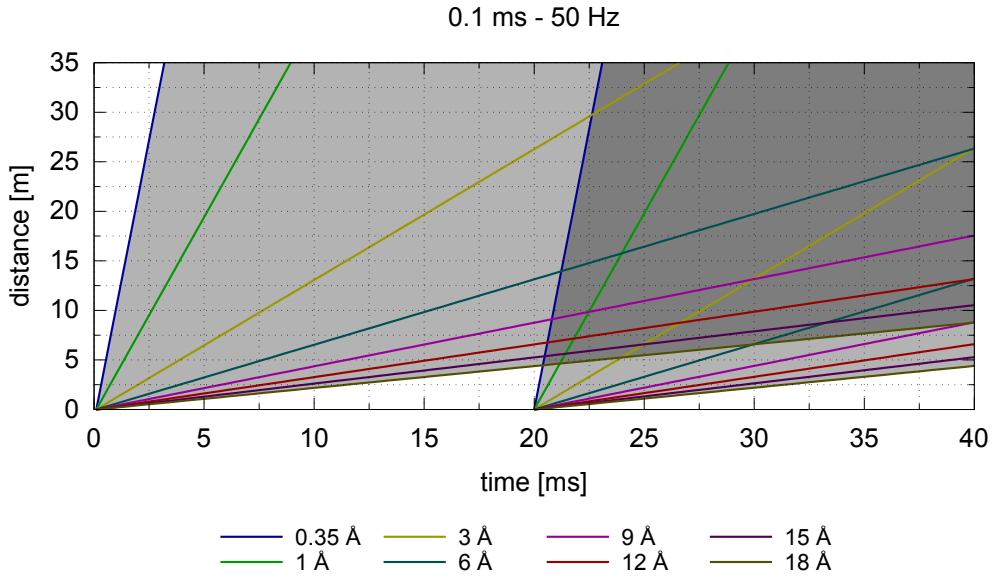

Figure 3-7: Time-space diagram of serveral wavelengths for the short pulse

Hence, it is necessary to identify which is the dynamic range useful for a particular experiment in order to improve the resolution as much as possible moving away the detector.

Figure 3-10 shows the evolution of dynamic range with distance. If it is supposed that To-chopper will allow the 0.35-18 Å-neutron range to pass through, these wavelegths will be mixed from 4.46 m. Belong this distance the dynamic range will decrease as showed by the red line (ratio of the dynamic range related to the initial range from the To-chopper). Once the useful dynamic range for the experiment will be selected, the longest distance that allows this range should be selected. Figure 3-11 shows the same analysis for the long pulse operation mode, where for a similar dynamic range than the short pulse, the detector can be placed farther.

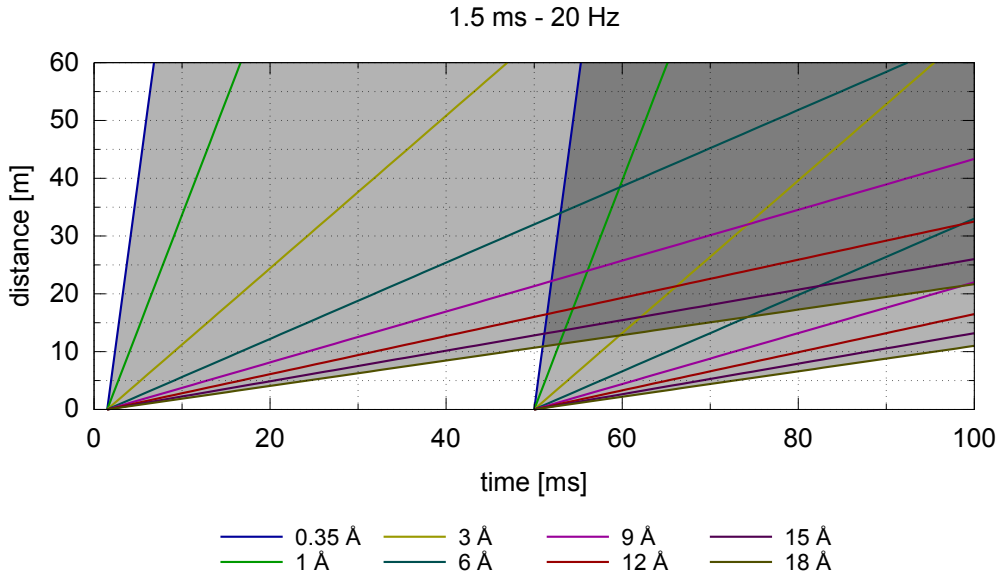

Figure 3-8: Time-space diagram of serveral wavelengths for the long pulse

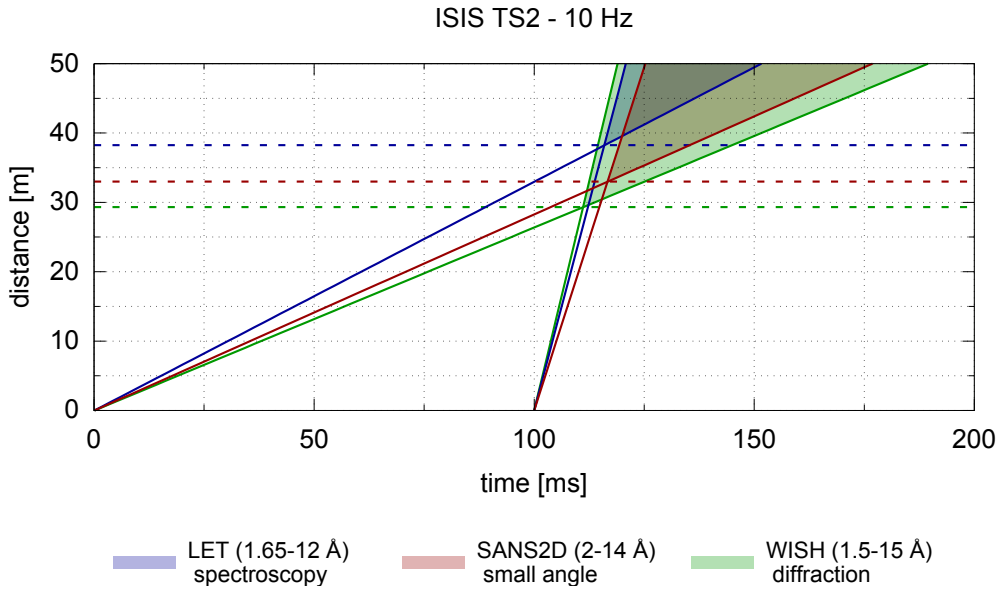

Figure 3-9: Time-space diagram for some instruments of ISIS-TS2

So the the long pulse can provide a higher dynamic range than the short one for the same distance.

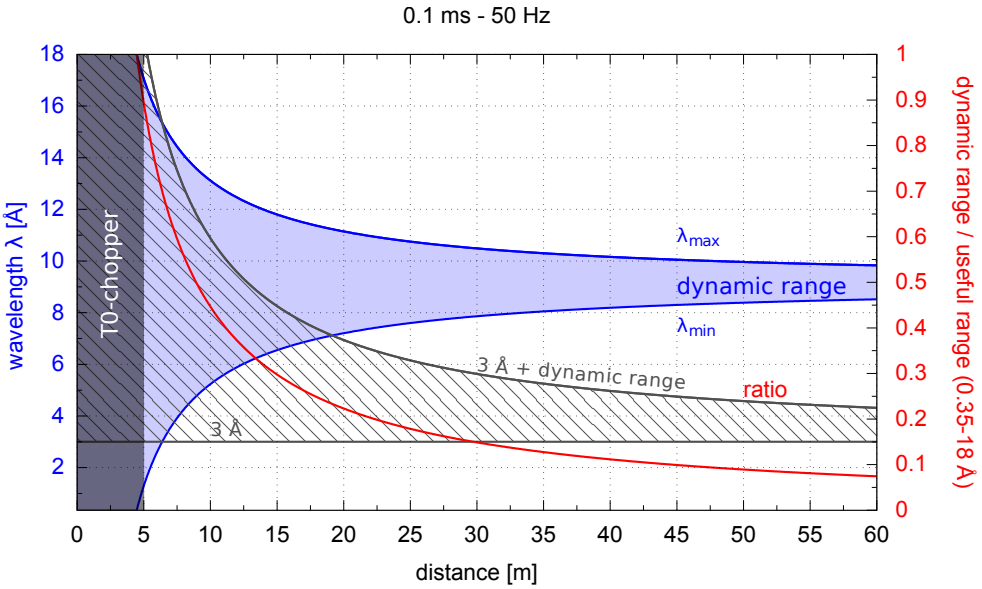

Figure 3-10: Evolution of the dynamic range for the short pulse

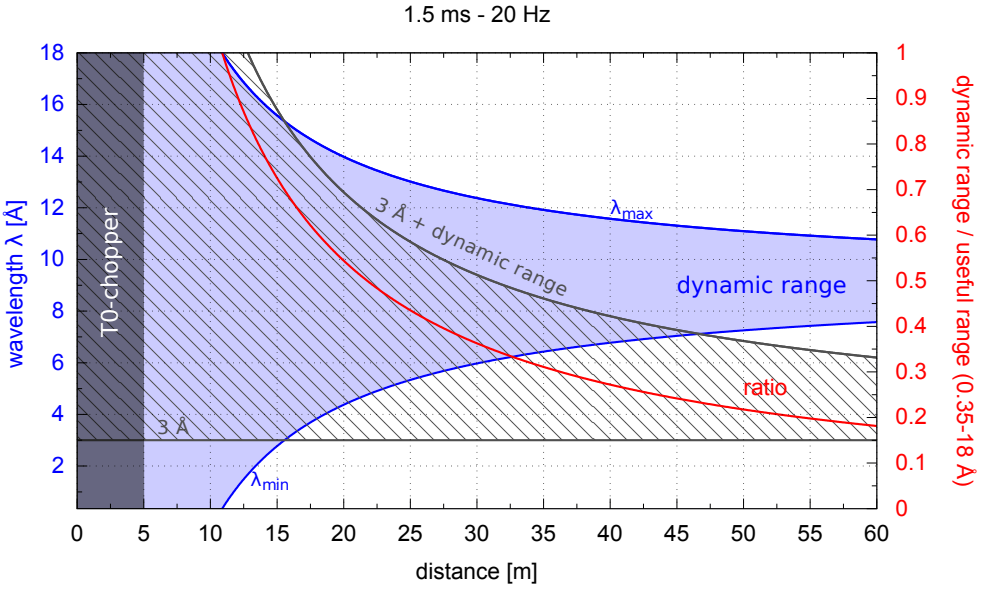

Figure 3-11: Evolution of the dynamic range for the long pulse

3.5 Resolution and dynamic range comparison

At the same distance, the short pulse can provide better spectral resolution than the long pulse. But also for the same distance, the dynamic range of the short pulse will be lower due to its higher repetition rate. So it will be intereseting to compare these two operation modes taken into account the resolution and the dynamic range together.

Figures 3-12 and 3-13 showthe resolution as function of the wavelength and the dynamic range. The secondary y-axis represents the maximum distance that will allow to pass a specific dynamic range, i.e. the better resolution that can be achieved for this range. These Figures show that for every particular dynamic range the short pulse can provide better resolution even at lower distances.

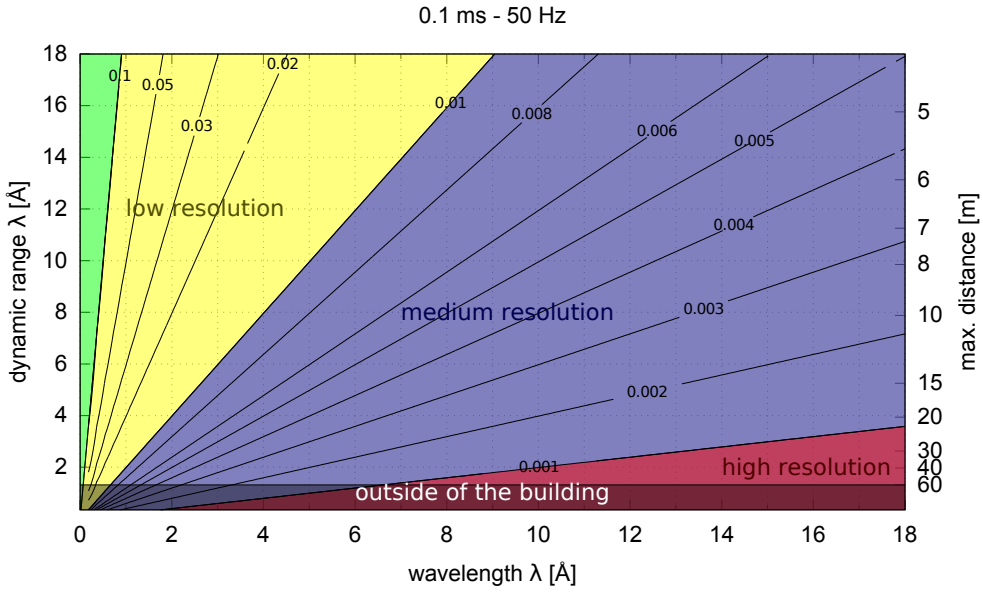

Figure 3-12: Spectral resolution as function of the wavelength and the dynamic range for the short pulse

Hence, if it is not considered coarse or low resolution applications, where the long pulse can provide higher amount of neutrons per second, the short pulse will be better from the point of view of resolution for any particular dynamic range. Also the short pulse will requiere lower distances that could be translanted in a lower cost on neutron guides and lower neutron leaks.

3.6 The fast chopper

Previous sections showed that the short pulse can provide neutron signals with better quality than the long pulse operation mode. But it is also noticed that the long pulse can provide around double of neutrons per second around its pulse peaks (for the baseline configuration).

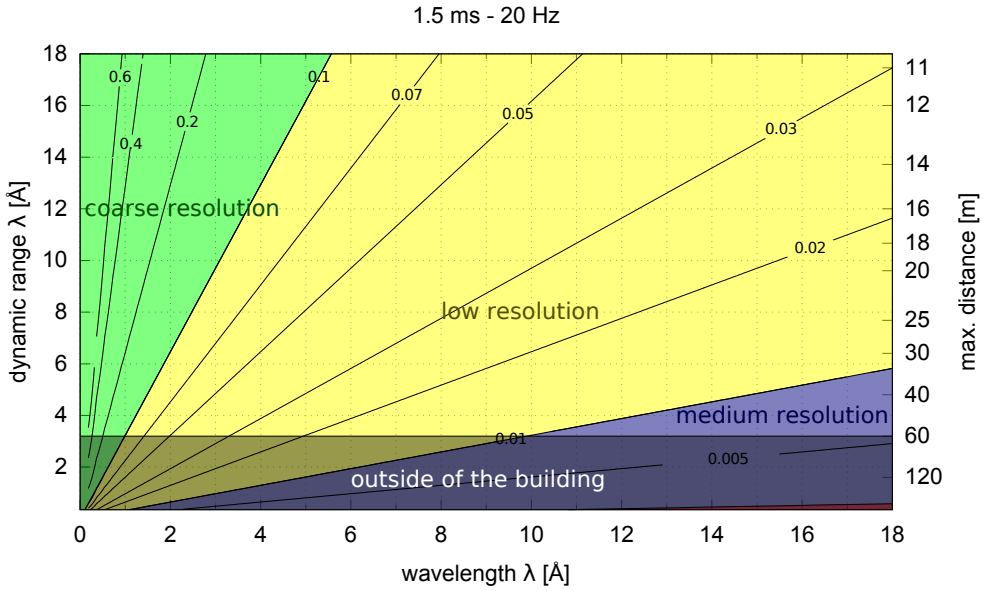

Figure 3-13: Spectral resolution as function of the wavelength and the dynamic range for the long pulse

It could be taken the advantage of this higher peak flux of the long pulse with the use of a fast chopper. A fast chopper will serve as a pulse shape chopper. It can adjust the pulse width to a wished value, so it can adjust the spectral resolution for a particular distance.

This proposal could be analyzed with two choppers rotating in opposite direction at 400 Hz each other as shown by Figure 3-14. Figure 3-15 shows the spectral resolution of the long pulse cut by these choppers. This speed will produce pulse widths of 0.07 ms over a 12 cm-window. It can be noticed that for any dynamic range the resolution will be better than the short pulse mode, even delivering higher flux. So ESSB could accede to the high resolution applications. This chopper system also will cut the tails of the pulses then the signal quality will be better.

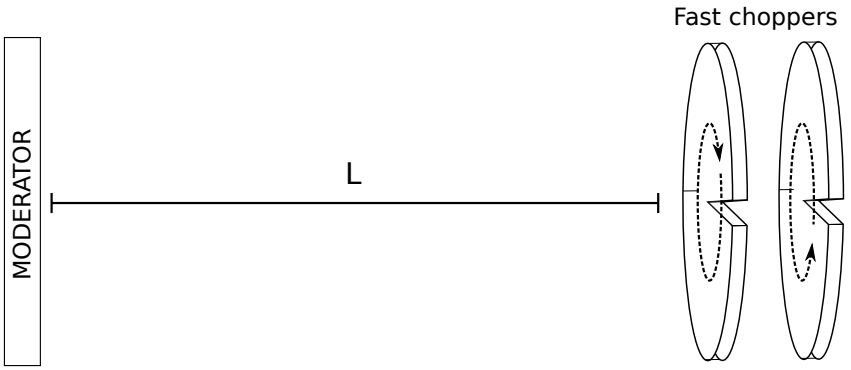

Figure 3-14: A conceptual sketch of two fast choppers rotating in opposite direction

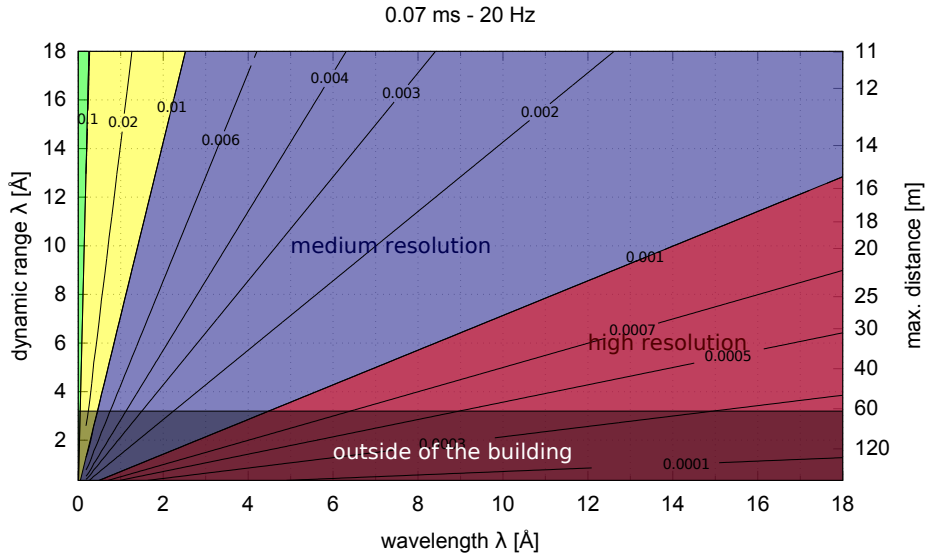

Figure 3-15: Spectral resolution as function of the wavelength and the dynamic range for the long pulse cut by two 400 Hz-chopper

The cut widths that can be achieved are related to a technical limitation on the tangential velocity of the chopper. And nowadays this velocity is limited around 24000 rpm with 80 cm-diameter [10]. So for a 12 cm-window, 0.14 ms will be minimum cut width archievable with this chopper. For this reason two choppers are placed together rotating in opposite directions in order to reach a relative rotation speed up to 48000 rpm, and a 0.07 ms-cut width could be achieved.

Figure 3-16 shows the chopper cutting effect at two distances (1.5 and 5 m) from the moderator surface. If the disk chopper is placed at 1.5 m then the pulses will be together enough when the chopper cut them, so the emerging wavelength range will be higher than a chopper placed at 5 m (outside of the Target Area [7])

Figure 3-17 shows the TOF at 10 m of the long pulses cut previously by the two 400 Hz-choppers system (0.07 ms of time window) placed at 1.5 m from the moderator face (outside of the Target Vessel). Figure 3-18 shows the same but the chopper system located at 5 m (outside of the Target Station Area). It can be checked that the choppers at 1 m can provide a higher wavelength range than the choppers at 5 m.

So two fast chopper disks could be useful to improve the resolution of the pulses (two 400 Hz-choppers will deliver 0.07 ms pulses and would let ESSB the access to high resolution instruments). On the other hand, a high resolution range longer than 1.5 Åwill requiered to place the chopper system as close as possible to the moderator face, even inside the Target Area (worse maintenance, radiation evironment).

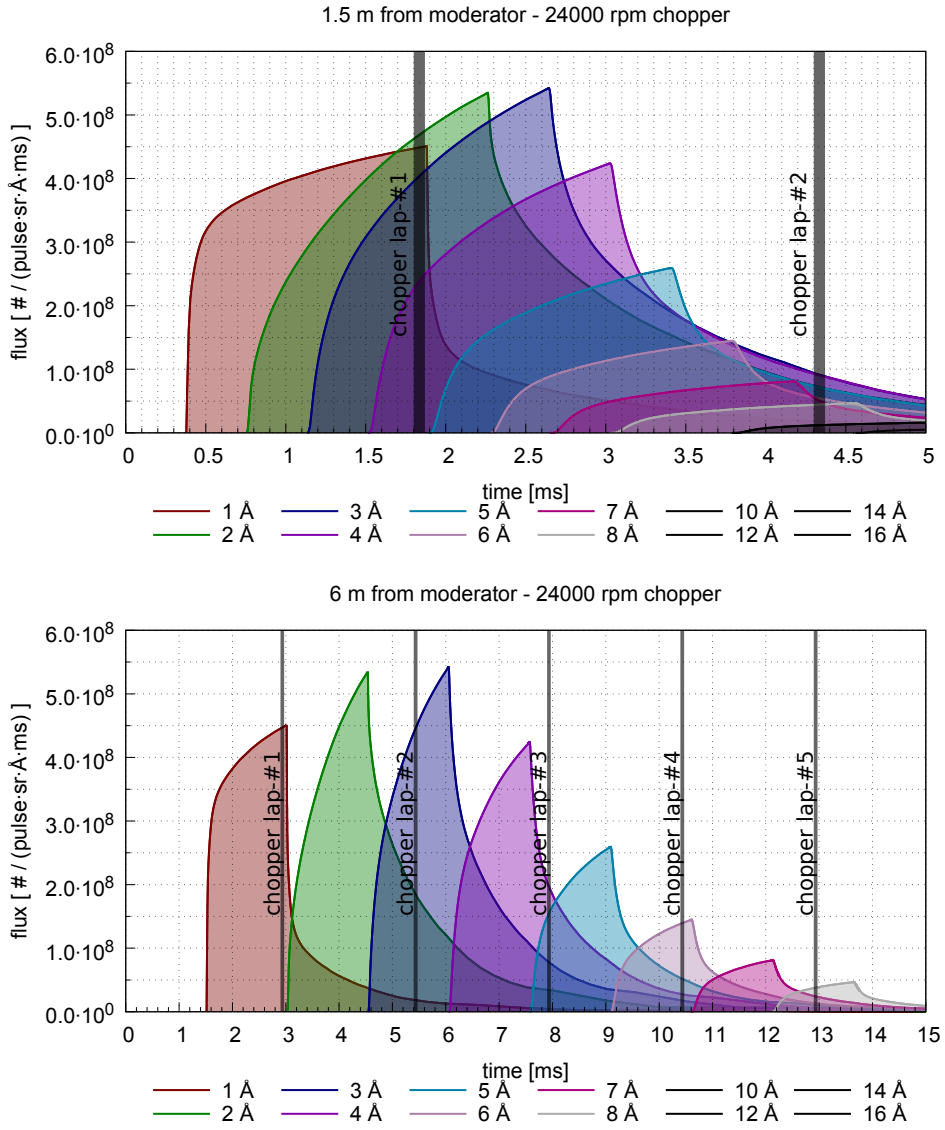

Figure 3-16: Pulse TOFs of several wavelengths at 1.5 (up) and 5 m (down)

3.7 Conclusions

The previous instrument anallysis has focused on quantifying background, resolution and dynamic range parameters. The following conclusions can be drawn:

- Background emerging from the source will reduce dynamic range at the sample due to contamination by high energy neutrons and it will damage some componets and the sample. A To-chopper placed outside the Target Area will be required to reduce this effect.
- In order to find the best operation mode for each instrument, pulse length and its repetition rate can be changed in operation. Long pulses and high repetition rates pro-

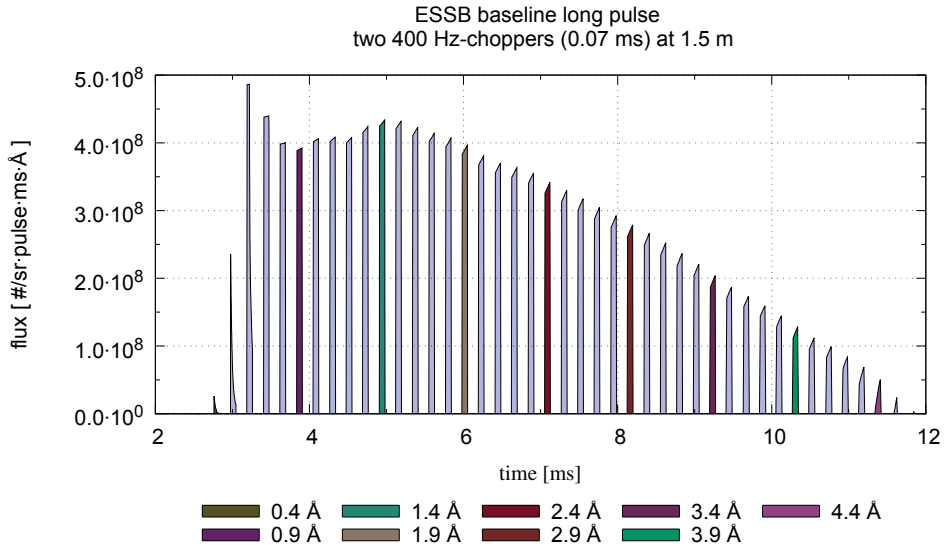

Figure 3-17: TOF at 10 m of baseline long pulses cut by two 400 Hz-choppers (0.07 ms) at 1.5 m from the moderator at 1.8 ms from the pulse zero-time

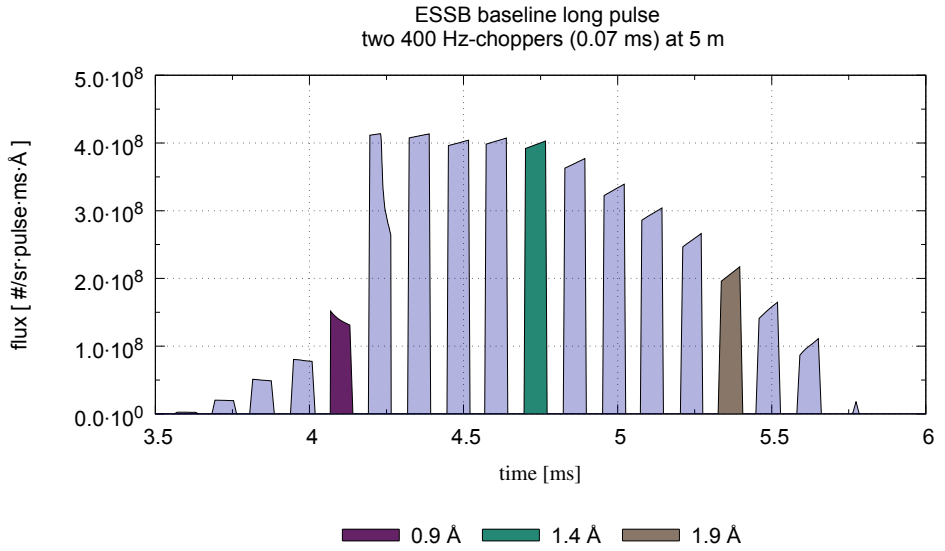

Figure 3-18: TOF at 10 m of baseline long pulses cut by two-400 Hz choppers (0.07 ms) at 5 m from the moderator at 1.8 ms from the pulse zero-time

duce higher neutron fluxes but worse resolution and dynamic range. On the other hand, short pulses ensure better resolution and low repetition rates ensure wider dynamic ranges.

- The shortest ESSB pulse length can achieve just up to medium resolution with a considerable dynamic range. However, it will be possible to get high resolution with the

use of a set of two disk choppers rotating at 24000 rpm in opposite directions. These choppers should be inside the Target Area as close as possible to the moderator in order to guarantee a considerable dynamic range.

4 INSTRUMENT DEFINITION

Previous chapters have established the general ESSB framework for neutron scattering instuments. This chapter will try to define the conceptual design of the candidate to the first ESSB neutron instrument, i.e a *Small Angle Neutron Scattering* instument.

In neutron science facilities the natural flow for instrument selection uses to start with the definition of "*what kind of science yo want to do*", then focus the optimization of your facility to the instruments whose perform this kind of science. Nevertheless ESSB has not a unique objective of making neutron science, it expects to serve as a testing facility for the components of the European Spallation Source (ESS). Hence ESSB has the limitation of following the main ESS parameters.

SANS instrument is not a great neutron beam quality demanding, also its design is not one of the most complicated instrument designs. So SANS could be a candidate for the first neutron instrument at ESSB.

This chapter will also try to show the flux at the sample for a SANS instrument in order to compare with other facilities.

4.1 The small angle neutron scattering technique

Small angle neutron scattering (SANS) is an experimental technique for probing large structures. It is a coherent elastic neutron scattering technique (neutron diffraction) for the mesoscopic scale (10-10000 Å). The SANS technique has been an effective characterization method in many area of research including Polymers, Complex Fluids, Biology, and Materials Science [11].

Neutron diffraction bases on the Bragg law (7) which emerges from the Van Hove formalism [incluir referencia]. This law shows that probing larges structures requires low values for the *scattering vector* ($\vec{Q}$). This *scattering vector* is the difference between the incoming ($\vec{k}$) and the outgoing ($\vec{k'}$) *wave vector*.

$$|\vec{Q}| = |\vec{k} - \vec{k'}| = n\left(\frac{2\pi}{d}\right) \tag{7}$$

where,

Q, is the scattering vector, in inverted angstroms
n, is an integer
d, is the characteristic distance of the structure, in angstroms

For elastic scattering (diffraction) Q can be expressed as a function of the incident neutron wavelength (λ) and the *scattering angle* (2θ) (the angle between the incoming and the outgoing waves), as shown by Expression (8). Hence low-Q can be achieved with large incident wavelengths and/or low *scattering angles*.

$$Q = \frac{4\pi sin\theta}{\lambda} \tag{8}$$

No actual spallation source produces neutrons with wavelengths of the same order of magnitude than the mesoscopic scale in an efficient way. Nevertheless SANS technique takes the advantage of the constructive interference between the incoming and outgoing neutron waves, producing a new wave with larger wavelength (9), which is useful for probing large structures. Although it requires low *scattering angles* between the *scattering vectors*.

$$\lambda_{probe} = \frac{\lambda}{2sin\theta} = \frac{2\pi}{Q} \tag{9}$$

When the *scattering angle* is small, Expression (9) can be approximated by Expression (10).

$$\lambda_{probe} \approx \frac{\lambda}{2\theta} \tag{10}$$

where,

2θ*, is the scattering angles, in radians*

4.2 Selection of the source operation mode

Previous chapters showed that ESSB can operate on short or long pulse operation mode. We will try to justify which one iof them could be the best for the operation of the ESSB neutron small angle instrument.

Long operation mode can deliver more neutrons per second than the short one but its spectral pulse resolution would be worse, as shown by Figure 3-6. Nevertheless the SANS technique measures the *scattering vector* Q hence the uncertainty in the detection is not only associate to the espectral resolution, as shown by Expression (11), where small angle approximation was made. Then angular considerations need also to be taken into account.

$$\frac{\Delta Q}{Q} \approx \left(\left(\frac{\Delta\lambda}{\lambda} \right)^2 + \left(\frac{\Delta\theta}{\theta} \right)^2 \right)^{1/2} \tag{11}$$

Figure 4-1 let K. Lieutenant [12] show that the angular resolution depends only on the geometry of the source, the sample and the area detection when pinhole configuration is used, as Expression (12) shows.

Common SANS values for Expression (12) could be $d_1 = 3\ cm$, $d_2 = 1\ cm$, $D = 2.5 - 50\ cm$ and $\Delta D = 1\ cm$, which produce an angular resolution values between 0.02 (in the corner of the detector) and 0.40 (in the corner of the beam-stop). On the other hand Figure 3-6 show that long pulse can deliver an epectral resolution ($\Delta\lambda/\lambda$) below 0.03 for wavelengths above

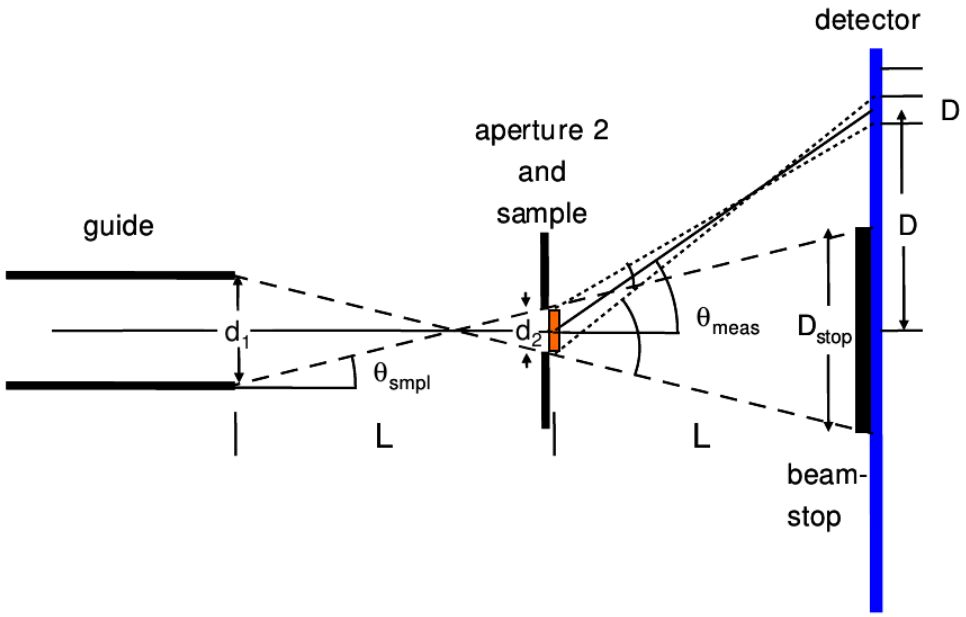

From K. Lieutenant [12]

Figure 4-1: Geometric parameters for ngular divergence at pinhole SANS instrument

$$\frac{\Delta\theta}{\theta} \approx \frac{\left(\left(d_1+d_2\right)^2+\left(d_2+\Delta D\right)^2\right)^{1/2}}{4D} \tag{12}$$

where,

d_1, *is the size of the aperture of the neutron guide exit*
d_2, *is the size of the sample*
D, *is the position position of the detection*
ΔD, *is size of the detector pixel*

4 Å and long flight paths longer than 50 m (for short pulse the espectral resolution would be even lower). This resolution values (espectral and angular ones) let Expression (12) show that the total resolution (scattering vector resolution) is determined in most detector area by the angular one, which is a fixed value for every experiment with the same instrument configuration.

Then the espectral resolution of the ESSB pulses is not a crucial parameter for the total resolution of the SANS. Then it would be better to operate the instrument with the long pulse operation mode because it can deliver higher flux over the sample (Figure 2-6) and the repetition rate is lower that the short pulse one, alowing a higher usable dynamic range, i.e., lower frameoverlap (Figure 3-8).

On the other hand the proposal of the band-width choppers operation for the SANS should avoid neutron wavelengths below 4 Å because the espectral resolution below this wavelength could be significant relative to the angular one. Nevertheless the moderator advanced proposal of ESSB, i.e., the use of a beryllium filter, has its optimal working point above 4 Å,

as shown by Figure 2-6, and can deliver higher flux than the baseline configuration above this wavelength.

Then the optimal operation mode of the source for a SANS at ESSB would be the long pulse over the moderator advanced proposal (beryllium filter) becasue it can provide higher flux with the same resolution as a shorter pulse length.

4.3 The sketch of SANS

Neutron scattering instruments use to be to much longer in order to get access to very low-Q values with low scattering angles. This section will try to decribe the general sketch of the proposed ESSB-SANS, but no detailed instrumentation is taking into account.

A common SANS instrument sketch is shown by Figure 4-2. At the begining there is a neutron extraction system from the Target Station. The selected system will be a bender guide in order to prevent the direct view of modetor removing the gamma radiation from the beryllium target. The coating of the bender should be selected to transport the usable neutron wavelength range, i.e. $4 - 7.8$ Å.

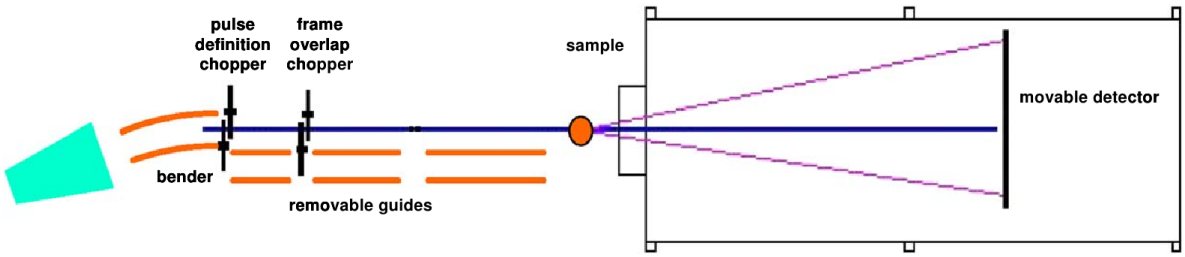

From K. Lieutenant [12]

Figure 4-2: General sketch of the proposed ESSB-SANS

Neutrons extracted from the Target Station are contaminaited with neutrons of other wavelengths. So it is necessary to filter them with a bandwidth chopper system. The first chopper will avoid to pass neutrons of wavelengths below 4 Å while the second one will avoid to pass neutrons of wavelengths above 7.8 Å.

A flexible instrument is proposed in order to optimize the Q-range, the count rate and the Q-resolution for any particular experiment. This flexibility could be achieved with removables neutrons guides which change the *effective source* (the exit of the last neutron guide) and also the free flight paths of the neutrons. Also a movable detector in a evacuated tank (in order to avoid nitrogen collision that could modify the scattering angle) is proposed.

In order to achive this flexibility a pinhole geometry is proposed rather than a collimation system. The pinhole geometry optimizes the intensity at the detector producing a sharp image. This kind of geometry requires that the free flight path (the distance between the *effective source* and the sample) and the detection distance (the distance between the sample and the detector) to be equal. It can be achivieved with the movable detector.

A common detector area is 1 x 1 m^2 with 1 x 1 cm^2 cells. The center of the detector hosts a beam-stop which avoid the radiation damage of the non-scattered neutrons from the sample. This beam-stop uses to be made of ^{10}B or Cd.

Diaphragms could be used in order to adjust the size of the *effective source* which is related with the total Q-resolution.

The gravity effect is not taking into account in this chapter, but it is of significant importance in a SANS instrument since neutrons of 7.8 Å will be on fligth during 108 ms. This effeThis effect can bee regulated with a gravity focuser (fixed and moving apertures).

4.4 Reference goals to achieve

One the most important parameter of SANS is the length of the instrument since it is related with the largest object that can be measured. Angular divergence of neutrons leaving the *effective source* (the exit the last neutron guide before the sample) produces that neutrons of the same wavelength go over different distances before hitting the sample. But they need to generate an interference pattern in order to be registered by the detector. This interference condition needs the phase different between the paths to be a 2π-multiple. Under this reasoning R. Pynn [13] shows that the largest object that SANS can be measured is related with geometrical parameters by expression (13).

$$d = 10^{-2} \cdot \left(\frac{\lambda}{a}\right) L \tag{13}$$

where,

d, is the largest object that can be measured, in micrometer,
λ, is the largest neutron wavelength, in angstroms,
a, is the size of the effective source exit aperture, in centimeters,
L, is the distance between the effective source exit and the sample, in meters.

The reference wavelength value is 4 Å which is the optimal one for a ESSB-SANS instrument (advanced proposal) as shown by previous section. On the other hand, the maximum distance to place the detector, i.e., the maximum time of flight, would be 50 m from the moderator (bulding constraint). So the maximum usable wavelengh (without frameoverlap) would be 7.8 Å as estimated by expression (6). A minimum value for the aperture of the *effective neutron source* exit could be 1 cm (d_1 at Figure 4-1) which could be achieved with a diaphragm. A pinhole geometry rather than a collimaion system is proposed in order to get a sharp image, hence the maximum effective source-sample distance (subtracting 5 m inside the target area) would be $L = (50 - 5)/2 = 22.5\ m$. Taking into account all of this values, the largest object that the proposed ESSB-SANS could measuse would be 1.7 μm.

According to Equation (9) the minimum Low-Q would be $3.7 \cdot 10^{-4}$ Å^{-1}, which is of the same order than other instruments like SANS at ESS ($3 \cdot 10^{-4}$ Å^{-1}), BIO-SANS ($9 \cdot 10^{-4}$ Å^{-1}) and HFIR ($7 \cdot 10^{-4}$ Å^{-1}) at SNS or SANS2D ($2 \cdot 10^{-3}$ Å^{-1}) at ISIS.

The *scattering angle* (2θ) required to achive a Low-Q of $3.7 \cdot 10^{-4}$ Å^{-1}, using 7.8 Å neutron wavelengths, would be 0.026°, as shown by Expression (8). Hence the outgoing scattering

vector will hit a detector, located at 22.5 m from the sample, at 1.03 cm from the center line. Then every neutron hitting the detector below this height is considered like a non-scattered neutron by the sample. All of these non-scattered neutrons add an important fraction of the sample-incident beam so they could damage the detector. In order to avoid this damage a beam-stop of 2 x 1.03 = 2.06 cm is placed at the center of the detector.

Figure 4-1 lets also determine the optimal size of the sample (d_2) as a function of the effective source aperture (d_1) and the size of the beam-stop D_{stop}, as Expression (14) shows. Although this optimal value is about 0.5 cm, it can be increased for another configurations.

$$D_{stop} = d_1 + 2d_2 \tag{14}$$

where,

d_1, *is the size of the effective neutron source aperture,*
d_2, *is the size of the sample,*
D_{stop}, *is the size of the beam-stop*

The maximum Q-value should be enough to probe sizes of the order of about 15 Å. This size needs a scattering vector of about 0.4 $Å^{-1}$. The best neutron wavelength to achive it would be 4 Å because it has the maximum flux at the ESSB avanced proposal moderator. The scattering angle (2θ) produced in this situation would be 14.6°. Taking into account a common detector area of 1 x 1 m^2 the minimum distance between the detector and the sample should be 1.92 m (removable neutron transport guides and movable detector).

The proposed ESSB-SANS will not try to achieve an extended Q range that makes possible the combination of small angle scattering technique and medium resolution diffraction, like EQ-SANS of SNS does. The limitation of this is due to the awful spectral resolution of the ESSB long pulse.

This section has established the scattering vector range to achieve by the proposed SANS at ESSB, i.e, $3.7 \cdot 10^{-4} - 0.4$ $Å^{-1}$ (15 Å − 1.7 μm). This range has not been optimzed by any particular area of science becuase there is no science directive at the moment of this proposal, nevertheless a general instrument for a wide Q-range was proposed.

4.5 Neutron extraction from the Target Area

Neutron extraction system needs to transport neutrons outside the Target Station in the more efficient way. It includes not only the transportation of the useful neutrons but also the elimination of the fast neutrons and the gamma radiation from the neutron source (they produce signal noise and radiation damage at the detectors). This task can be carried out by a mechanical device like a To-chopper, described in Section 3.2, pag. 27 . But the ESSB-SANS needs to transport neutrons above 4 Å-wavelengths so optical solutions can be implemented also like a bender system. In addition a bender system improves the transmission over a To-chopper for long wavelengths as showed by a technical report of EQ-SANS at SNS [14].

The coating bender system will be of a supermirror material that allows neutrons above 4 Å to be transported outside of the Target Area. It will avoid neutrons bellow this wavelength and gamma radiation to reach the exit preventing the direct view of the source by the sample.

In order to collect as much neutrons as possible, ESSB moderator system design allows to approach the bender until 30 cm from the moderator. Taking into account the Target Area radius is about 5 m then the characteristic bender length (L_1 in Figure 4-3) will be 4.7 m.

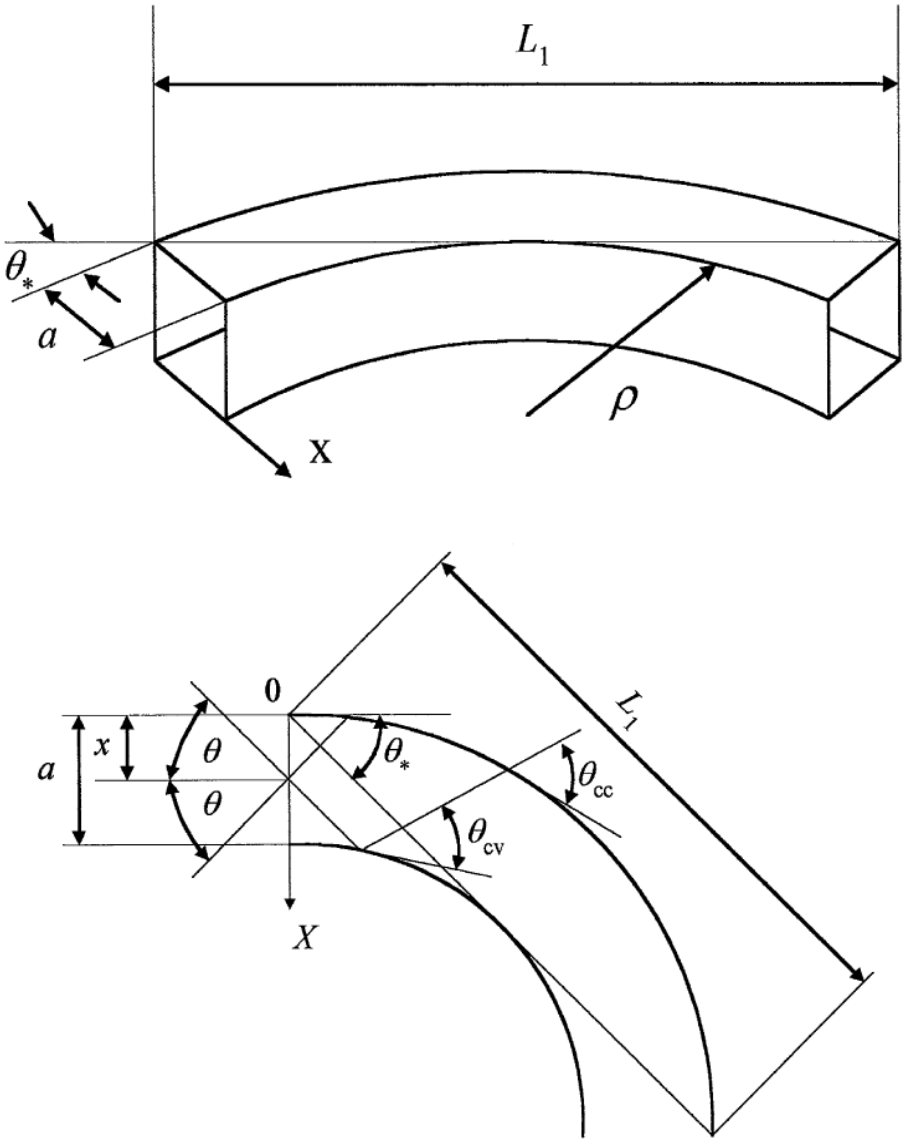

From A. Schebetov [15]

Figure 4-3: A schematic view of the neutron guide bender

Given $a^2 = 4\ x\ 4\ cm^2$ for the bender cross section, trigonometric relations (assuming small angle approximation) on Figure 4-3 lets establish the requiered bender radius in order to avoid the direct view of the bender entry and its exit, Expression (15). Then the proposed

bender radius is 69 m. Also the *characteristic angle* (θ_*), which is the maximum glancing angle of a non-divergence trajectory, can be determined by Expression (16); its value is 1.95°.

$$\rho = \frac{L_1^2}{8a} \tag{15}$$

where,

ρ, *is the bender radius,*
L_1, *is the bender length,*
a, *is the bender cross section size.*

$$\theta_* = \frac{4a}{L_1} \tag{16}$$

where,

θ_*, *is the characteristic angle.*

But neutrons with divergence trajectory at the entry can have a glancing angle higher than the *characteristic angle*. A. Shebetov [15] defines the glancing angle of a divergent trajectory over the concave (17) and the convex (18) sides.

$$\theta_{cc} = \theta_* \sqrt{\left(\theta/\theta_*\right)^2 + x/a} \tag{17}$$

where,

x, *is the coordinate of the intersection point of the trajectory and the bender entrance,*
θ, *is the angle between the incident trajectory and the entrance normal.*

$$\theta_{cv} = \theta_* \sqrt{\left(\theta/\theta_*\right)^2 + x/a - 1} \tag{18}$$

Since $\theta_{cc} > \theta_{cv}$, the condition to transport a neutron trajectory is a glancing angle (θ_{cc}) [in degrees] lower than $\theta_{cc} < 0.099 \cdot m \cdot \lambda$, where m is the supermirror coating number (multiples of the momentum transfer of natural Ni), and λ [in angstroms] is the minimum wavelength to be transported. So Expression (17) lets determine the admittance angle θ_1 by Expression (19), which is the maximum angle of the incoming neutron trajectory (with the normal of the bender entrance) to be transported by a m-supermirror coating.

$$\theta_1 = \theta_* \sqrt{\left(\frac{0.099 \cdot m \cdot \lambda}{\theta_*}\right)^2 - \frac{x}{a}} \tag{19}$$

In spite of the bender cost, the maximum current m-supermirror coating is 7. This coating will allow to transport 4 Å neutrons wavelengths until a divergence of 2.77°. Taking into account this angle, the moderator-bender distance of 30 *cm*, the moderator size of 12 *cm* and the bender entrance size of 4 *cm*, there will be a large waste amount of neutrons from the moderator.

Alternatives to a high m-supermirror value could be channels inside the bender, which reduce the *characteristic angle*, and polarising devices.

Then the main parameters of a bender guide have been proposed in order to extract neutrons from the Target Station preventing the direct view of the moderator, which avoid the direct gamma radiation from the beryllium target. This bender will have a 69 m-radius of curvature, a 4 x 4 cm^2 cross section and length of 4.7 m. A supermirror coating of $m = 7$ was proposed in order to transport a much 4 Å neutron wavelengths as possible.

4.6 Bandwidth definition

In spite of the bender system is optimized to transport wavelengths above 4 Å, there are some lower wavelengths that will be also transmitted due to theis low glancing angle at the bender entrance. Then bandwidth-choppers defining the wavelength range (4-7.8 Å) are needed.

The bandwidth choppers rotate at the frequency of the long pulse (1.5 ms) operation mode, i.e. 20 Hz. The first one will be located just outside of the Target Station at a distance of 5.5 m. In order to block neutrons below 4 Å it will allow to pass the beam at $t = 4$ Å $\cdot\, 5.5\ m/3.96 = 5.56\ ms$ (zero time is assumed when the first neutron emerges from the moderator for every pulse). But neutrons, emerging from the tail of the proton pulse, until $\lambda = 3.96 \cdot (5.56 - 1.5\ ms)/5.5\ m = 2.92$ Å wavelength will also pass also.

The other bandwidth chopper should be located as a certain distance from the first one, e.g 9 m from the source. It should avoid to pass the rest of the beam when the 7.8 Å wavelength neutrons have passed. It happens at $t = 7.8$ Å $\cdot\, 9\ m/3.96 + 1.5\ ms = 19.23\ ms$. Also neutrons until $\lambda = 3.96 \cdot 15.29\ ms/7\ m = 8.46$ Å wavelength will pass.

Two bandwidth choppers are needed to define the usable wavelength range, i.e. $4 - 7.8$ Å. This section has tried to define the timing of both choppers. The first one located at 5.5 m from the source should allow pass the beam at 5.56 ms. On the other hand the second chopper should avoid to pass the beam at 19.23 ms. Both of them should rotated at the same frequency than the source, i.e. 20 Hz.

4.7 Neutron transport guides

The mission of the ESSB-SANS guides is the transportation of neutron wavelengths above 4 Å. But only those with a divergence lower that a certain value.

The maximum glancing angle of a neutron hitting the sample is given for the shortest flight path, i.e 1.92 m. Figure 4-3 let establishes the $\theta_{smpl} = atan\big(1/2(d_1 + d_2)/L\big) = 0.22°$. Then it is the maximum glancing angle the guides need to transport. Normal nickel allows angles of 0.446° so it would be enough for the guide coating.

As anticipated on a previous section, a flexible instrument is intended to be built at ESSB. So removable neutron guides and a movable detector in a evacuated tank is proposed. A first design approach could host three different configurations. The first one will be a no-guide

after the bender configuration. Then the effective source will be the exit of the bender. It corresponds to a total free flight path of 45 m (equal distance of 22.5 m for effective-sample and sample-detector as established by the pinhole configuration). The second one will be the shortest free flight path, i.e. 1.92 m which correspond to a guide length of $22.5 - 2.95 = 19.55$ m and 1.92 m of sample-detector distance (movable detector). The third one will be an intermediate case of 11.25 m of neutron guides and the same length for the free flight path and the sample-detector distance.

An incoming wavelength range of $4 - 7.8$ Å produces the following scattering vector ranges for the three proposed configurations. The 22.5 m free flight path configuration produces the range 3.7 10^{-4} $\text{Å}^{-1} - 0.035$ Å^{-1}. The 11.25 m one produces 7.4 10^{-4} $\text{Å}^{-1} - 0.07$ Å^{-1}. And the 1.92 m one produces the range 4.32 10^{-3} $\text{Å}^{-1} - 0.4$ Å^{-1}. All of then with different Q-resolutions.

A proposal of three removable guides and a movable detector has been established in order cover a wide Q-range with different Q-resolutions adjustable for experiment requirements.

5 CONCLUSIONS

The ESS-Bilbao neutron source has been characterized from the point of view of neutron scattering instruments. Two main proton pulse lengths, i.e. the long pulse (1.5 ms at 20 Hz) and the short one (0.1 ms at 50 Hz) have been analyzed. While the long pulse could deliver a higher flux rate than the short one its neutron beam quality would be worse for most of the neutron scattering applications.

Nevertheless an intermediate choice of high peak flux and high quality neutron could be achived with the use of a fast chopper which could be useful for high resolution applications.

The proposed quality parameters for a general analysis were the wavelength or spectral resolution and the dynamic range at the sample. They have been analyzed depthly.

These parameters were compared with ISIS-TS2 facility showing that ESSB is a modest neutron source. The ESSB long pulse could deliver between 20 and 30% of total cold neutrons per pulse than this large facilitie, but with an awful time distribution, limiting its applications to coarse resolution applications.i

The ESSB short pulse could produce a similar time distribution than ISIS-TS2 (their moderator response shapes would be similar), but it would be limited to the 5% of ISIS-TS2 cold neutron flux per pulse.

One of the key feature of ESSB is the option of changing the pulse length and its repetition rate during operation. Long pulses and high repetition rates produce higher neutron fluxes but worse resolution and dynamic range. On the other hand, short pulses ensure better resolution and low repetition rates ensure wider dynamic ranges.

A conceptual design of a Small Angle Neutron Scattering instrument was proposed. This instrument could take the advantage of the long pulse in order to it does not require a good spectral resolution. This instrument could address a Q-range between $3.7 \cdot 10^{-4}$ and 0.4 Å^{-1}, which is on the same order than other facilities.

References

[1] The European Spallation Source, 2012. http://ess-scandinavia.eu/. Quoted in page 3.

[2] F. Sordo, A. Ghiglino, M. Magan, F. Martinez, S. Terron, R. Vivanco, and J. de Vicente. Proyecto del Laboratorio de Aplications Neutronicas de ESS-Bilbao. Technical report, January 2012. Quoted in pages 3 y 5.

[3] The ESSB front-end, an injector for light ion accelerator, Conference at UCANS III, jul 2012. Quoted in pages 4 y 5.

[4] ESS-Bilbao Target Station Status, Conference at UCANS III, aug 2012. Quoted in pages 5, 6 y 7.

[5] F. Sordo, S. Terrón, M. Magán, G. Muhrer, A. Ghiglino, F. Martínez, P.J. de Vicente, R. Vivanco, J.M. Perlado, and F.J. Bermejo. Neutronic design for ESS-Bilbao neutron source. Nuclear Instruments and Methods in Physics Research Section A: Accelerators, Spectrometers, Detectors and Associated Equipment, 707(0):1–8, 2013. Quoted in page 8.

[6] I. Tilquin, P. Froment, M. Cogneau, Th. Delbar, J. Vervier, and G. Ryckewaert. Experimental measurements of neutron fluxes produced by proton beams (23–80 MeV) on Be and Pb targets. Nuclear Instruments and Methods in Physics Research Section A: Accelerators, Spectrometers, Detectors and Associated Equipment, 545(1-2):339–343, 2005. Quoted in page 8.

[7] ESS-Bilbao. Technical Design Report: ESS-Bilbao Target Station. Technical report, ESS-Bilbao, May 2013. Quoted in pages 9, 26 y 39.

[8] Raúl Vivanco Sanchez. Análisis de diseño y optimización nuetrónica del moderador frío de ESS-Bilbao. Technical report, ESS-Bilbao - Instituo de Fusion Nuclear UPM, 2013. Quoted in pages 9, 10 y 26.

[9] Roger Pynn. Neutron Scattering - A primer. Quoted in page 25.

[10] Aernnova engineering, editor. Neutron shielding of a carbon epoxy chopper disc with high strength boron 2012. Quoted in page 39.

[11] Boualem Hammouda. Probing Nanoscale structures - The SANS toolbox. National Institute of Standards and Technology, national institute of standards and technology edition, December 2010. Quoted in page 43.

[12] K. Lieutenant, T. Gutberlet, A. Wiedenmann, and F. Mezei. Monte-Carlo simulations of small angle neutron scattering instruments at European spallation source. Nuclear Instruments and Methods in Physics Research Section A: Accelerators, Spectrometers, Detectors and Associated Equipment, 553(3):592–603, 2005. Quoted in pages 44, 45 y 46.

[13] Roger Pynn. Neutron Scattering - Lecture 5: Small Angle Scattering. NIST Center for Neutron Research, 2013. Quoted in page 47.

[14] Jinkui Zhao. Conceptual Design and Performance Analysis of the Extended Q-range, High Intensity, High Precision Small Angle Diffractometer. Technical report, SNS, Oak Ridge, May 2000. Quoted in page 48.

[15] A Schebetov, A Kovalev, B Peskov, N Pleshanov, V Pusenkov, P Schubert-Bischoff, G Shmelev, Z Soroko, V Syromyatnikov, V Ul'yanov, and A Zaitsev. Multi-channel neutron guides of PNPI: results of neutron and X-ray reflectometry tests. Nuclear Instruments and Methods in Physics Research Section A: Accelerators, Spectrometers, Detectors and Associated Equipment, 432(2-3):214–226, 1999. Quoted in pages 49 y 50.

[16] K. Lefmann and K. Nielsen. McStas, a general software package for neutron ray-tracing simulations. Neutron News, 10(3):20–23, 1999. Quoted in page 58.

[17] DB Pelowitz, JS Hendricks, JW Durkee, ML Fensin, MR James, GW McKinney, SG Mashnik, and LS Waters. MCNPX 2.7. A Extensions. Los Alamos National Laboratory, 2008. Quoted in page 58.

[18] Esben Klinkby, Bent Lauritzen, Erik Nonbøl, Peter Kjær Willendrup, Uwe Filges, Michael Wohlmuther, and Franz X. Gallmeier. Interfacing MCNPX and McStas for simulation of neutron transport. Nuclear Instruments and Methods in Physics Research Section A: Accelerators, Spectrometers, Detectors and Associated Equipment, 700(0):106–110, 2013. Quoted in page 58.

[19] Shinichi Itoh, Kenji Ueno, Ryuji Ohkubo, Hidenori Sagehashi, Yoshisato Funahashi, and Tetsuya Yokoo. {To} chopper developed at {KEK}. Nuclear Instruments and Methods in Physics Research Section A: Accelerators, Spectrometers, Detectors and Associated Equipment, 661(1):86–92, 2012. Quoted in page 82.

[20] J.J. Yugo, E.D. Blakeman, R.A. Lillie, and J.O. Johnson. Three-dimensonal shielding simulations and activation calculations of the SNS neutron beam lines To, Eo and bandwidth choppers. Technical report, Oak Ridge National Laboratory, 2008. Quoted in page 83.

[21] Masakuni Narita and Koichi Narita. Average number of collisions necessary for slowing down of neutrons. Jounal of Nuclear Science and Technology, 26:819–825, September 1989. Quoted in page 83.

MÁSTER EN CIENCIA Y TECNOLOGÍA NUCLEAR

DOCUMENT 2: **APPENDICES**

APPENDIX A

THE ESS-BILBAO MCSTAS COMPONENT

A.1 GENERAL DESCRIPTION

The amount, and the time-distribution, of neutrons emerging from a pulsed neutron source depend on the TMR (Target Moderator Reflector) configuration and on the proton pulse from the accelerator. The whole process of neutron producction can be correctly simulated by codes like MCNPX. But the moderation process produces slow neutrons, which wavelengths are at the same order than the interatomic distances, then they would be sentitive to the material structure, so interference phenomena between the neutron waves could appear. Also the reflection phenomenon between surfaces could be considerable. MCNPX does not consider these phenomena for the slow neutron transport (beyond the moderator along the the neutron guides), so another code which would take it into account should be used. At this point the connection of MCNPX to another code would be required.

McStas [16] is a code that can take into account these phenomena along the neutron guides, i.e, the wave reflection and the constructive interferences (coherent transport) in supermirrors. It is also a popular code for neutron scattering instruments because it incorporates a large ammount of components, so the scientific can properly predict the neutron flux over his sample. McStas provides some neutron pulse *source components* for several analytic distributions. Nevertheless ESSB aims to try new advanced moderator concepts whose analytic distributions for emerged neutrons are not established yet. Hence it is mandatory to join the neutron production from MCNPX [17] to McStas. Several ways to do that are nowadays under development [18]. One of these is by a McStas component, that reads the MCNPX output and transforms it to a McStas input. A homemade McStas source component for ESSB (BILBAO_source component) will try to connect MCNPX to McStas.

This appendix will try to briefly review how this component works, and what information it could supply regardless of the connection with McStas.

A.1.1 Inputs of the component

The inputs of the BILBAO_source component are the MCNPX tally output file (energy and time tally) and some other parameters. The table A.1-1 lists these inputs. Those marked with an asterisk are mandatory and otherwise the default value is indicated. It is recommended the use of the same moderator width and height than used for MCNPX. Neutrons emerge in all directions isotropically from moderator. Hence it is necessary for simulation performance the use of a focusing element that collect only neutrons whose could really reach the next instrument component. On the other hand, sometimes it is useful simulate only a particular energy or time range, instead of the whole spectrum. These ranges could be selected from the component inputs. The time distribution of protons from the accelerator uses to be uniform (squared shape), nevertheless the component would be ready to model other shapes.

Table A.1-1: Inputs of the BILBAO_source component

input	value	units	description
double width	*	cm	width of the moderator face rectangle
double height	*	cm	height of the moderator face rectangle
double xw	*	cm	width of the focusing rectangle
double yh	*	cm	height of the focusing rectangle
int target index	+1		component whose position is used as focusing distance
double dist	0.0	cm	distance of the focusing element (alternative to the use of target_index)
double Emin	min.avail.	meV	minimum selected energy
double Emax	max.avail.	meV	maximum selected energy
double Lmin	min.avail.	Å	minimum selected wavelength
double Lmax	max.avail.	Å	maximum selected wavelength
double tmin	min.avail.	s	minimum selected time
double tmax	max.avail.	s	maximum selected time
int shape	0		shape of the incident proton pulse (only squared shape available)
double FWHM	1.5	ms	full with at half maximum of the proton pulse
double current	75.0	mA	max. electric current of the proton pulse
double protonEnergy	50.0	MeV	proton energy
char* source_file	*		mcnpx outp file (MCNPX tally should have total bins)
int tally	105		number of the MCNPX tally to read
double distTally	10.0	m	distance of the MCNPX point detector (useful to estimate values per steradian in the MCNPX FU card from SNS)
double* lambdas	*	Å	array of wavelengths to plot in an output file

A.1.2 Outputs of the component

The main output of the component is the production of a continuous neutron TOF distribution useful to McStas simulations.

Nevertheless several text files in column format are produced (*.dat). Some of them store the proton signal distribution, the intrinsic moderator response, the neutron pulses, some central moments, the FWHM of the pulses or the time distributions at wavelengths specified by the user.

protonSignal.dat stores the proton signal distribution. *moderatorResponse.dat* and *moderatorResponse3D.dat* store the intrinsic moderator response. *neutronPulse.dat* and *neutronPulse3D.dat* store the convolved neutron source. *moments.dat* stores a statistical analysis. *fastChopper.dat* stores the energy-time distribution of chopped neutrons emerging from a fast chopper. And *lambdas.dat* stores the time distribution for some wavelengths specified on the variable *lambdas* by the user.

What we understand by intrinsic moderator response, neutron pulse and central moments should be commented and developed in previoust sections of this report.

A.1.3 The model of the source component

The BILBAO_source component follows the same methodology as the SNS_source component but has some particularities.

Figure A.1-1 shows us how it works. First it reads an energy-time distribution of neutrons from a MCNPX tally. This should be the intrinsic moderator response per proton, i.e. the energy-time distribution of neutrons emerging from the moderator face as the moderation process of simultaneous neutrons from a just one nuclear reaction in the target by just one proton. This response would be function of wavelength and time. Next this response is going to be convolved with a set of protons from the accelerator (the proton pulse).

So the result would be discrete neutron pulse, as a function of wavelength and time, which would be interpolated by the BILBAO_source component (in these two variables) in order to produce a continuous pulse, required for McStas simulations.

Some of the particularities of the component are,

a an automatic convolution based on the user input parameters. Some facilities like ISIS do not need an important convolution tool because their proton pulse lengths use to be too much lower than their intrinsic moderator responses. Hence this moderator response would be the neutron pulse directly,

b the use of Hermite and Bicubic interpolation in some cases, specially at few microseconds from the peak of the pulses in order to obtain a good estimate of the peak shape. In the other cases lineal interpolation is used,

c cluster working successfully and managing of the tracing for every core,

d possibility of the use of wavelength and time ranges in order to narrow the energy and time distribution simulated in order to improve the simulation performance,

e central moments analysis of the neutron pulses, i.e. the time integrated values, the mean, the deviation, the skewness and the kurtosis of the distributions as well as the peak as function of the wavelength, the FWHM and the HWHMs. Another parameters that could estimate the central moments are also supplied. All of them could be interesting in order to analyze the shape of the pulses in detail,

f the production of text files that store the proton signal, the intrinsic moderator response, the TOF distribution and the central moments analysis, fast chopper cuts, and text files that allow their 3D plotting with Gnuplot, and

g the component would be ready to include a proton signal shape different than the squared one.

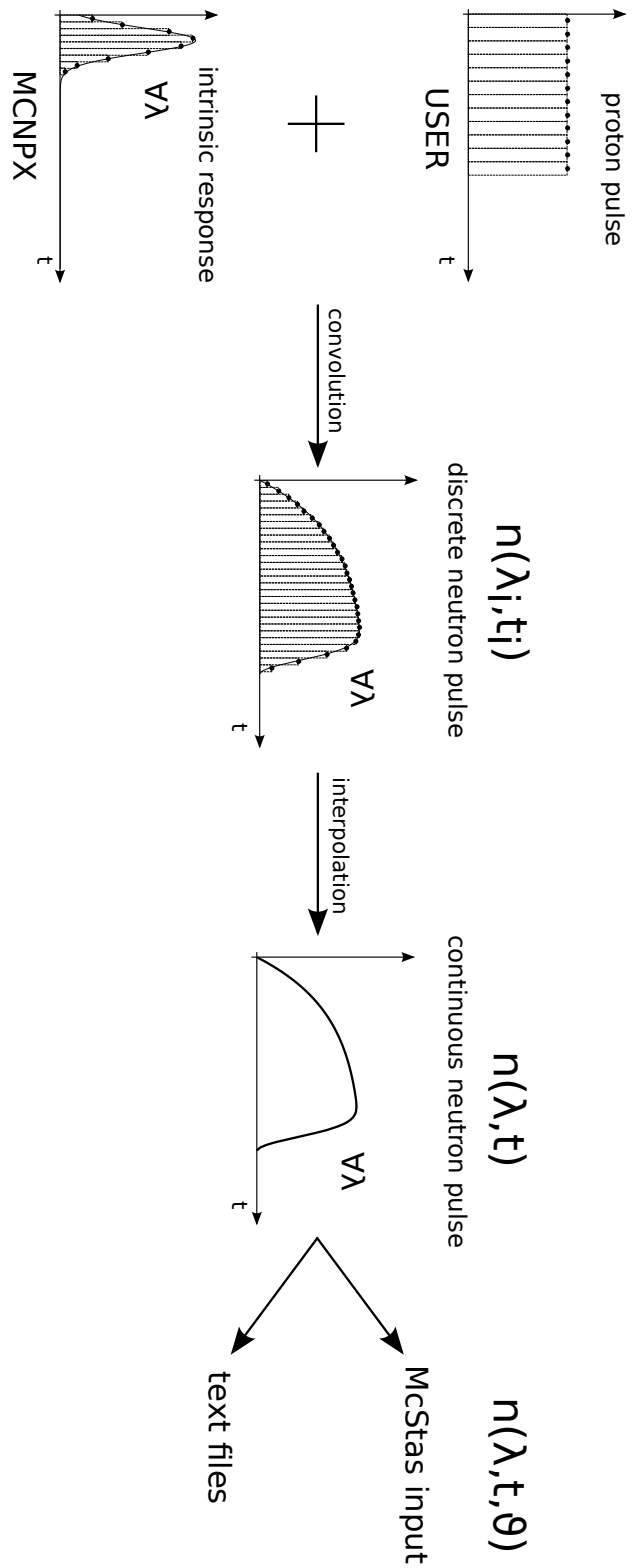

Figure A.1-1: Sketch of the inner working for BILBAO_source component

A.2 THE SOURCE CODE

The McStas source code of BILBAO_source component could be downloaded from the following link:

https://docs.google.com/file/d/0B6loJORHvdLbeWdfb0xwMXdSbWc/edit?usp=sharing

APPENDIX B

THE ESS-BILBAO MODERATOR RESPONSE

B.1 INTRINSIC MODERATOR RESPONSE

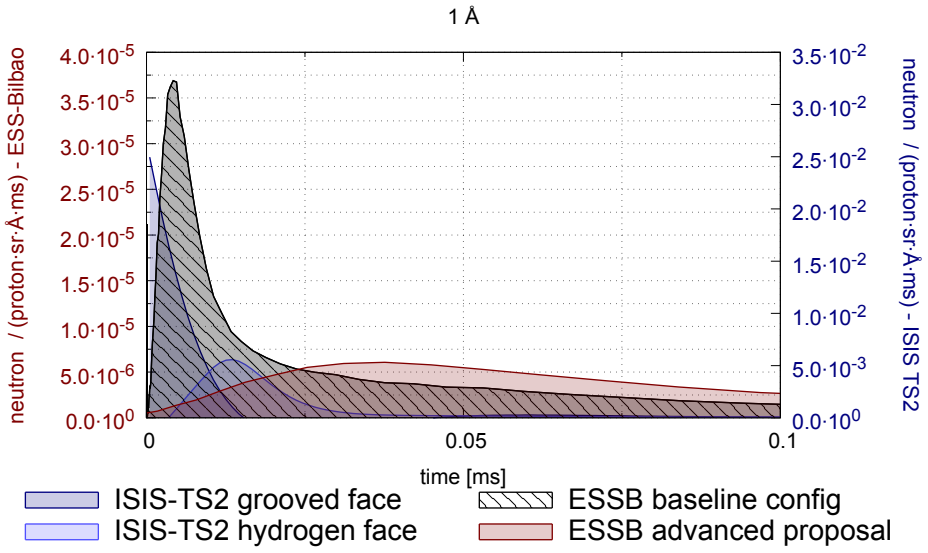

Figure B.1-1: Intrinsic moderator response ESSB vs ISIS-TS2 at 1 Å

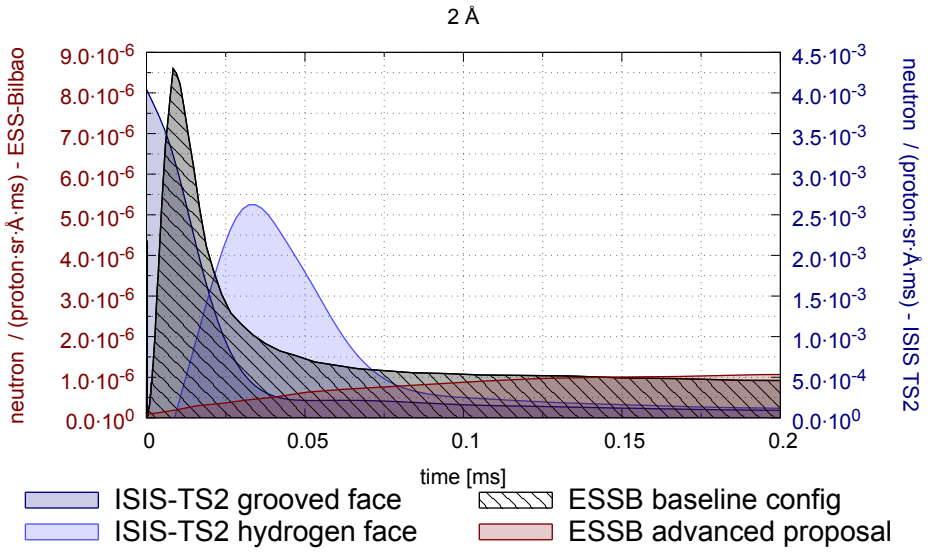

Figure B.1-2: Intrinsic moderator response ESSB vs ISIS-TS2 at 2 Å

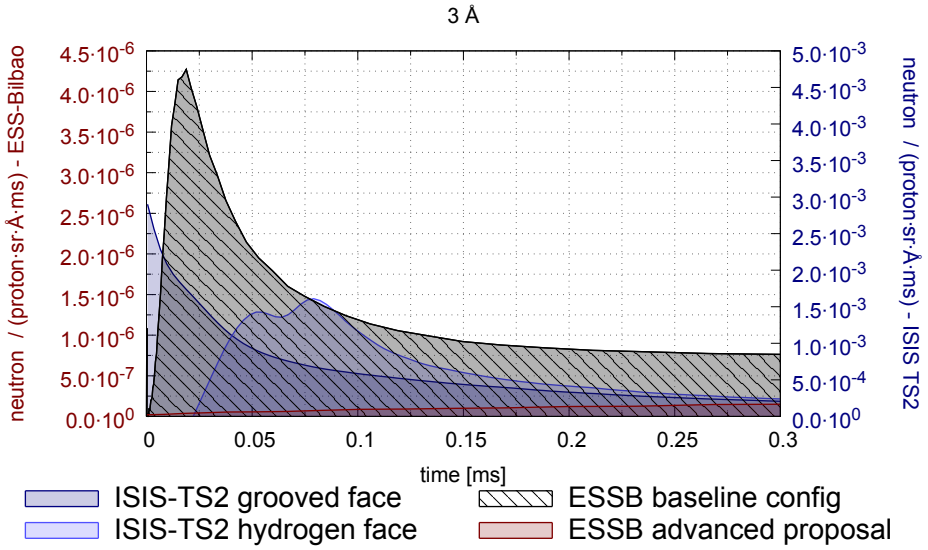

Figure B.1-3: Intrinsic moderator response ESSB vs ISIS-TS2 at 3 Å

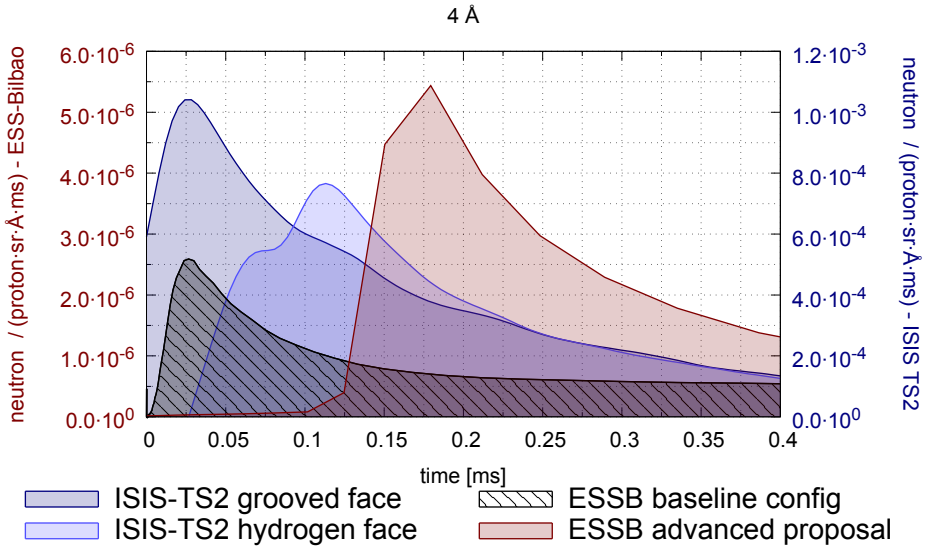

Figure B.1-4: Intrinsic moderator response ESSB vs ISIS-TS2 at 4 Å

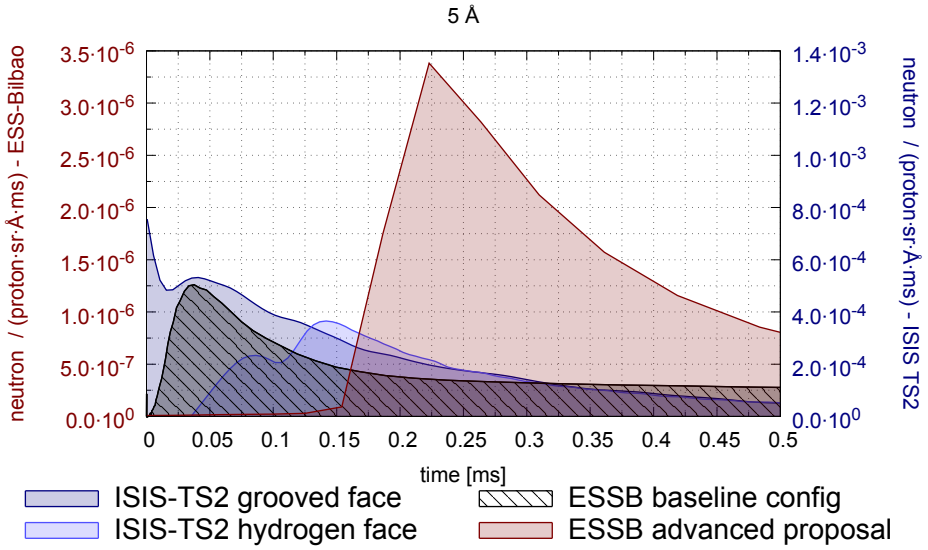

Figure B.1-5: Intrinsic moderator response ESSB vs ISIS-TS2 at 5 Å

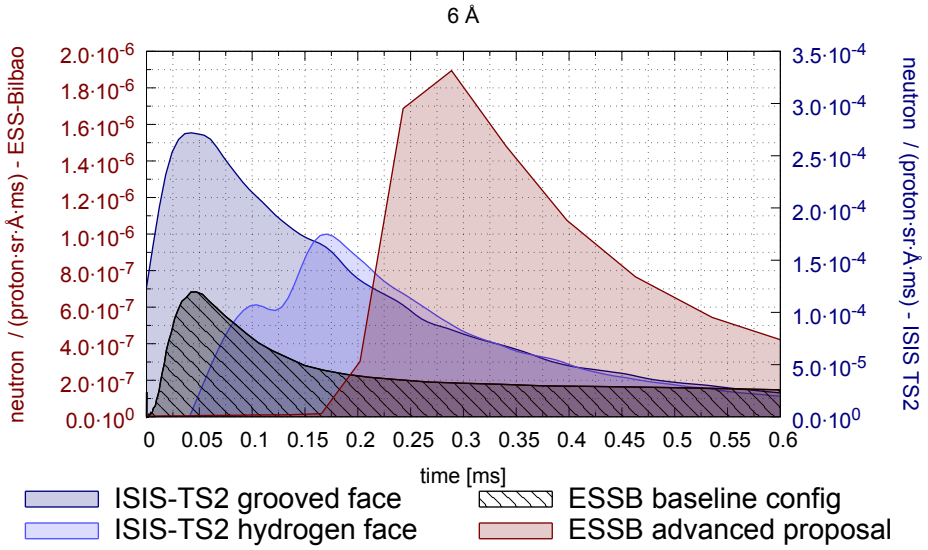

Figure B.1-6: Intrinsic moderator response ESSB vs ISIS-TS2 at 6 Å

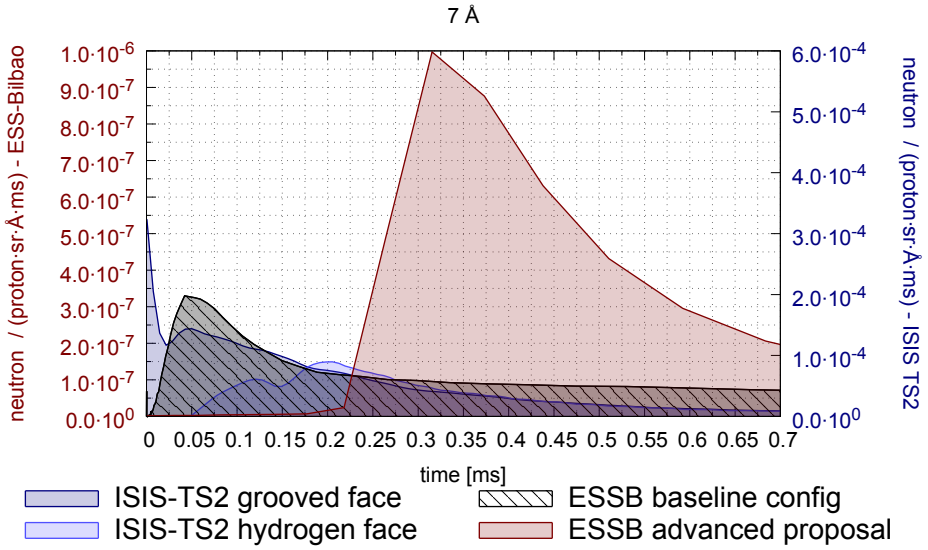

Figure B.1-7: Intrinsic moderator response ESSB vs ISIS-TS2 at 7 Å

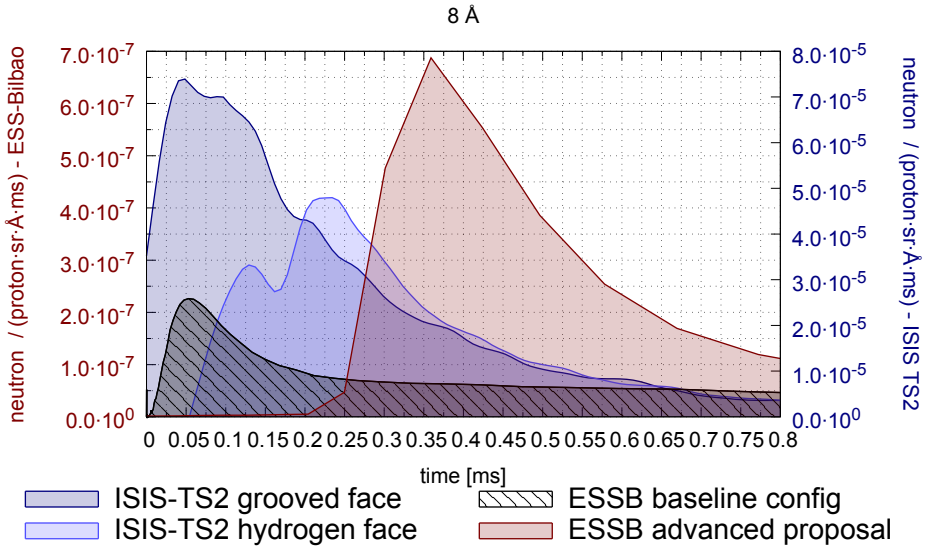

Figure B.1-8: Intrinsic moderator response ESSB vs ISIS-TS2 at 8 Å

APPENDIX C

THE ESS-BILBAO NEUTRON PULSES

C.1 LONG NEUTRON PULSES

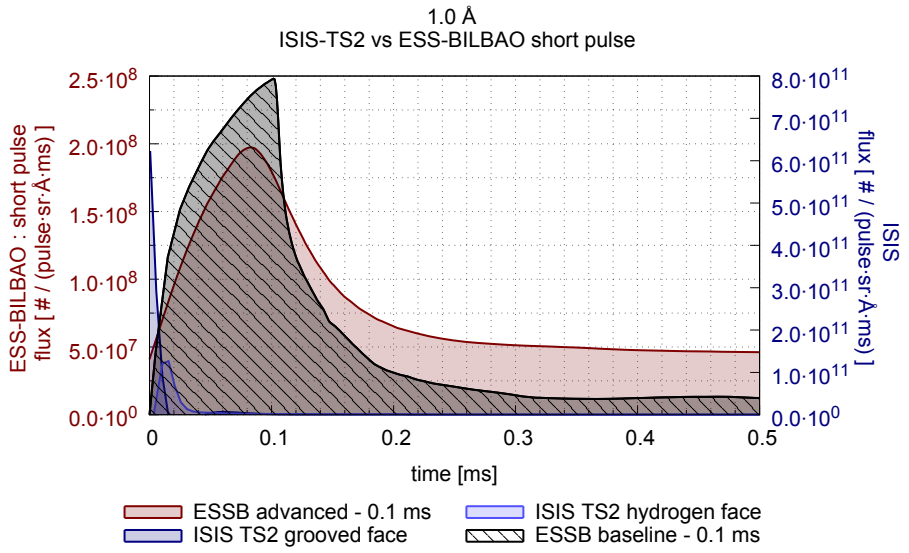

Figure C.1-1: Neutron pulse for the ESSB short pulse cases vs ISIS-TS2 at 1 Å

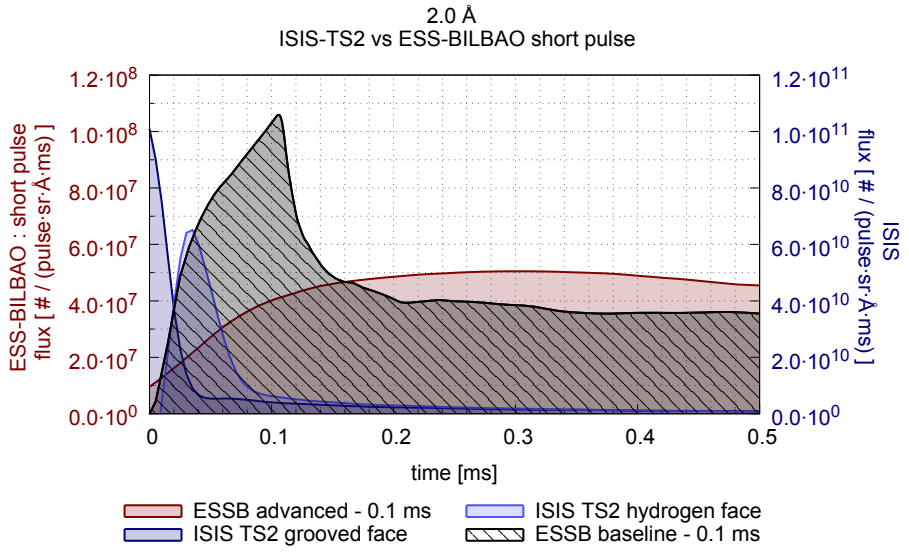

Figure C.1-2: Neutron pulse for the ESSB short pulse cases vs ISIS-TS2 at 2 Å

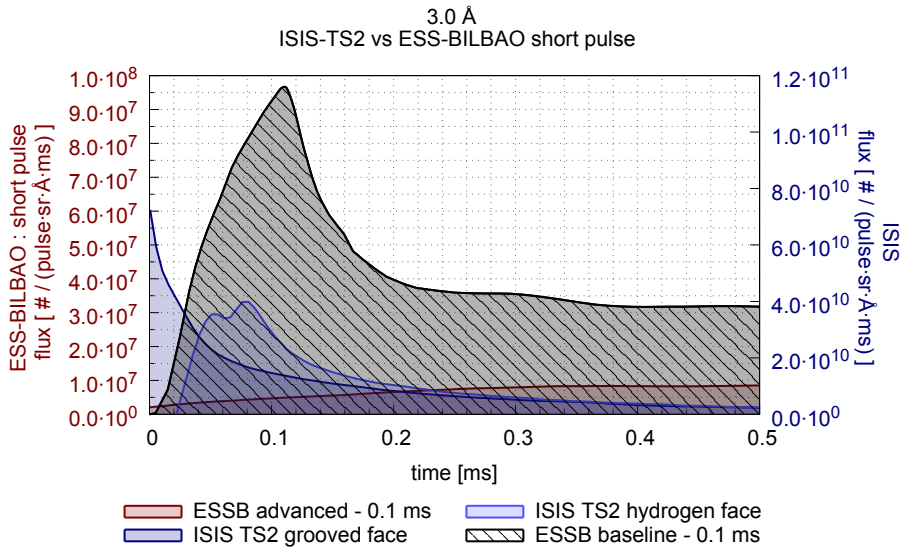

Figure C.1-3: Neutron pulse for the ESSB short pulse cases vs ISIS-TS2 at 3 Å

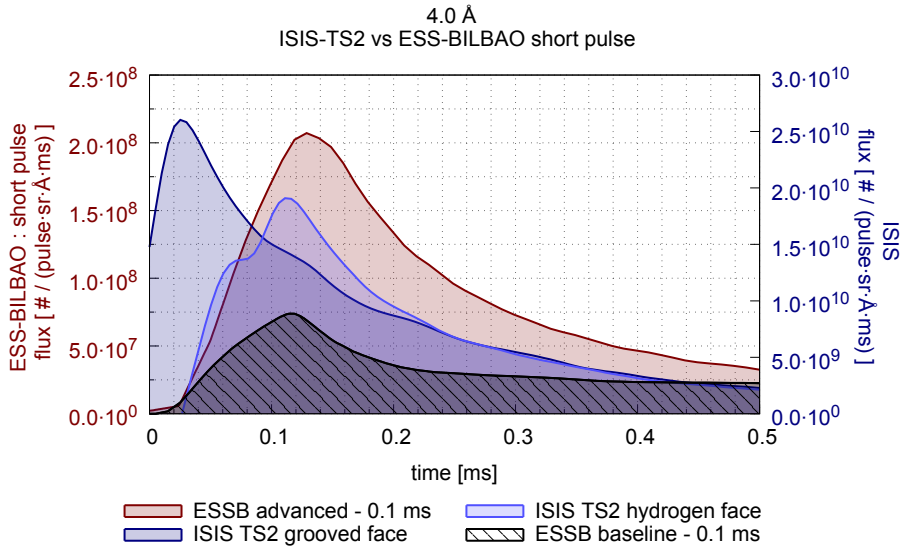

Figure C.1-4: Neutron pulse for the ESSB short pulse cases vs ISIS-TS2 at 4 Å

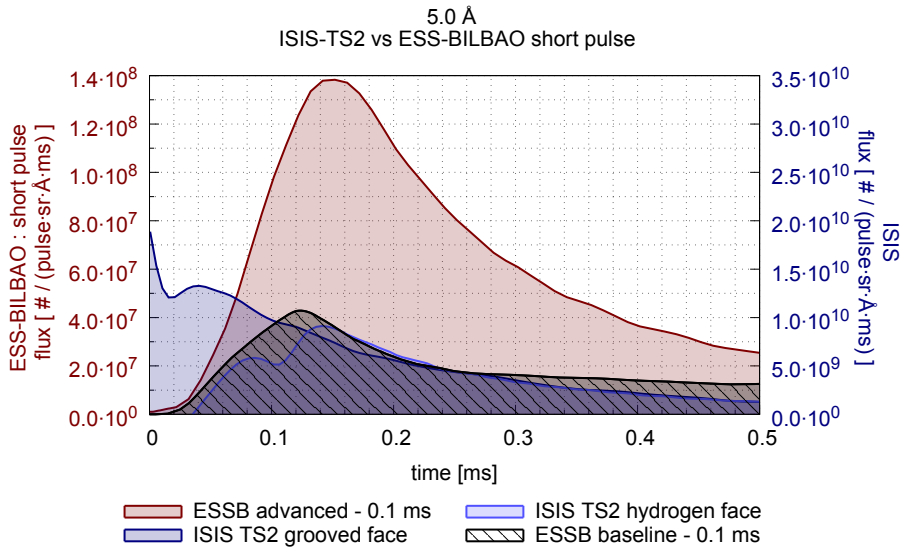

Figure C.1-5: Neutron pulse for the ESSB short pulse cases vs ISIS-TS2 at 5 Å

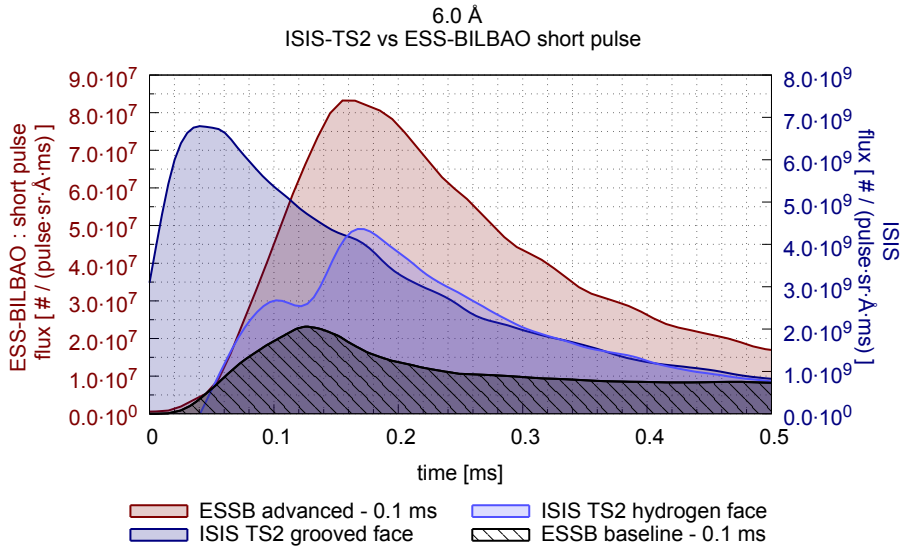

Figure C.1-6: Neutron pulse for the ESSB short pulse cases vs ISIS-TS2 at 6 Å

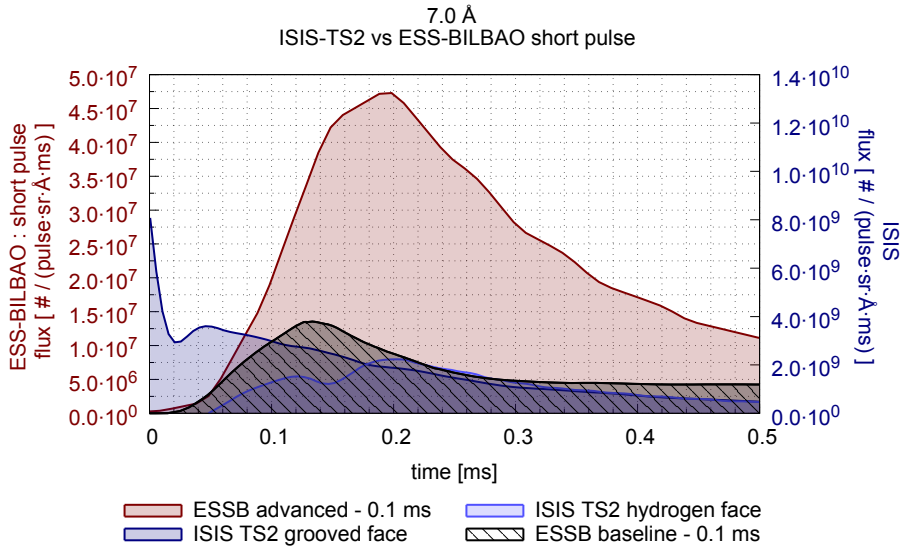

Figure C.1-7: Neutron pulse for the ESSB short pulse cases vs ISIS-TS2 at 7 Å

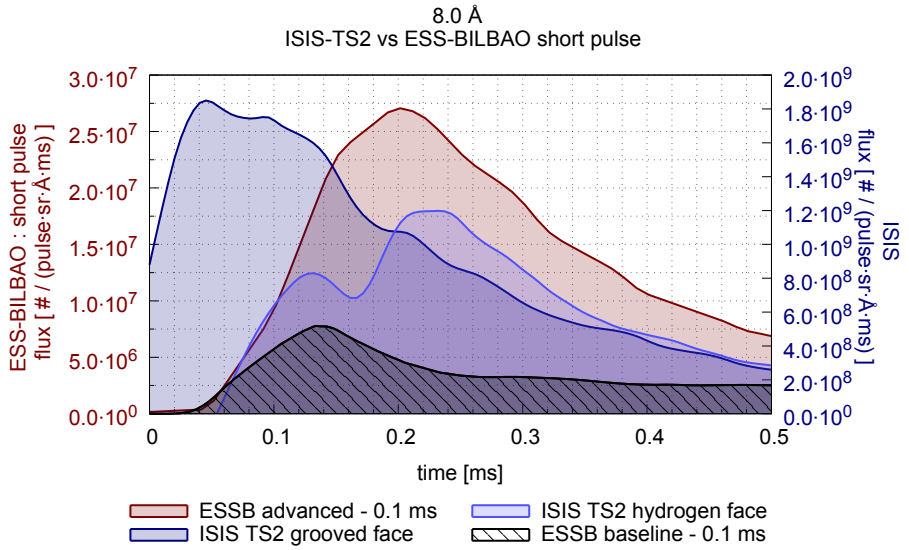

Figure C.1-8: Neutron pulse for the ESSB short pulse cases vs ISIS-TS2 at 8 Å

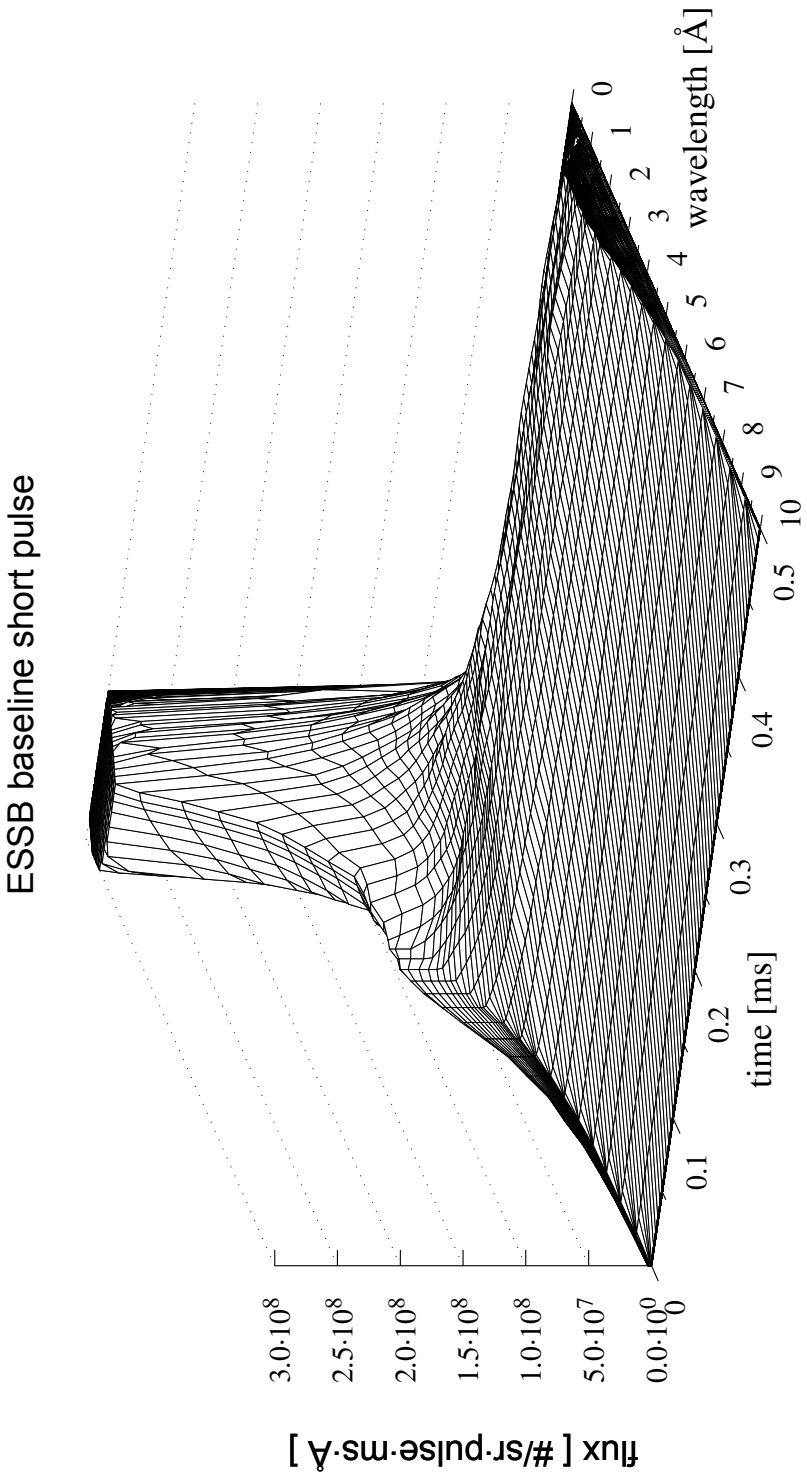

Figure C.1-9: Neutron pulses for the ESSB baseline configuration

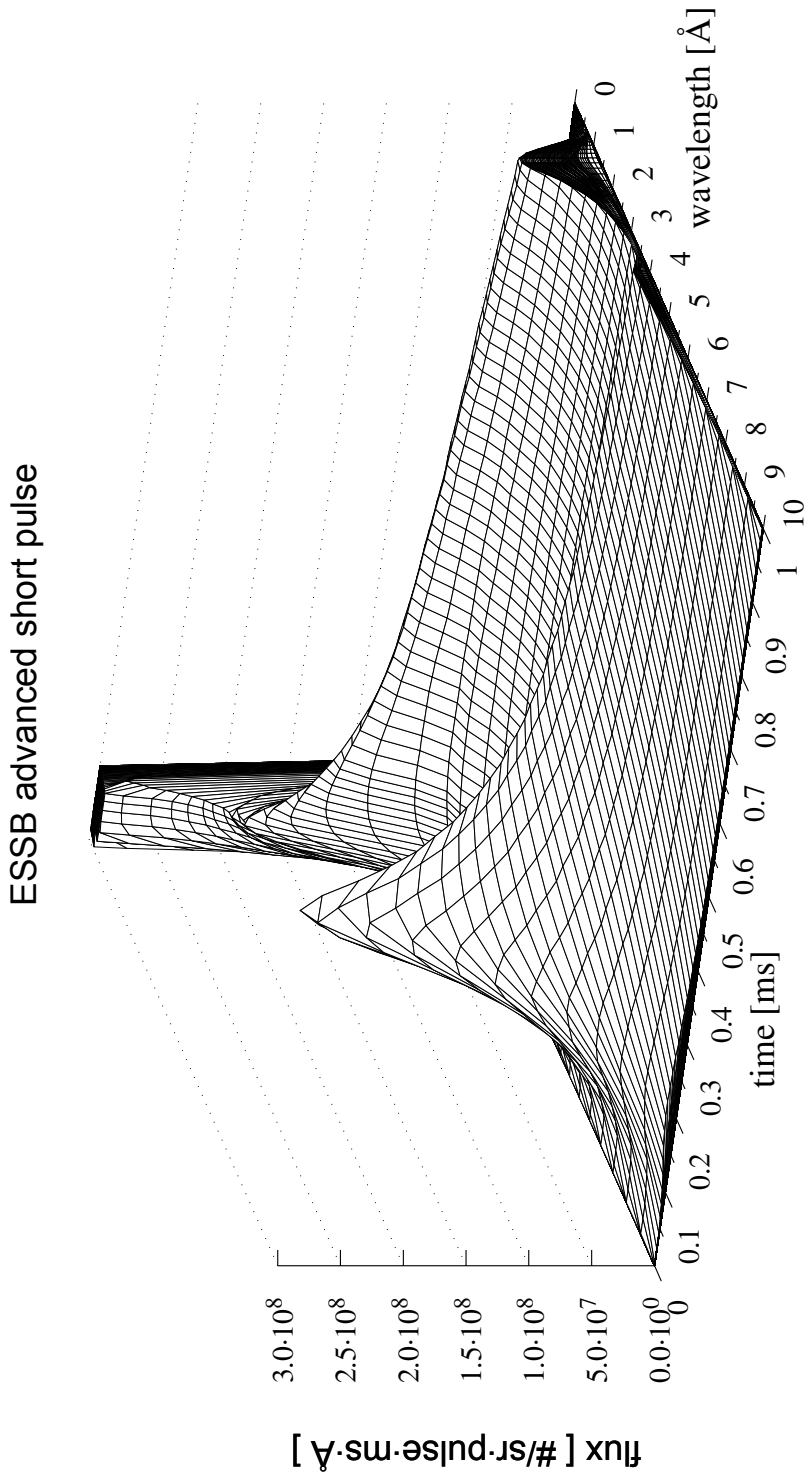

Figure C.1-10: Neutron pulses for the ESSB short advanced proposal

C.2 SHORT NEUTRON PULSES

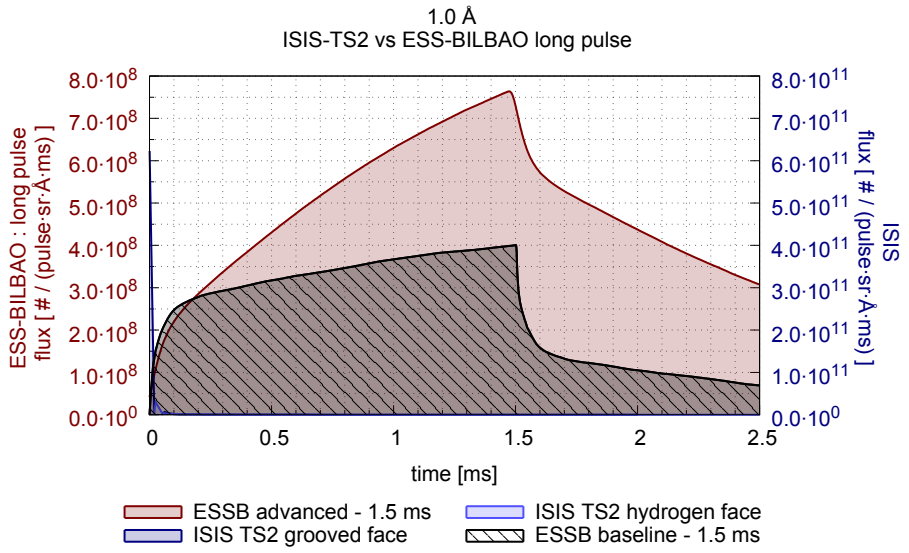

Figure C.2-1: Neutron pulse for the ESSB long pulse cases vs ISIS-TS2 at 1 Å

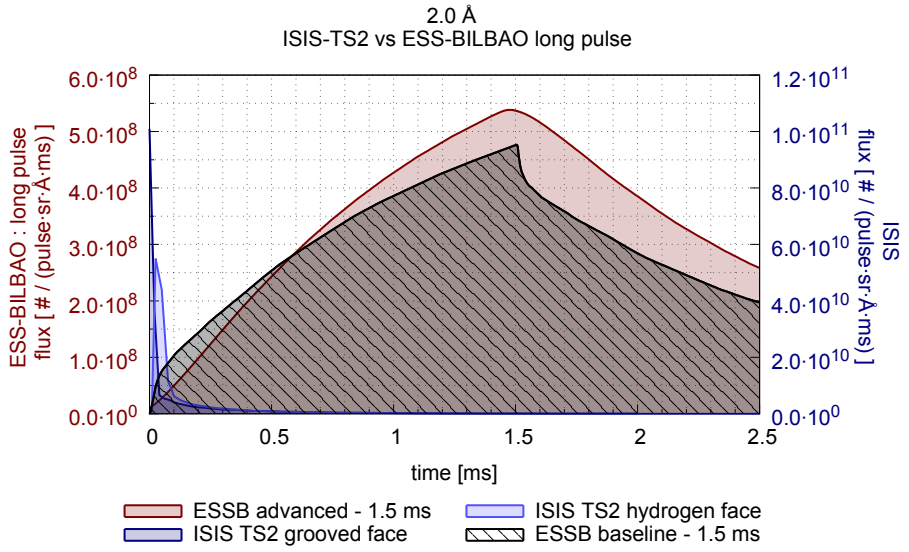

Figure C.2-2: Neutron pulse for the ESSB long pulse cases vs ISIS-TS2 at 2 Å

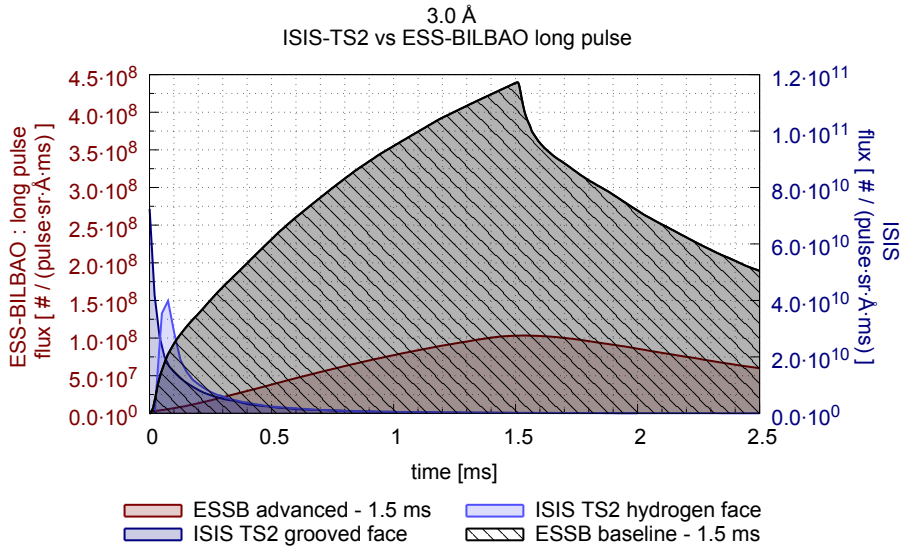

Figure C.2-3: Neutron pulse for the ESSB long pulse cases vs ISIS-TS2 at 3 Å

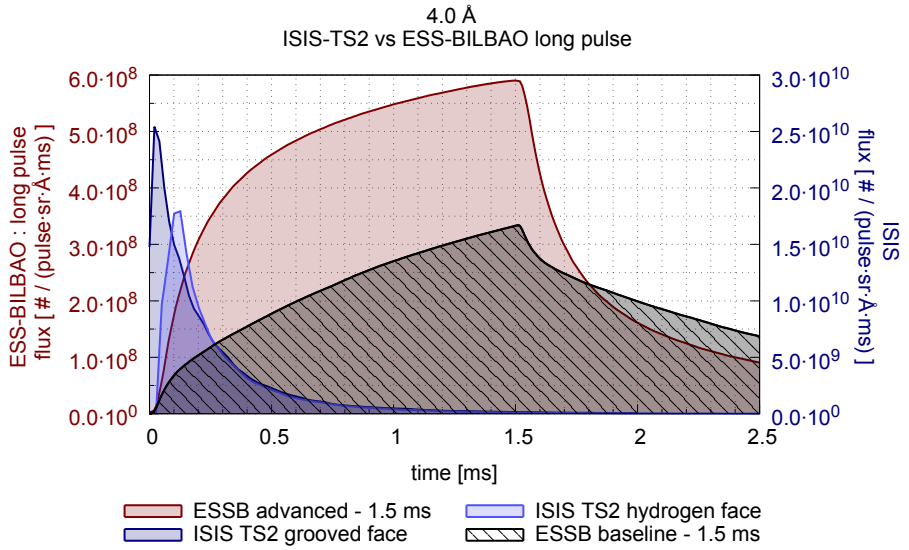

Figure C.2-4: Neutron pulse for the ESSB long pulse cases vs ISIS-TS2 at 4 Å

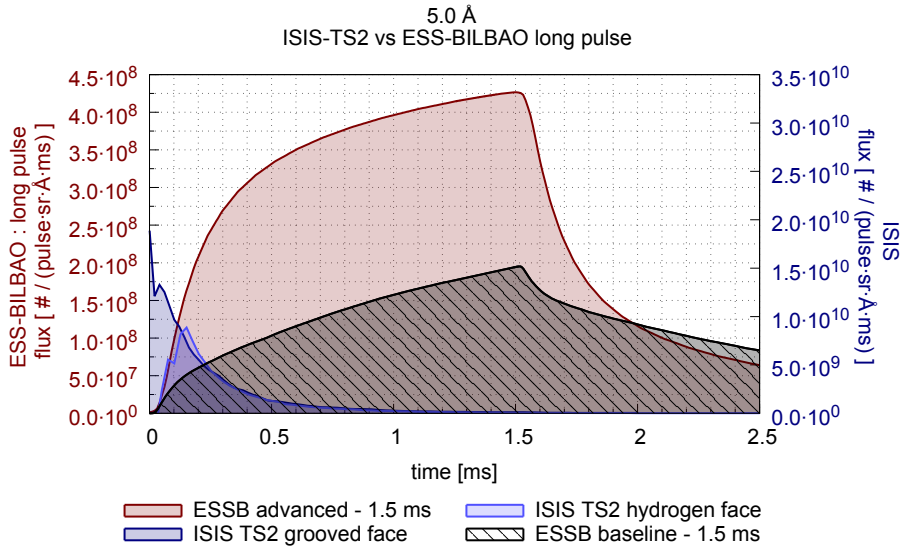

Figure C.2-5: Neutron pulse for the ESSB long pulse cases vs ISIS-TS2 at 5 Å

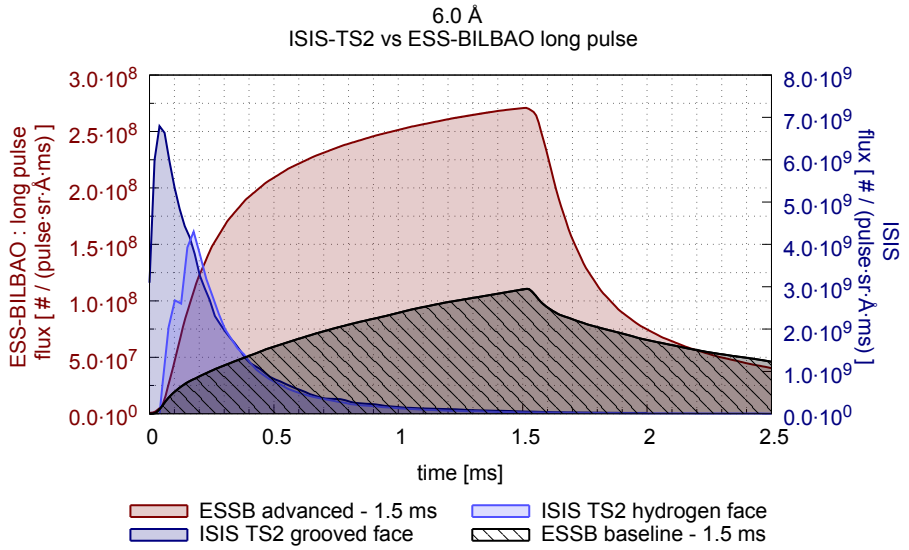

Figure C.2-6: Neutron pulse for the ESSB long pulse cases vs ISIS-TS2 at 6 Å

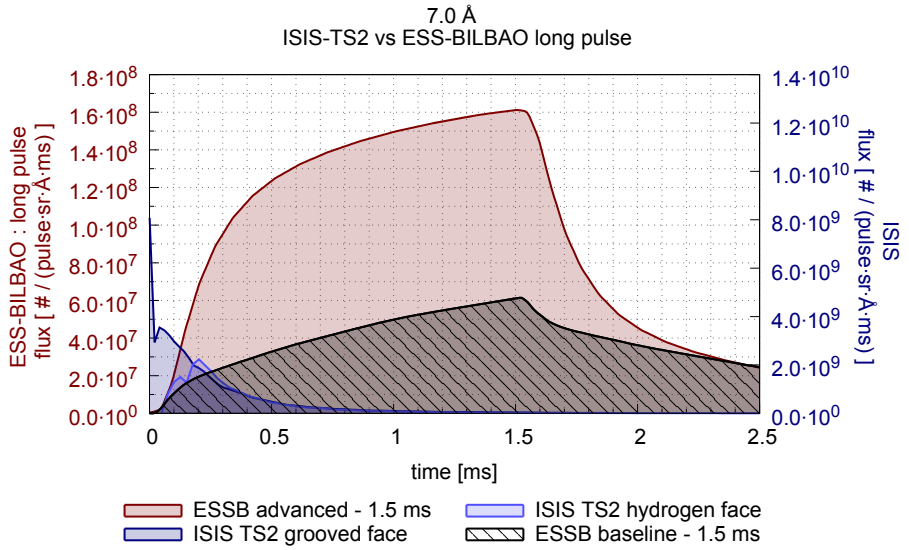

Figure C.2-7: Neutron pulse for the ESSB long pulse cases vs ISIS-TS2 at 7 Å

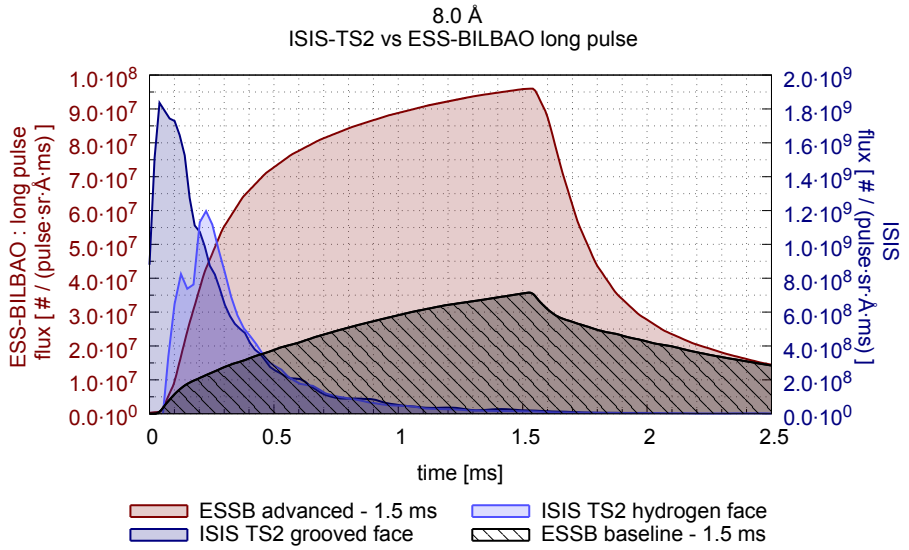

Figure C.2-8: Neutron pulse for the ESSB long pulse cases vs ISIS-TS2 at 8 Å

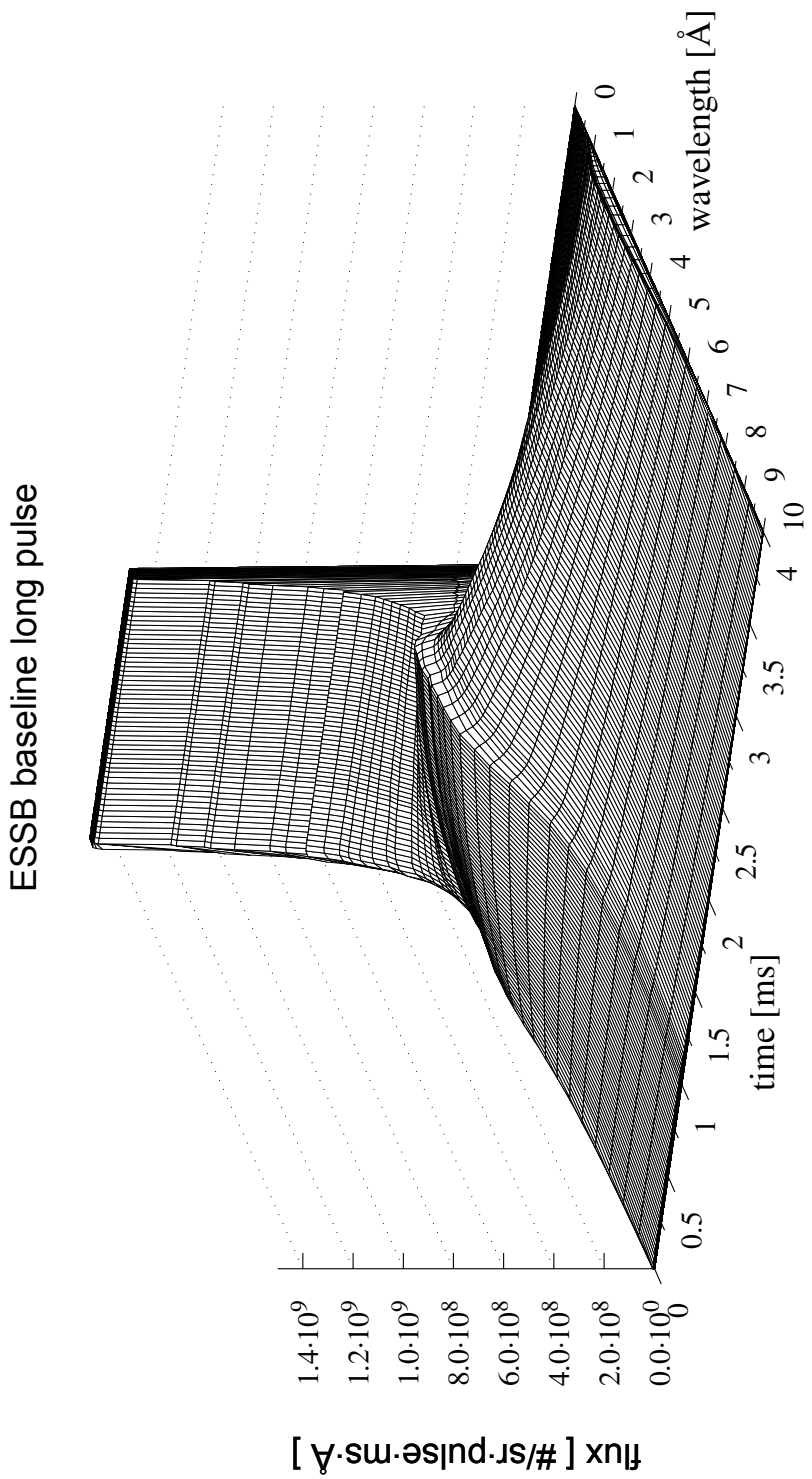

Figure C.2-9: Neutron pulses of the ESSB long baseline configuration

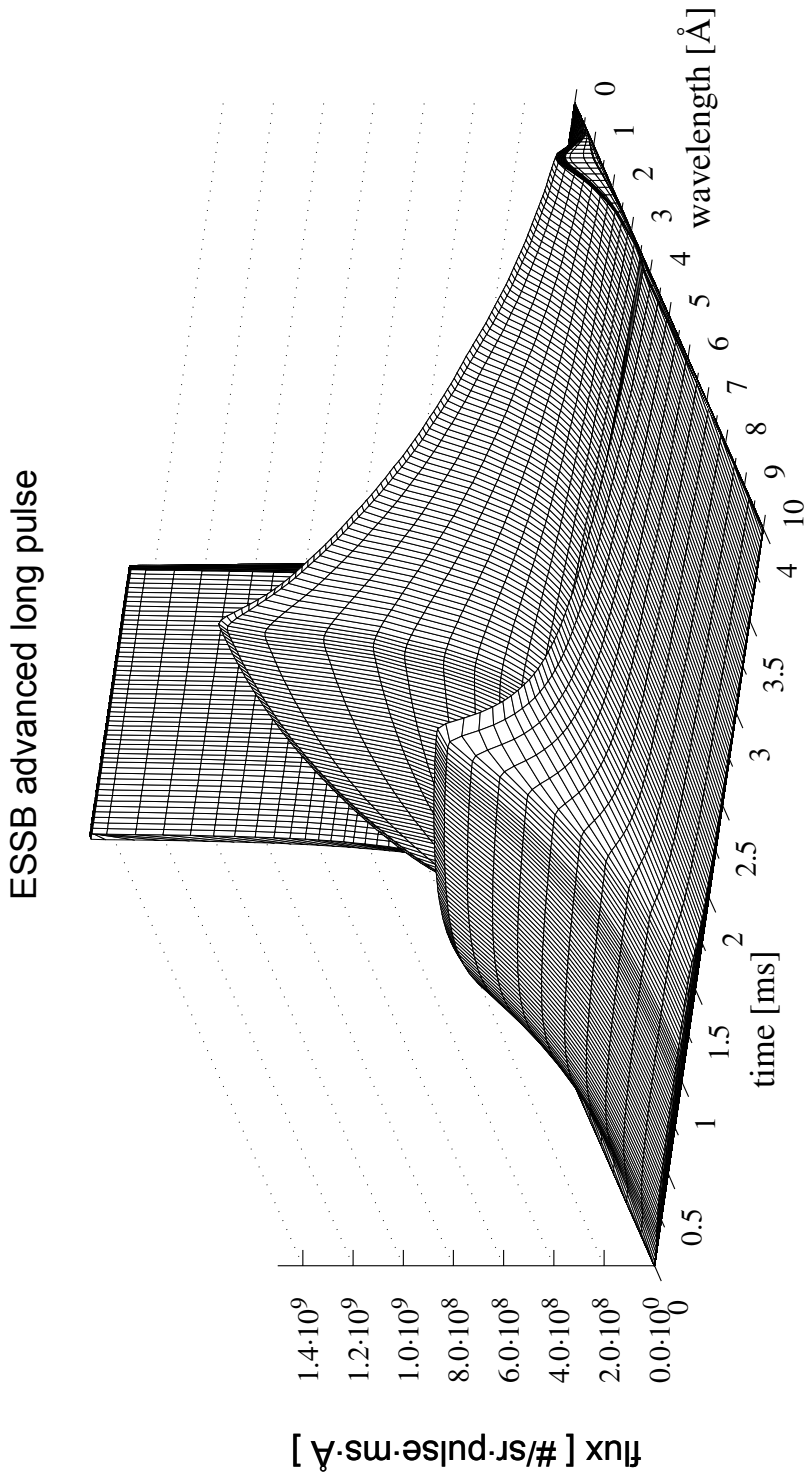

Figure C.2-10: Neutron pulses for the ESSB long advanced proposal

APPENDIX D

ESTIMATION OF THE To-CHOPPER DEPTH

D.1 GENERAL CONSIDERATIONS

This appendix will try to estimate the required depth of the To-chopper blades in order to block the high energy neutrons and the gamma radiation from the target (background).

It was assumed that the mean free path of high enery neutrons is greater than the gamma radiation one. Hence a To-chopper depth estimation was carried out only under neutron transport radiation criteria.

A analytical estimation assuming the history of a 50-MeV neutron particle was performed. No simulation of the neutron beam was carried out becuase the exact position of the To-chopper is required in order to take into account the solid angle.

The employed material for the blades was Inconel X-750 (chemical composition in table D.1-1), used for a To-chopper developed at KEK for J-PARC [19], because it collects good mechanical and radiation activation properties.

Table D.1-1: Chemical composition (%) of the Ni-based superalloy Inconel X-750

Ni	Cr	Fe	Co	Ti	Al	Nb + Ta
73.8	15	7	-	2.5	0.7	1.0

Figure D.1-1 shows an sketch of the To-Chopper from KEK. It shows how the requiered depth for the blades is around 30 cm.

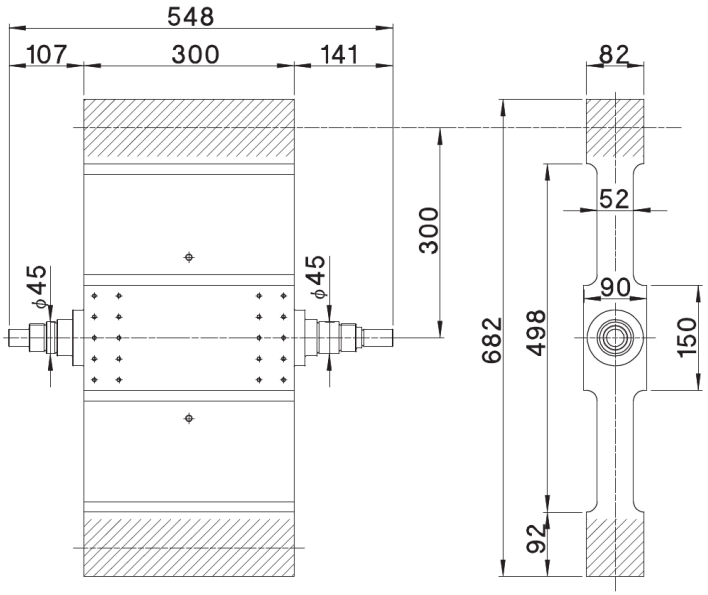

Figure from S. Ithoh et al. [19]

Figure D.1-1: Sketch of the To-Chopper developed at KEK (units is millimeters)

D.2 ANALYTICAL ESTIMATION

Figure D.2-1 plots the elastic, inelastic, radiative capture and total cross sections of the Inconel X-750 material. It shows how above a few hundreds of millielectrovolts the predominant nuclear reaction will be the elastic collion one. Below this limit the elastic collision will compite with the radiative capture which will emit gamma radiation.

So the first step of the analythical proccess would be to estimate the penetration range of 9 MeV-neutrons (the mean energy of neutrons emerging from the ESSB baseline configuration) until their energies go down to a few electronvolts [20] due to only elastic interactions.

The nickel contribution to the macroscopic elasttic cross section is the greatest one because this element is the main component of the Inconel X-750. Nevertheless the elastic cross section is not a direct measure of the material stopping power because it does not take into account the energy loss per collision. Expression D-1 shows the mean lethargy variation that can be an indirect measure of the previous energy loss.

$$\xi = \Delta \langle u \rangle = ln\frac{E_i}{E_f} = 1 + \frac{(A-1)^2}{2A} ln\left(\frac{A-1}{A+1}\right) \tag{D-1}$$

where,

ξ, *is the variation of lethargy*
u, *is the lethargy*
E_i, *is the neurton energy before collision*
E_f, *is the neutron energy after collision*
A, *is the atomic mass of the nucleus*

The lethargy variation is not dependent of the neutron energy (only depends on the atomic mass of the element), so its exponential could be multiplied by the macroscopic elastic cross section, Expression D-2, to get a direct measure of the material neutron stopping power.

$$e^{\xi} \cdot \Sigma = \frac{E_i}{E_f} \cdot \Sigma \tag{D-2}$$

Figure D.2-2 plots the previous multiplication and confirms that nickel is the most powerful inconel-component for stopping neutrons. So it can be taken the nickel element only for neutron transport estimations.

As mentioned the mean lethargy variation does not depend on the neutron energy, so Expression D-3 [21] lets to get the number of collisions to reducing neutron energy from E_i to E_f. Taken into account that ξ for nickel is 0.034, then it would be needed around 335 collisions to stop neutrons from 9 MeV to 100 eV.

On the other hand, the mean macroscopic nickel elastic cross section of the energy range taken into account is around 11 cm^{-1} so 335 collisions will happen along the 30.5 cm.

$$n = \frac{u}{\xi} = \frac{1}{\xi} \cdot ln\frac{E_i}{E_f} \tag{D-3}$$

Hence 30.5 cm will be enough to stop 9 MeV-neutrons to a hundred of electrovolts. But this is not an optimized value because another reactions that stop neutron energy have not been taken into account like radiative capture. Then Monte-Carlo simulations will be required. Also the radiation dose that is allowed to pass through the blades and the solid angle reduction of the radiation are needed in order to estimate the blades width.

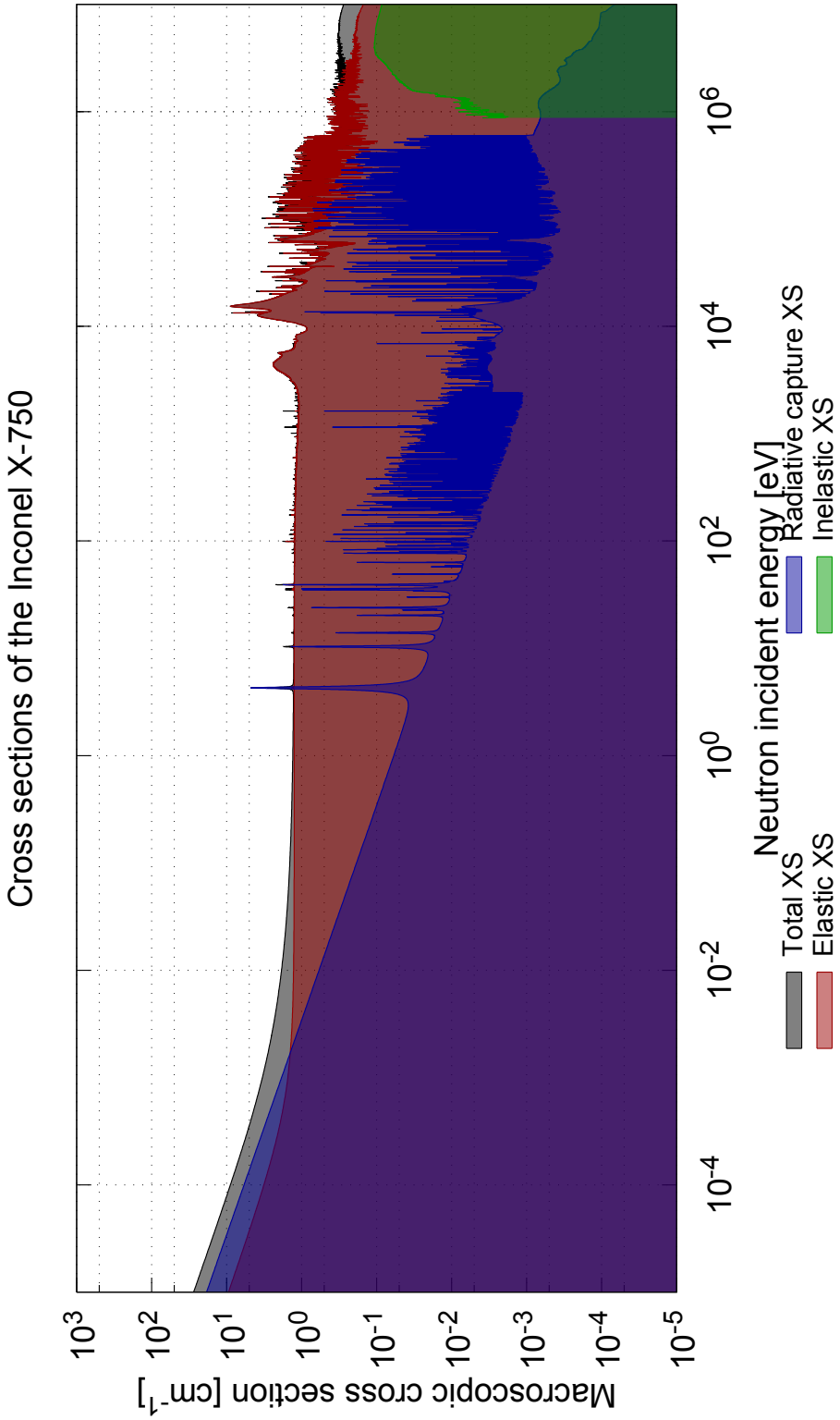

Data from the Chinise Evaluated Nuclear Data Library v2.1 & v3.1

Figure D.2-1: Total, elastic, inelastics and radiative capture XS of Inconel X-750

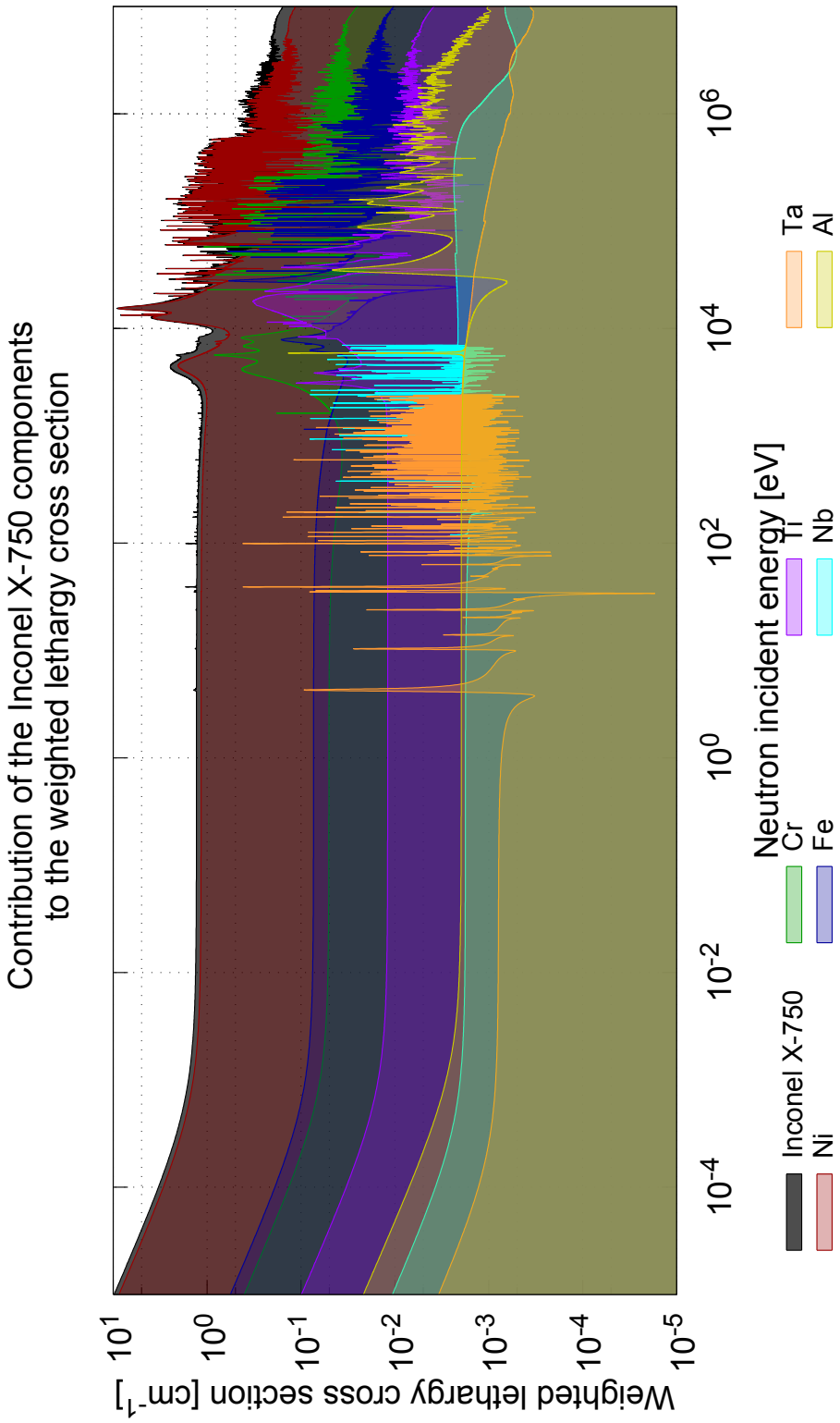

Data from the Chinise Evaluated Nuclear Data Library v2.1 & v3.1

Figure D.2-2: Relative contribution of Inconel X-750 components to weighted lethargy cross section